

Summer November 2014

EVALUATING EFFECTS OF MOLECULAR HETEROGENEITY ON THE NON-LINEAR MECHANICAL BEHAVIOR OF EPOXY NETWORKS

Zhan Hang Yang

Follow this and additional works at: https://scholarworks.umass.edu/dissertations_2



Part of the [Polymer Science Commons](#)

Recommended Citation

Yang, Zhan Hang, "EVALUATING EFFECTS OF MOLECULAR HETEROGENEITY ON THE NON-LINEAR MECHANICAL BEHAVIOR OF EPOXY NETWORKS" (2014). *Doctoral Dissertations*. 277.
<https://doi.org/10.7275/8ra4-sr44> https://scholarworks.umass.edu/dissertations_2/277

This Open Access Dissertation is brought to you for free and open access by the Dissertations and Theses at ScholarWorks@UMass Amherst. It has been accepted for inclusion in Doctoral Dissertations by an authorized administrator of ScholarWorks@UMass Amherst. For more information, please contact scholarworks@library.umass.edu.

**EVALUATING EFFECTS OF MOLECULAR HETEROGENEITY ON THE
NON-LINEAR MECHANICAL BEHAVIOR OF EPOXY NETWORKS**

A Dissertation Presented

by

ZHAN HANG YANG

Submitted to the Graduate School of the
University of Massachusetts Amherst in partial fulfillment
of the requirements for the degree of

DOCTOR OF PHILOSOPHY

September 2014

Polymer Science and Engineering

© Copyright by Zhan Hang Yang 2014

All Rights Reserved

**EVALUATING EFFECTS OF MOLECULAR HETEROGENEITY ON THE
NON-LINEAR MECHANICAL BEHAVIOR OF EPOXY NETWORKS**

A Dissertation Presented

by

ZHAN HANG YANG

Approved as to style and content by:

Alan J. Lesser, Chair

David A. Hoagland, Member

H. Henning Winter, Member

David A. Hoagland, Department Head
Polymer Science and Engineering

DEDICATION

To my patient and loving parents

ACKNOWLEDGMENTS

I would like to thank my advisor, Professor Alan Lesser, for his significant contributions to my intellectual growth. His curiosity, enthusiasm, and creativity have continuously motivated me throughout my study. I appreciate his patience and guidance in helping me develop critical thinking and effective communication skills. I would also like to extend my gratitude to my committee members, Professor David Hoagland and Professor Henning Winter. They have provided me valuable suggestions for my projects, and taught me the importance of thinking across different perspectives and disciplines.

I would like to thank past and present Lesser Group members for my wonderful time at UMass: Joonsung, Scott, Donna, Andrew, Jared, Sinan, Naveen, Rousty, Jan, Wei, Polina, Angela, Brian, Connor, Ranadip, Nihal, and Maheen. It is my pleasure to work with them and have them as friends. I would also like to thank my classmates and friends for the trips and joyful time we have together, especially Dayong, Xinyu, and Yu.

My acknowledgments to CUMIRP, MRSEC, Stonhard, BASF, and Gates Foundation for all the funding and support through the years. The graduate life becomes easier with continuous assistance from the PSE staff - Lisa, Sophie, Maria, Jessica, Ann, and Alyssa. Many thanks to Jack, Lou, Sekar, Andre, Dennis, John, Greg, and Jim.

I would like to thank my housemates who are not only great friends, but create a family away from home. Li, Ziwen, and Zhou are like brothers to me and are always there in my good and bad times. I also appreciate their sense of humor.

I would also like to thank my mother and father for their love, patience, and trust. I am fortunate to have them as my family. I would not be where I am today without them.

ABSTRACT

EVALUATING EFFECTS OF MOLECULAR HETEROGENEITY ON THE NON-LINEAR MECHANICAL BEHAVIOR OF EPOXY NETWORKS

SEPTEMBER 2014

ZHAN HANG YANG, B.E., STATE UNIVERSITY OF NEW YORK STONY BROOK

M.S., UNIVERSITY OF MASSACHUSETTS AMHERST

Ph.D., UNIVERSITY OF MASSACHUSETTS AMHERST

Directed by: Professor Alan J. Lesser

This thesis describes synthetic and processing strategies to formulate epoxies resins with molecular heterogeneity to achieve enhanced engineering properties. The network heterogeneities include chemical differences in stiffness and crosslink density, as well as mechanical difference in baseline energy state. The focus is to understand the fundamental structure-process-property relationships in these unusual network polymers, especially the post-yield responses and fracture toughness. The main characterization techniques to probe the complex network architectures are dynamic mechanical spectroscopy and compression tests. Ductility and governing parameters are also proposed to describe the relationships between molecular structures and physical properties.

Three different staged fabrication strategies are studied, with increasing complexity in network architectures. In the Topologically Heterogeneous Network approach, a rigid multi-functional prepolymer is prepared first and then reacted with flexible reagents to generate within the resulting materials regions of varying stiffness and crosslink density. In the Prestressed Double Network approach, deformation is imposed between cure

reactions to alter the energy state of the resulting materials. In the Asymmetric Double Network approach, lightly crosslinked aliphatic network and highly crosslinked aromatic network are introduced as the major and minor components. All three strategies produce macroscopically homogeneous epoxies with improved toughness. Combinations of the approaches are also evaluated.

The observed changes in the dynamic mechanical spectra include broadening and shifting of the transitions with imposed molecular heterogeneity. A ductility parameter based on mechanical spectroscopy is proposed to quantify the influence of segmental mobility on large strain deformation. Compression test is also investigated to extract intrinsic network characteristics of thermosets. A second ductility parameter based on equilibrium and kinematic considerations is proposed to correlate with fracture toughness. Both the glass transition temperature and cohesive energy density are correlated with the non-linear mechanical behavior, including rejuvenated stress and strain hardening modulus.

TABLE OF CONTENTS

	Page
ACKNOWLEDGMENTS	v
ABSTRACT.....	vi
LIST OF TABLES	xiii
LIST OF FIGURES	xiv
CHAPTER	
1. INTRODUCTION	1
1.1 Structure-Property Relationships of Epoxies	1
1.2 Background.....	3
1.2.1 Dynamic Mechanical Spectroscopy.....	3
1.2.2 Compression Testing	5
1.2.3 Fracture Toughness.....	5
1.3 Main Characterization Techniques	6
1.3.1 Dynamic Mechanical Analysis	6
1.3.2 Compression Testing	7
1.3.3 Fracture Toughness.....	7
1.4 Dissertation Overview	8
1.5 References	11
2. PREPARATION AND CHARACTERIZATION OF TOPOLOGICALLY HETEROGENEOUS NETWORK EPOXIES	14
2.1 Introduction	14
2.2 Experimental.....	16

2.2.1 Materials	16
2.2.2 Network Formation.....	17
2.2.2.1 Homologous Curatives Approach	17
2.2.2.2 Multifunctional Prepolymer Approach	17
2.2.3 Characterization	18
2.2.3.1 Differential Scanning Calorimetry	18
2.2.3.2 Dynamical Mechanical Analysis.....	18
2.2.3.3 Compression Testing.....	18
2.2.3.4 Fracture Toughness	19
2.2.3.5 Thermogravimetric Analysis.....	19
2.3 Results and Discussion	19
2.3.1 Homologous Curatives Approach.....	19
2.3.1.1 Crosslink Density from Stoichiometry.....	19
2.3.1.2 Differential Scanning Calorimetry	20
2.3.1.3 Dynamic Mechanical Analysis	21
2.3.1.4 Compressive Behavior	22
2.3.1.5 Fracture Toughness	23
2.3.2 Multifunctional Prepolymer Approach.....	24
2.3.2.1 Crosslink Density from Stoichiometry.....	24
2.3.2.2 Dynamic Mechanical Properties	25
2.3.2.3 Compressive Behavior	29
2.3.2.4 Fracture Toughness	31
2.3.2.5 Thermal Stability.....	32

2.4 Conclusion.....	33
2.5 Future Work.....	34
2.6 References	35
3. PREPARATION AND CHARACTERIZATION OF PRESTRESSED DOUBLE	
NETWORK EPOXIES.....	37
3.1 Introduction	37
3.2 Experimental.....	39
3.2.1 Materials	39
3.2.2 Network Formation.....	39
3.2.3 Characterization.....	40
3.2.3.1 Thermomechanical Analysis	40
3.2.3.2 Dynamic Mechanical Analysis	41
3.2.3.3 Tensile Testing.....	41
3.2.3.4 Fracture Toughness	41
3.3 Results and Discussion	41
3.3.1 Molecular Weight between Crosslinks	41
3.3.2 Thermomechanical Properties	42
3.3.3 Dynamic Mechanical Properties.....	48
3.3.4 Tensile Response	52
3.3.5 Fracture Toughness.....	54
3.4 Conclusion.....	58
3.5 Future Work.....	59
3.6 References	60

4. PREPARATION AND CHARACTERIZATION OF ASYMMETRIC DOUBLE NETWORK EPOXIES	62
4.1 Introduction	62
4.2 Experimental.....	66
4.2.1 Materials	66
4.2.2 Network Formation.....	66
4.2.3 Characterization	67
4.2.3.1 Differential Scanning Calorimetry.....	67
4.2.3.2 Dynamic Mechanical Analysis	67
4.2.3.3 Compression Testing.....	67
4.2.3.4 Tensile Testing	67
4.2.3.5 Fracture Toughness	68
4.3 Results and Discussion	68
4.3.1 Molecular Weight between Crosslinks.....	68
4.3.2 Differential Scanning Calorimetry.....	69
4.3.3 Dynamic Mechanical Properties	72
4.3.4 Compressive Behavior	77
4.3.5 Tensile Responses.....	82
4.3.6 Fracture Toughness.....	84
4.4 Conclusion	86
4.5 Future work	87
4.6 References	89
5. DUCTILITY AND GOVERNING PARAMETERS	91

5.1 Introduction	91
5.1.1 DMA-based Ductility Parameter	91
5.1.2 Compression-based Ductility Parameter	93
5.1.3 Glass Transition Temperature and Cohesive Energy Density	95
5.2 Experimental.....	95
5.3 Results and Discussion	96
5.3.1 DMA-based Ductility Parameter	96
5.3.2 Compression-based Ductility Parameter	98
5.3.3 Glass Transition Temperature and Cohesive Energy Density	99
5.4 Conclusion.....	104
5.5 Future Work.....	105
5.6 References	106
BIBLIOGRAPHY.....	108

LIST OF TABLES

Table		Page
Table 2.1	Chemical structures of epoxide monomers and amines.....	17
Table 2.2	Mechanical Properties of the Epoxies	24
Table 2.3	Physical properties of the epoxies.	30
Table 3.1	Chemical structure of new amine.	39
Table 3.2	Estimated molecular weights between the crosslinks of PDN epoxies	42
Table 3.3	Tensile testing results.....	54
Table 4.1	Chemical structure of new amines.	64
Table 4.2	Molecular weights between crosslinks of the epoxies.....	69
Table 4.3	Physical properties of the epoxies.	80
Table 4.4	Tensile properties of DDM-based asymmetric epoxies.....	84
Table 5.1	Physical properties of the reagents.	100
Table 5.2	Molecular weights between crosslinks, and cohesive energy densities of Topologically Heterogeneous Networks.....	101
Table 5.3	Molecular weights between crosslinks, and cohesive energy densities of Double Networks.....	101
Table 5.4	Molecular weights between crosslinks, and cohesive energy densities of Asymmetric Networks.....	102

LIST OF FIGURES

Figure		Page
Figure 1.1	Research overview.....	1
Figure 2.1	(a) Structurally diverse THN prepolymer. Colored segments: black, stiff tetrafunctional epoxide; and red, rigid difunctional amine. (b) THN prepolymer reacted with flexible tetrafunctional amine (blue segments), (c) THN prepolymer reacted with flexible tetrafunctional amine (blue segments) and soft difunctional epoxide (orange segments).	16
Figure 2.2	DSC thermograms of DGEBA-D400 and DGEBA-D230-D2000 8.9-1.1. The numbers on the curves are glass transition temperatures of the epoxies.....	20
Figure 2.3	Dynamic mechanical spectra of DGEBA-D400 and DGEBA-D230-D2000 8.9-1.1. (a) Storage moduli labeled with glass transition temperatures, (b) Loss moduli labeled with full width at half maximum (FWHM) of alpha transitions.	22
Figure 2.4	Stress-strain curves of DGEBA-D400 and DGEBA-D230-D2000 8.9-1.1 tested in compression.	23
Figure 2.5	Crosslink densities (solid circles), and volumetric densities (unfilled triangles) of epoxies.	25
Figure 2.6	(a) Storage moduli and (b) Loss moduli of epoxies. (c) Network repeat segment of DGEBA-based resin with hydroxypropylether unit and	

phenyl group highlighted. (d) Network repeat segment of TGDDM-based resin.	26
Figure 2.7 (a) Glass transition temperature (solid circle) and storage moduli (unfilled triangle). (b) Comparison between crosslink densities obtained from rubbery plateau moduli, and stoichiometry.	26
Figure 2.8 (a) Normalized alpha transitions, (b) Corresponding full widths at half maximum (FWHM) of the transitions.	29
Figure 2.9 (a) Stress-strain curves of THN epoxies and control samples tested in compression, (b) Comparison of crosslink densities obtained from strain hardening moduli and stoichiometry.	30
Figure 2.10 Fracture toughness of epoxies.	32
Figure 2.11 (a) TGA thermograms of epoxies, (b) Decomposition temperatures (solid circle) and residues (unfilled triangle).	33
Figure 3.1 Sample preparation scheme of PDN epoxies. The black and red wavy lines stand for D230 and DDS, respectively. After the first cure (Step I), essentially all D230 had reacted to form the first network while most DDS remained unreacted. The partially cured resin was then compressed by 50% compressive strain (Step II). While in the deformed state, DDS was reacted to introduce the second network (Step III). The resulting epoxy is unrelaxed because of the latent free energy stored in it. It became relaxed and had some thickness recovery after heating above its glass transition temperature.	40

Figure 3.2	Dimension changes of epoxies during first heating on TMA. The numbers 0.2, 0.5, and 0.8 denote the molar fractions of DDS used to synthesize the resins. Control: DN epoxies without prestress; Prestressed, Unrelaxed _{//} : unrelaxed PDN epoxies tested parallel to the prestressing direction; Prestressed, Unrelaxed _⊥ : unrelaxed PDN epoxies tested perpendicular to the prestressing direction.	43
Figure 3.3	Dimension changes of epoxies going from glassy to rubbery state normalized by thickness prior to testing.	45
Figure 3.4	Dimension changes of epoxies during second heating on TMA. Prestressed, Relaxed _{//} : relaxed PDN epoxies tested parallel to the prestressing direction; Prestressed, Relaxed _⊥ : relaxed PDN epoxies tested perpendicular to the prestressing direction.	46
Figure 3.5	Glass transition temperatures of epoxies measured on TMA. (a) Parallel to the prestressing direction, (b) Perpendicular to the prestressing direction.....	47
Figure 3.6	Coefficients of linear thermal expansion of epoxies. (a) Measured parallel to the prestressing direction, (b) Measured perpendicular to the prestressing direction.....	48
Figure 3.7	Dynamic mechanical measurements of some representative epoxies. (a) Storage moduli, (b) Loss moduli.....	49
Figure 3.8	Glass transition temperatures of epoxies measured on DMA.	49
Figure 3.9	Normalized beta transitions.....	50

Figure 3.10 (a) Normalized alpha transitions, (b) Full width at half maximum (FWHM) of the transitions.....	51
Figure 3.11 Tensile stress-strain curves of epoxies. DN 0: cured purely with D230; DN 1: cured purely with DDS; DN 0.5: cured with 50% DDS content; PDN 0.5U: prestressed, unrelaxed resin with 50% DDS content.	53
Figure 3.12 Fracture toughness of unrelaxed PDN epoxies and control samples.	55
Figure 3.13 (a) Fracture toughness of unrelaxed PDN epoxies with 50% DDS content tested along different precrack directions, (b) Precrack directions.	56
Figure 3.14 Polarized digital images of representative miniature compact tension specimens after fracture. (a) control sample with 50% DDS content, (b) unrelaxed PDN epoxy with 50% DDS content.	57
Figure 3.15 Fracture surfaces of an unrelaxed PDN epoxy with 50% DDS content. The sketch at the left shows the relative positions where the images are taken on the mini-CT specimen.	58
Figure 4.1 Schematic presentation of Asymmetric Double Network epoxies. The loosely crosslinked aliphatic network is colored blue. The densely crosslinked aromatic network is colored red.....	63
Figure 4.2 (a) Chain-extended prepolymer, (b) DGEBA-Aniline-D230-SD231-DDM 5-4-1. Colored segments: black, DGEBA; red, aniline; orange, SD231; blue, D230; and green, DDM.....	65
Figure 4.3 (a) DSC thermograms of partially cured resins, (b) DSC thermograms of postcured resins. The numbers next to the curves are glass transition temperatures of the epoxies. Exothermic direction up.....	71

Figure 4.4	(a) DSC thermograms of resins with the same T_g values, (b) DSC thermograms of partially cured and postcured DGEBA-Aniline-D230-SD231-DDM 5-4-1. The numbers next to the curves are glass transition temperatures of the epoxies.....	72
Figure 4.5	(a) Storage moduli of epoxies. The numbers on the curves are glass transition temperatures of the epoxies. (b) Loss moduli of the same epoxies.....	73
Figure 4.6	(a) Normalized alpha transition, (b) Full width at half maximum (FWHM) of the transitions.....	74
Figure 4.7	(a) Storage moduli (solid lines) and loss moduli (dash lines) of DGEBA-D230-SD231-DDM 5-4-1 resins without and with prestress, (b) Normalized alpha transitions of the same epoxies. The numbers on the curves are the full widths at half maximum (FWHM) of the transitions.	75
Figure 4.8	Storage and loss moduli of DGEBA-Aniline-D230-SD231-DDM 5-4-1.	76
Figure 4.9	(a) Stress-strain curves of partially cured resins. The numbers next to the curves are molecular weights between crosslinks of the aliphatic networks. (b) Stress-strain curves of postcured resins. The numbers next to the curves are the average molecular weights between crosslinks of the epoxies.....	78
Figure 4.10	Stress-strain curves of postcured resins with the same T_g values, and DGEBA-Aniline-D230-SD231-DDM 5-4-1. The numbers next to the curves are the average molecular weights between crosslinks for the epoxies.....	82

Figure 4.11 (a) Stress-strain curves of DDM-based asymmetric networks tested in tension, (b) Polarized images of tensile bars after test. 5-4-1 & 6-2-2: amine hydrogen ratio of the curing agents D230-SD231-DDM. The boxed regions indicate the onsets of necking and shear banding.....	84
Figure 4.12 Fracture toughness of DGEBA-based epoxies.....	86
Figure 5.1 (a) Delta function approach; (b) Weighted integral approach.....	92
Figure 5.2 (a) Before baseline subtraction. Inset shows how the onset of beta transition is defined; (b) After baseline subtraction.....	93
Figure 5.3 Correlations between the DMA-based ductility parameter and (a) yield stress; (b) fracture toughness.....	97
Figure 5.4 Correlation between the DMA-based ductility parameter and process zone size.....	97
Figure 5.5 Correlations between estimated process zone size and (a) equilibrium factor; (b) kinematic factor.....	98
Figure 5.6 Correlation between estimated process zone size and compression-based ductility parameter λ_E / λ_K	99
Figure 5.7 Molecular weight between crosslink versus cohesive energy density. THN: Topologically Heterogeneous Networks; DN: Double Networks; DN*: Reference [16]; AN: Asymmetric Networks.....	103
Figure 5.8 Normalized non-linear mechanical properties plotted against normalized test temperature. (a) Yield stress; and (b) Rejuvenated stress.....	103
Figure 5.9 Normalized strain hardening modulus against normalized test temperature.....	104

CHAPTER 1

INTRODUCTION

1.1 Structure-Property Relationships of Epoxies

The primary objective of this research is to evaluate the effects of chemical and mechanical heterogeneity introduced through unusual synthetic and processing routes on the non-linear mechanical behavior of epoxy networks. The size of network heterogeneity will not be quantified, but is expected to be on the molecular or nanometer scale. We fabricate unusual molecular architectures, specifically Topologically Heterogeneous Network, Prestressed Double Network, and Asymmetric Double Network. We interrogate non-linear engineering properties, such as strain softening, strain hardening, and fracture toughness. We impose new test methods, dynamic mechanical spectroscopy and compression testing, to correlate network structures to mechanical performance.

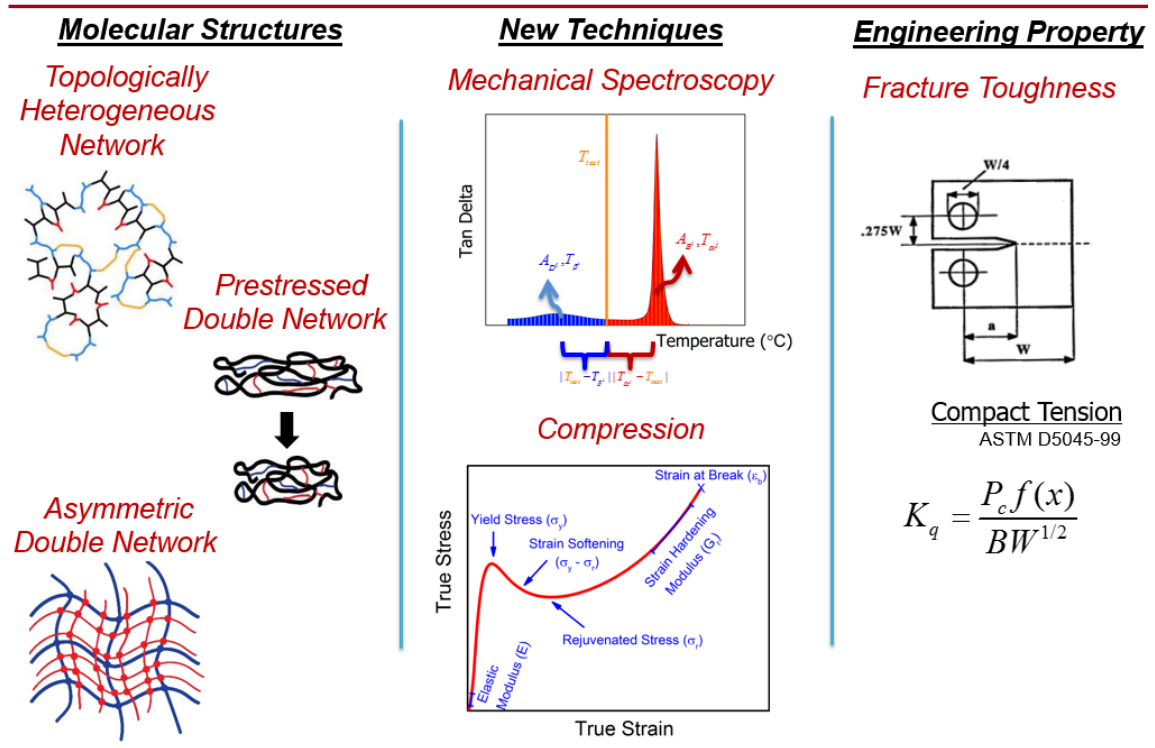


Figure 1.1 Research overview.

Epoxy resins are one of the thermosets commonly employed in coatings, adhesives, electronics, and aerospace applications. They are known for their small cure shrinkage, good chemical and creep resistance, as well as broad service temperature range. However, they are susceptible to brittle failure due to their highly crosslinked network structures¹.

Most epoxy formulations found in the open literature are below their glass transition temperatures (T_g 's) at room temperature. The resins are typically prepared by curing a difunctional epoxide diglycidyl ether of bisphenol A (DGEBA) with a single aliphatic or aromatic diamine¹⁻⁵. Few studies have investigated the use of miscible blends of amines with different molecular weights and functionalities⁶⁻¹⁷. There are even fewer reports on homogenous mixtures of epoxide monomers^{18,19}. Furthermore, there is no previous work on 1) complex formulations containing mixtures of epoxides and amines with varying stiffness and functionalities, 2) prestressing between staged cure reactions, or 3) double networks with highly asymmetric stiffness between the constituents.

The linear, yield, and fracture behavior of epoxies have been investigated in the past decades²⁰⁻²³. The elastic modulus is a linear property associated with network connectivity^{22,23}. The modulus is influenced by thermal treatment or physical aging²¹. Yielding is considered the onset of plastic deformation, and the process is described as thermally activated²¹. A generalized yield criteria is proposed based on the Eyring flow model and von Mises criterion to predict the effects of stress states, strain rate, test temperature, crosslinker functionalities, and crosslink densities^{8,9}. The activation volume stays the same for all the controlled epoxy networks studied except for the most densely crosslinked. In contrast, the internal friction coefficient is insensitive to molecular structure and strain rate. The yield strength of aliphatic and aromatic epoxies with various crosslink

densities collapse together when normalized by the cohesive energy density (E_c), and plotted against test temperature normalized by T_g ^{12,13}. The correlation suggests that E_c and T_g are molecular parameters that govern yielding.

1.2 Background

The theoretical background of dynamic mechanical spectroscopy, compression testing, and fracture toughness are briefly highlighted in this section. The detailed experimental and data analysis procedures are provided in the next section. Since the same techniques are used throughout our investigations, the information will be referred to in subsequent chapters of this dissertation.

1.2.1 Dynamic Mechanical Spectroscopy

The glass or alpha transition of an amorphous polymer is characterized by significant change in viscosity and other physical properties²¹. With decreasing temperature, a polymer eventually reaches the glassy state, where the motion of its chains is much slower than the time scale of the experiment. Conversely, with increasing temperature, a polymer ultimately becomes free to explore all possible configurational states. Partly due to the dependence on cooling and heating rates, the transition is considered a kinetic process, instead of a true second-order thermal transition.

As discussed later in the fracture toughness section, the alpha transition temperature or T_g is strongly correlated with the toughness of polymers. T_g is dependent on stiffness of structural repeat unit, molecular weight, crosslink density, and intermolecular interaction²⁴.

The measured T_g values can vary among different characterization techniques due to different experimental time scales.

The beta transition is a secondary transition that occurs below the alpha transition, often at sub-ambient temperatures²¹. The transition is due to localized motion of small polymer chain segments. Such molecular rearrangements include the rotation of the side group about the bond linking it to the backbone, and rotation of main chain segments about the backbone bonds. For example, the beta transition of poly(methyl methacrylate) (PMMA) is attributed to intramolecular rotation of the ester group.

The low temperature secondary transition has also been associated with the toughness of polymers²¹. In the case of polycarbonate (PC), two neighboring carbonate units are thought to undergo trans-trans and tran-cis conformational interchange. This interchange propagates rapidly down the polymer chain, resulting in high energy dissipation.

Govaert and coworkers²⁵ have illustrated that, depending on the proximity of the test temperature to the alpha and beta transitions, the non-linear mechanical properties of amorphous thermoplastics would show two different slopes of temperature dependence. Changing strain rate has equivalent effects because of the principle of time-temperature-superposition. For example, the yield stress of PC is known to follow the prediction of Eyring model and exhibit a linear dependence on temperature and logarithmic strain rate. In marked contrast, the yield stress of PMMA shows an abrupt change in the slope of dependence at certain test conditions. The discrepancy is attributed to the difference in the locations of the beta transitions of the two polymers. While the beta transition of PC occurs far below room temperature, the beta transition of PMMA occurs at room temperature.

1.2.2 Compression Testing

Compression test is considered a better measure of intrinsic material properties than tension test, since geometric instabilities such as necking and crazing are suppressed^{26,27}. The toughness of amorphous glassy polymers has been associated with their ability to effectively de-localize strain, which is typically characterized by small strain softening and large strain hardening modulus. Strain softening is the difference between the yield stress and rejuvenated stress, which are the maximum and minimum of the stress-strain curve, respectively (Figure 1.1). The yield stress is related to network strength and stiffness¹³, and influenced by the thermomechanical history^{21,27}. Taking an amorphous glassy polymer beyond the rejuvenated stress is akin to heating above its glass transition temperature^{28,29}. The strain hardening modulus is related to network connectivity^{30,31}, and depends strongly on entanglement in thermoplastics and chemical crosslink in thermosets^{26,32,33}.

The evolution of yield stress, strain softening, rejuvenated stress, and strain hardening modulus during network formation has recently been reported for epoxies cured with ethylene diamine³². Systematic changes are also observed for epoxies cured with two miscible amines in different molar ratios¹⁶. However, it is unclear how these non-linear mechanical behavior are affected by more complex molecular structures or enhanced network heterogeneities.

1.2.3 Fracture Toughness

Fracture toughness is an important engineering property used to evaluate materials for structural applications^{20,34}. The testing measures the resistance of a material to crack initiation or fast crack growth. In this study, fracture toughness is the critical stress intensity

factor obtained under plane-strain condition in Mode I, or opening failure mode using compact tension geometry. Fracture resistance may also be characterized using energy release rate, or energy dissipation per unit area. Under small-scale yielding condition, the stress intensity factor and energy release rate can be interconverted.

Fracture toughness is sensitive to intrinsic material properties and changes in network structures, since the precrack acts as the largest flaw in the material³⁵. Depending on the combination of testing rate and temperature, a crack can propagate in a continuous or “stick-slip” manner^{36,37}. As the stress at the crack tip approaches and eventually exceeds the yield stress of a polymer, a process zone containing damages or inelastically deformed materials develops. The size of the process zone may be estimated using the ratio of fracture toughness to yield stress²⁰. A highly crosslinked epoxy tends to have high T_g and yield stress but low toughness. The reason is that its small process zone can only provide limited energy dissipation^{20,34,38}.

1.3 Main Characterization Techniques

1.3.1 Dynamic Mechanical Analysis

Dynamic mechanical analysis was conducted either on DMA Q800 (TA Instruments) in tension film mode or DMA 2980 (TA Instruments) in single cantilever mode at 0.1% strain with a single frequency of 1 Hz and heating rate of 3 °C/min. Instead of tan delta-temperature curves, the loss modulus-temperature curves are presented in Chapter 2 through 4 because they provide better visualization of the beta transitions of epoxies. The T_g values were taken as the maxima of the loss moduli (E''). The full width at half maximum (FWHM) was calculated from E'' in the alpha transition region with the

limits taken as the minimum between the beta and alpha transitions, and the peak value of the alpha transition.

1.3.2 Compression Testing

Uniaxial compression test was performed on an Instron 5800 universal tester at 20 °C and a constant strain rate of 1 min⁻¹. Cylindrical bullets (Diameter ~ 11.3 mm) with 1:1 height-to-diameter ratio were machined. Soapy water and thin PTFE films were used for lubricating the ends of the specimens. The strain hardening modulus (G_R) was computed at 90% of the ultimate true strain using the following equation:

$$G_R = \frac{\partial \sigma_t}{\partial (\lambda^2 - 1/\lambda)} \quad (1.1)$$

where σ_t is the true stress, $\lambda^2 - 1/\lambda$ is the Neo-hookian strain, and λ is the compression ratio.

1.3.3 Fracture Toughness

Fracture toughness measurements were made with 3 mm thick miniature compact tension (mini-CT) specimens with 20 mm width following ASTM standard D5045-99. The use of mini-CT specimens for testing glassy polymers had been reported by Jones and Lee³⁵, and Hinkley³⁹. The thickness satisfied the requirement for achieving plane-strain condition across the crack front, namely $B \geq 2.5 (K_q/\sigma_y)^2$, where K_q is the measured fracture toughness and σ_y is the yield stress estimated from the compression data. The pre-notches were introduced with a diamond wafering blade. After conditioning the samples at -10°C for an hour, a sharp precrack was generated on each specimen by inserting a fresh razor blade into the pre-notch and tapping lightly with a hammer. Load-displacement curves

were recorded by Instron 4411 at a crosshead speed of 0.5 mm/min and 20 °C. Fracture toughness (K_q) was computed using the following equation:

$$K_q = \frac{P_c f(x)}{BW^{1/2}} \quad (1.2)$$

where P_c is the critical load in kilonewton (kN), B is the specimen thickness in centimeter (cm), W is specimen width in cm, and K_q is in $\text{MPa}\cdot\text{m}^{1/2}$. The use of K_q instead of K_{IC} denotes the use of a mini-CT specimen. The geometric factor $f(x)$ is a dimensionless power function in terms of x , which is equal to a/W , or the ratio of the precrack length to specimen width.

$$f(x) = \frac{(2+x)(0.886 + 4.64x - 13.32x^2 + 14.72x^3 - 5.6x^4)}{(1-x)^{3/2}} \quad (1.3)$$

All mini-CT specimens in this study failed in a brittle fashion, thus the maxima in load-deflection curves were taken as the critical loads in calculating fracture toughness. Each reported fracture toughness value was an average of 4 to 8 measurements.

1.4 Dissertation Overview

In Chapter 2, we report the synthesis and characterization of Topologically Heterogeneous Network (THN) epoxies. In homologous curative approach, a THN epoxy was prepared from amine curatives with different molecular weights but the same structure repeat unit. The resulting material contains both stiff and flexible chain segments, as well as polydisperse crosslink density. Compared to control sample with the same average crosslink density, the THN resin shows broadened glass transition, and bifurcated dynamic mechanical transition. It exhibits identical post-yield behavior as the control sample, suggesting that the non-linear properties are dictated by network connectivity. In

multifunctional prepolymer approach, a rigid multifunctional prepolymer is first prepared from a stiff tetrafunctional epoxide and difunctional amine at off-stoichiometric ratio. It is then reacted with a flexible tetrafunctional amine, or a combination of the flexible amine and a diepoxide to produce ultimate THN epoxies with regions of varying stiffness and crosslink density. The crosslink density estimated from stoichiometry correlates well with experimental values. Broadening of the beta and alpha transitions suggests enhanced segmental mobility and is attributed to chemical heterogeneities in stiffness and crosslink density. The 70% decrease in strain softening and two-fold increase in strain hardening modulus indicate that the materials have improved strain localization response or reduced propensity for premature failure. A THN resin with relatively high toughness and T_g is obtained.

In Chapter 3, we present the synthesis and characterization of Prestressed Double Network epoxies. The preparation involves a judicious selection of miscible aliphatic and aromatic curing agents to generate materials with constant crosslink density but different stiffness over the composition range. The non-overlapping reaction kinetics of the amine crosslinkers provide a model system for imparting compressive prestress to the partially cured resin, which contains unreacted aromatic curing agent. The second network is then introduced while the first is deformed by 50% compressive strain. Drastic dimensional change of the unrelaxed glass during the glass transition is related to strong release of the imposed latent free energy. However, the glassy and rubbery coefficients of thermal expansion are unaffected by prestressing. Systematic changes in the width of alpha transition is attributed to the chemical heterogeneity in stiffness and mechanical heterogeneity in baseline energy states. About 30% increase in fracture toughness is

achieved without changing glass transition temperature (T_g), or elastic modulus. The enhancement is associated with the combination of opening and in-plane shear failure modes.

In Chapter 4, we describe the synthesis and characterization of Asymmetric Double Network epoxies. We also investigate the effects of hydrogen bonding, and combining the fabrication strategies discussed in previous chapters. The major constituent of the asymmetric resins is a lightly crosslinked aliphatic network, and the minor component a highly crosslinked aromatic network. The asymmetric stiffness or chemical heterogeneity does not alter the breadth of the dynamic mechanical transitions but generates stronger and more ductile epoxies. Instead of brittle failure, the materials show yielding and onset of necking when tested in tension. Fracture toughness in certain case is comparable to prestressed resin in Chapter 3. The asymmetric epoxy can be prestressed by 70% compressive strain. The toughness increases further, but the relative improvement stays the same or around 30%. A formulation incorporating a chain-extended prepolymer also shows enhancement in fracture toughness despite its relatively high T_g .

In Chapter 5, we propose the use of two ductility parameters to correlate with non-linear mechanical performance. The first is based on dynamic mechanical analysis, and utilizes a weighted integral approach to quantify the effects of chemical and mechanical heterogeneities on segmental mobility. The second is based on compression testing, and incorporates the effect of chemical heterogeneity on strain localization and extensibility. We also demonstrate that the rejuvenated stress and strain hardening modulus are governed by the glass transition temperature and cohesive energy density.

1.5 References

1. Lee, H., and Neville, K., Handbook of Epoxy Resins. McGraw-Hill, New York, (1967).
2. Wang, X. R., and Gillham, J. K., J Appl Polym Sci, 47, 425-446 (1993).
3. deNograro, F. F., Guerrero, P., Corcuera, M. A., and Mondragon, I., J Appl Polym Sci, 56, 177-192 (1995).
4. Ma, J., Mo, M. S., Du, X. S., Rosso, P., Friedrich, K., and Kuan, H. C., Polymer, 49, 3510-3523 (2008).
5. Laiarinandrasana, L., Fu, Y., and Halary, J. L., J Appl Polym Sci, 123, 3437-3447 (2012).
6. deNograro, F. F., LlanoPonte, R., and Mondragon, I., Polymer, 37, 1589-1600 (1996).
7. Pfaff, F. A. Mechanical Relaxation Effects in Amine Cured Epoxies. In: SPI Epoxy Resin Formulators Conference, New Orleans, LA, Nov. 3-5 1996.
8. Kody, R. S., and Lesser, A. J., J Mater Sci, 32, 5637-5643 (1997).
9. Lesser, A. J., and Kody, R. S., J Polym Sci Pt B-Polym Phys, 35, 1611-1619 (1997).
10. Crawford, E., and Lesser, A. J., J Polym Sci Pt B-Polym Phys, 36, 1371-1382 (1998).
11. Tan, N. C. B., Bauer, B. J., Plestil, J., Barnes, J. D., Liu, D., Matejka, L., Dusek, K., and Wu, W. L., Polymer, 40, 4603-4614 (1999).
12. Lesser, A. J., and Calzia, K. J., J Polym Sci Pt B-Polym Phys, 42, 2050-2056 (2004).
13. Calzia, K. J., and Lesser, A. J., J Mater Sci, 42, 5229-5238 (2007).
14. Lahlali, D., Naffakh, M., and Dumon, M., Polym Eng Sci, 45, 1581-1589 (2005).
15. Yang, G., Fu, S. Y., and Yang, J. P., Polymer, 48, 302-310 (2007).
16. Detwiler, A. T., and Lesser, A. J., J Mater Sci, 47, 3493-3503 (2012).
17. McAninch, I. M., Palmese, G. R., Lenhart, J. L., and La Scala, J. J., J Appl Polym Sci, (2013).

18. Bonnaud, L., Pascault, J. P., and Sautereau, H., *Eur Polym J*, 36, 1313-1321 (2000).
19. Park, S. J., and Lee, J. R., *J Mater Sci Lett*, 20, 773-775 (2001).
20. Kinloch, A. J., and Young, R. J., *Fracture Behaviour of Polymers*. Applied Science Publishers, Northern Ireland, (1983).
21. Haward, R. N. (ed) *The Physics of Glassy Polymers*. 2nd edn. Chapman & Hall, London, (1997).
22. Flory, P. J., *Principles of Polymer Chemistry*. Cornell University Press, Ithaca, (1953).
23. Nielsen, L. E., Landel, R. F., *Mechanical properties of polymers and composites*. 2nd edn. Marcel Dekker, New York, (1994).
24. Shaw, M. T., MacKnight, W. J., *Introduction to polymer viscoelasticity*. 3rd edn. John Wiley & Sons, Hoboken, (2005).
25. van Breemen, L. C. A., Engels, T. A. P., Klompen, E. T. J., Senden, D. J. A., and Govaert, L. E., *J Polym Sci Pt B-Polym Phys*, 50, 1757-1771 (2012).
26. van Melick, H. G. H., Govaert, L. E., and Meijer, H. E. H., *Polymer*, 44, 2493-2502 (2003).
27. van Melick, H. G. H., Govaert, L. E., and Meijer, H. E. H., *Polymer*, 44, 3579-3591 (2003).
28. Govaert, L. E., van Melick, H. G. H., and Meijer, H. E. H., *Polymer*, 42, 1271-1274 (2001).
29. Kierkels, J. T. A., Dona, C.-L., Tervoort, T. A., Govaert, L. E., *J Polym Sci B Polym Phys*, 46, 134-147 (2008).
30. Haward, R. N., and Thackray, G., *Proc R Soc A*, 302, (1968).
31. Haward, R. N., *Polymer*, 28, 1485-1488 (1987).

32. Detwiler, A. T., and Lesser, A. J., *J Appl Polym Sci*, 117, 1021-1034 (2010).
33. Hoy, R. S., and Robbins, M. O., *J Polym Sci Pt B-Polym Phys*, 44, 3487-3500 (2006).
34. Kanninen, M. F., and Popelar, C. H., *Advanced fracture mechanics*. Oxford University Press, New York, (1985).
35. Lee, C. Y. C., and Jones, W. B., *Polym Eng Sci*, 22, 1190-1198 (1982).
36. Yamini, S., and Young, R. J., *Polymer*, 18, 1075-1080 (1977).
37. Kinloch, A. J., Shaw, S. J., Tod, D. A., and Hunston, D. L., *Polymer*, 24, 1341-1354 (1983).
38. Crawford, E. D., and Lesser, A. J., *Polym Eng Sci*, 39, 385-392 (1999).
39. Hinkley, J. A., *J Appl Polym Sci*, 32, 5653-5655 (1986).

CHAPTER 2

**PREPARATION AND CHARACTERIZATION OF TOPOLOGICALLY
HETEROGENEOUS NETWORK EPOXIES**

2.1 Introduction

The aim of this research is to investigate the effect of chemical heterogeneity or topological differences in stiffness and crosslink density on the physical characteristics of epoxies. As discussed in Chapter 1, an epoxy is usually prepared by reacting a single epoxide monomer with a single amine curing agent¹⁻⁵. Few researchers studied miscible blends of amines^{6,10,11,14-16}, or epoxides^{18,19}. Furthermore, there is no previous work on complex formulations containing mixtures of epoxides and amines with varying stiffness and functionalities.

Chemical heterogeneity can include polydispersity in crosslink density and variation in backbone stiffness. Detwiler and Lesser¹⁶ studied Double Network epoxies with constant crosslink density but varying stiffness. They employed aliphatic and aromatic amines with the same functionality and similar molecular weights. The epoxies appear homogeneous on the macroscopic scale, since a single glass transition is detected for each resin. However, dynamic mechanical analysis reveals network heterogeneity on the molecular scale. The widths of the glass or alpha transitions are narrowest for resins cured with a single amine, and increase toward intermediate compositions for Double Networks. The physical properties of the resins are tunable over the entire composition range. For example, the strain localization response or propensity for premature brittle failure can be systematically varied by adjusting the molar ratio of the two curatives.

Topologically Heterogeneous Network (THN) epoxies with varying stiffness and crosslink densities may be prepared by blending amine curing agents with different molecular weights but the same backbone repeat unit. In addition to stiff and flexible chain segments, the resulting materials have highly polydisperse crosslink density. However, such networks can be designed to provide the same average crosslink density as a resin cured with a single amine.

THN epoxies may also be synthesized via the use of a multifunctional prepolymer. For example, a stiff tetrafunctional epoxide may be reacted with a short difunctional amine in 2:1 or off-stoichiometric ratio to obtain a viscous liquid containing a variety of potential structures [Figure 2.1(a)]. A linear dimer with 6 residual epoxide functionalities is the most probable reaction product. However, other species such as the cyclic dimer and linear trimer are also expected to form.

In the second step, a flexible tetrafunctional amine may be added to the viscous liquid to produce a resin with regions of high stiffness and crosslink density together with regions of lower stiffness and crosslink density [Figure 2.1(b)]. A diepoxide may be incorporated to further enhance the molecular heterogeneity. As seen in Figure 2.1(c), the ultimate network consists of a stiff tetrafunctional epoxide, rigid difunctional amine, flexible tetrafunctional amine, and soft diepoxide. The resulting materials are expected to have more composite-like behavior.

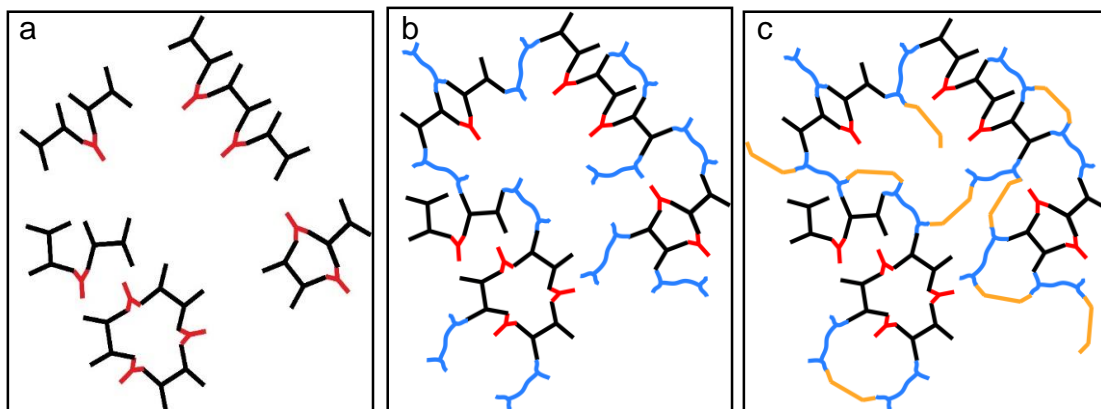


Figure 2.1 (a) Structurally diverse THN prepolymer. Colored segments: black, stiff tetrafunctional epoxide; and red, rigid difunctional amine. (b) THN prepolymer reacted with flexible tetrafunctional amine (blue segments), (c) THN prepolymer reacted with flexible tetrafunctional amine (blue segments) and soft difunctional epoxide (orange segments).

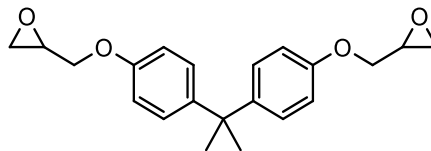
2.2 Experimental

2.2.1 Materials

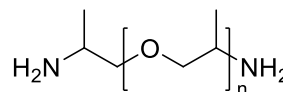
Diglycidyl ether of bisphenol A (DGEBA, DER 332, Epoxide equivalent weight: 171-175 g/eq, $n \sim 0.03$) was purchased from Dow Chemical. Polyetheramines (Jeffamine D230, MW ~ 240 g/mol; D400, MW ~ 450 g/mol; and D2000, MW ~ 2000 g/mol) as well as N,N,N',N'-Tetraglycidyl-4,4'-methylenebisbenzeneamine (TGDDM, Araldite 721, Epoxide equivalent weight: 109-116 g/eq, $n \sim 0.07$) were courtesy of Huntsman. Aniline (MW: 93 g/mol) was purchased from Acros Organic. The structures of the chemicals are given in Table 2.1.

Table 2.1 Chemical structures of epoxide monomers and amines

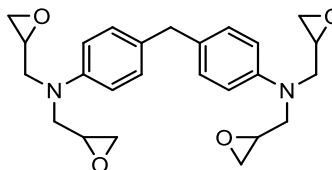
Diglycidyl ether of bisphenol A
(DGEBA, DER, $n \sim 0.03$)



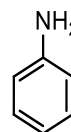
Polyetheramine
(D230, $n \sim 2.5$; D400, $n \sim 6.1$;
D2000, $n \sim 33$)



N,N,N',N'-Tetraglycidyl-4,4'-
methylenebisbenzeneamine
(TGDDM)



Aniline



2.2.2 Network Formation

2.2.2.1 Homologous Curatives Approach

DGEBA-D230-D2000 8.9-1.1 and DGEBA-D400 were cured at 80 °C for 3 h, and 120 °C for 3 h. The select ratio of D230 and D2000 yields a Topologically Heterogeneous Network (THN) epoxy with the same average crosslink density as DGEBA-D400, which is a control sample based on a single curing agent.

2.2.2.2 Multifunctional Prepolymer Approach

The multifunctional prepolymer for THN epoxies was synthesized by reacting 2 molar equivalent of TGDDM with aniline at 80 °C for 1 h, and 100 °C for 3 h. It was then mixed with either stoichiometric amount of D230 (TGDDM-Aniline-D230), *or* 2) one

molar equivalent of DGEBA and stoichiometric amount of D230 (TGDDM-Aniline-DGEBA-D230). They were cured at 80 °C for 3 h, 160 °C for 3 h, and 200 °C for 1 h.

For the control samples, TGDDM was mixed with stoichiometric amount of aniline (TGDDM-Aniline), and cured using the same schedule as THN epoxies. DGEBA and TGDDM were also separately mixed with stoichiometric amount of D230. These networks were first cured at 80 °C for 3 h, then postcured for 3 h at 120 °C (DGEBA-D230) or 160 °C (TGDDM-D230).

2.2.3 Characterization

2.2.3.1 Differential Scanning Calorimetry

Differential scanning calorimetry was conducted on DSC Q200 (TA Instruments) with a heating rate of 10 °C/min under nitrogen purge. The sample was sealed in an aluminum hermetic pan. The glass transition temperature (T_g) was taken as the inflection point of the thermogram.

2.2.3.2 Dynamical Mechanical Analysis

Tension film specimens were tested on DMA Q800 (TA Instruments). The detailed testing procedures, T_g assignments, and FWHM calculations are given in Chapter 1.

2.2.3.3 Compression Testing

Uniaxial compression testing was carried out as described in Chapter 1.

2.2.3.4 Fracture Toughness

Fracture toughness measurements were performed as described in Chapter 1.

2.2.3.5 Thermogravimetric Analysis

Thermogravimetric study was carried out on TGA Q500 (TA Instruments) at a heating rate of 10 °C/min under nitrogen purge. The decomposition temperature (T_d) was taken as the inflection point of the thermogram. The residue was the percentage of the original sample weight remaining at the end of the test.

2.3 Results and Discussion

2.3.1 Homologous Curatives Approach

2.3.1.1 Crosslink Density from Stoichiometry

Based on stoichiometry of the reagents, M_c for amine-cured epoxy is given by⁴⁰

$$M_c = \frac{2(M_e + \sum_{x=2}^{\infty} \frac{M_x}{x} \Phi_x)}{\sum_{x=3}^{\infty} \Phi_x} \quad (2.1)$$

where M_e is the epoxy equivalent weight of the epoxide monomer, x is the functionality of the amine, M_x is the molecular weight of the amine having x functionality, and Φ_x is the molar fraction of amine hydrogens from x -functional amine. The key assumptions for Equation 2.1 are one-to-one stoichiometry between epoxide and amine hydrogen and full conversion of the reagents at the end of cure.

The three curing agents, D230, D400, and D2000, have the same end groups but different numbers of the polypropylether repeat units as their backbones (Table 2.1). The control sample DGEBA-D400 has a M_c of 565 g/mol. The Topologically Heterogeneous

Network (THN) epoxy DGEBA-D230-D2000 8.9-1.1 has the same average M_c . However, the THN resin cured with homologous amines is expected to have a much broader M_c distribution. The D2000 segment is about 10 times longer than D230 and more flexible.

2.3.1.2 Differential Scanning Calorimetry

Despite having the same average crosslink density, DGEBA-D230-D2000 8.9-1.1 has higher T_g than DGEBA-D400 (Figure 2.2). The width of its glass transition is also broader. The reason for the discrepancies is that the THN epoxy has much larger variations in crosslink density and stiffness than the control sample cured with a single amine.

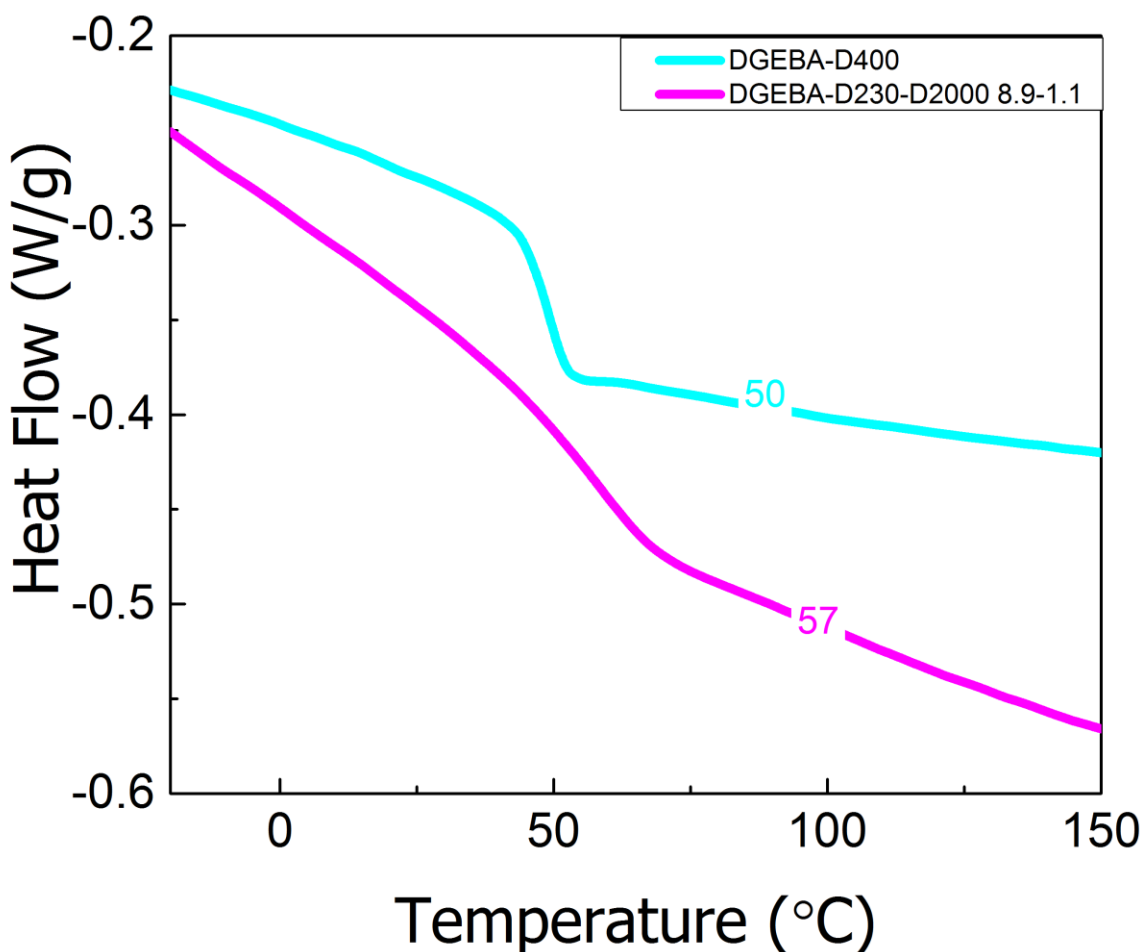


Figure 2.2 DSC thermograms of DGEBA-D400 and DGEBA-D230-D2000 8.9-1.1. The numbers on the curves are glass transition temperatures of the epoxies.

2.3.1.3 Dynamic Mechanical Analysis

The storage and loss moduli of DGEBA-D400 and DGEBA-D230-D2000 8.9-1.1 are plotted in Figure 2.3(a) and 2.3(b), respectively. The storage modulus exhibits a pronounced drop over several magnitudes at the glass or alpha transition. This drop also manifests itself as a highly stretched peak in the loss modulus. DGEBA-D400 has a rather sharp alpha transition at around 60 °C. In marked contrast, DGEBA-D230-D2000 8.9-1.1 has an earlier onset around 0 °C but more gradual and broader alpha transition. Unlike the DSC measurements discussed earlier, however, the THN epoxy appears to have a lower T_g than the control sample when tested on the DMA [Figure 2.3(a)]. This discrepancy is probably due to its much stretched alpha transition. The apparent increase in the T_g value of DGEBA-D400 measured on DMA over DSC is due to different experimental time scale²⁴.

As shown in Figure 2.3(a), the storage modulus of DGEBA-D230-D2000 8.9-1.1 is higher than DGEBA-D400 at sub-zero temperature. However, the trend is reversed at higher temperature due to earlier intervention of the much broader alpha transition of the THN epoxy. Compared to DGEBA-D400, the alpha transition of DGEBA-D230-D2000 8.9-1.1 are three times as broad [Figure 2.3(b)]. This increased width is due to the high polydispersity in crosslink density and variation in stiffness within the THN epoxy. Furthermore, the beta transition of the THN epoxy appears bifurcated [inset of Figure 2.3(b)]. The result is another indication of enhanced network heterogeneity on the molecular scale.

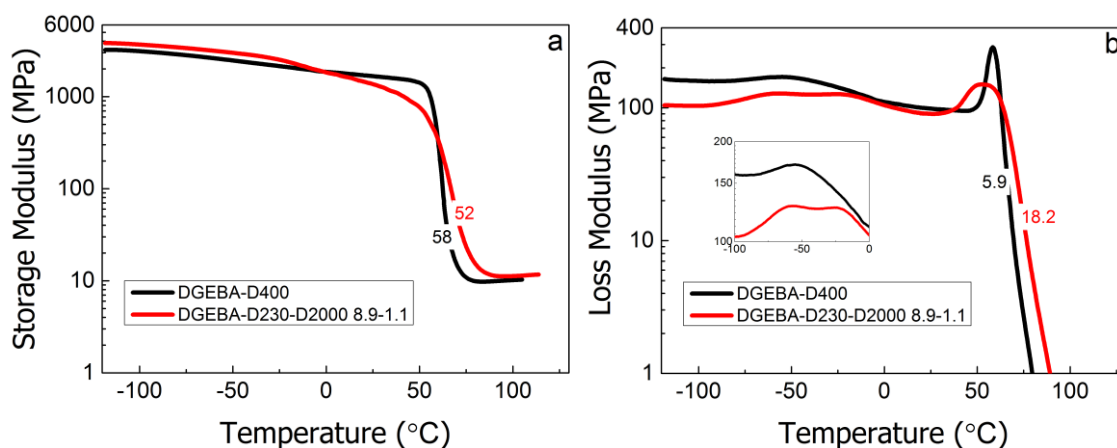


Figure 2.3 Dynamic mechanical spectra of DGEBA-D400 and DGEBA-D230-D2000 8.9-1.1. (a) Storage moduli labeled with glass transition temperatures, (b) Loss moduli labeled with full width at half maximum (FWHM) of alpha transitions.

2.3.1.4 Compressive Behavior

The stress-strain curves of DGEBA-D400 and DGEBA-D230-D2000 8.9-1.1 tested in compression are plotted in Figure 2.4, and the compressive properties are listed in Table 2.2. As discussed in the DMA section, the THN epoxy has lower elastic modulus than the control sample because its molecular heterogeneity results in much earlier and broader glass transition. Despite its higher T_g measured on DSC, DGEBA-D230-D2000 8.9-1.1 has lower yield stress than DGEBA-D400. Its slower aging kinetics appear to retard the densification process that increases the yield stress²¹. However, the two resins exhibit almost the same post-yield response. In agreement with previous work^{26,30-33}, the result suggests that the large strain behavior like strain hardening is dictated primarily by the network connectivity. Little effects of varying stiffness and crosslink density are observed.

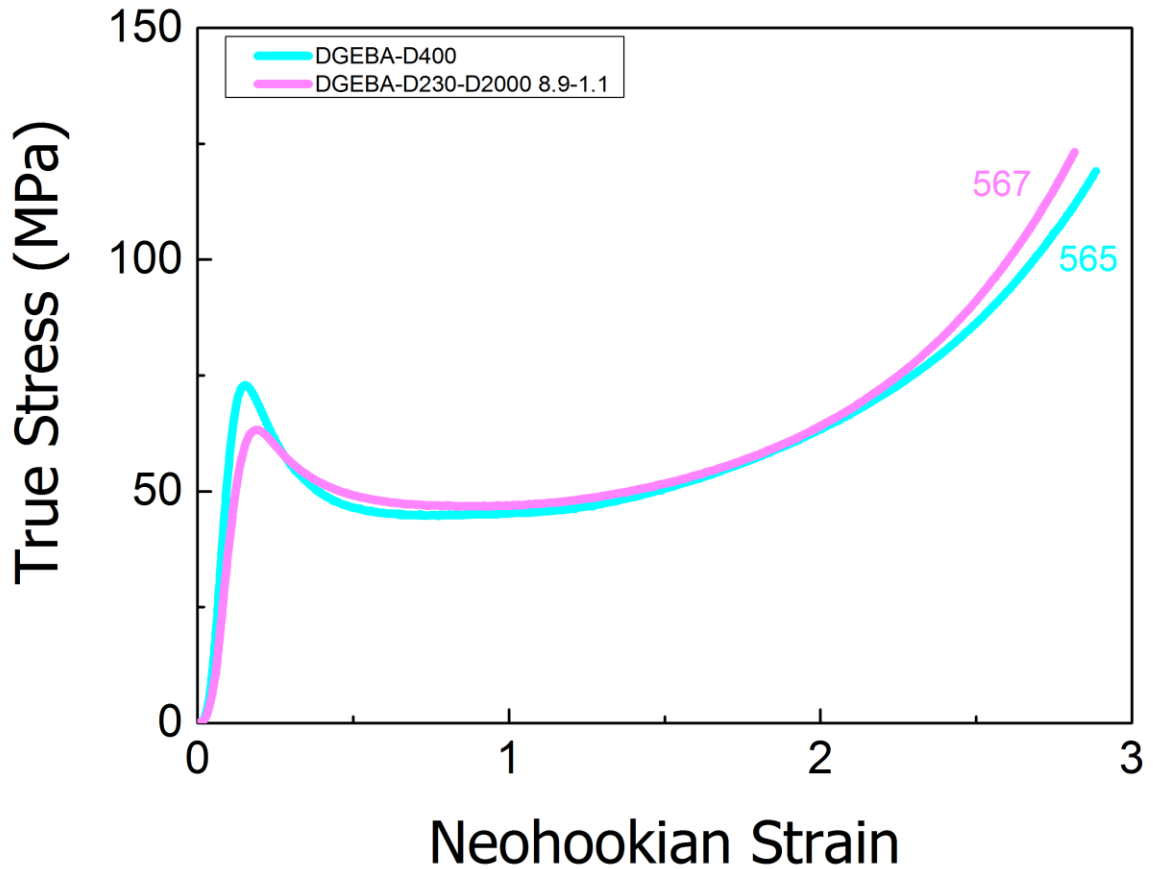


Figure 2.4 Stress-strain curves of DGEBA-D400 and DGEBA-D230-D2000 8.9-1.1 tested in compression.

2.3.1.5 Fracture Toughness

As listed in Table 2.2, the THN epoxy DGEBA-D230-D2000 8.9-1.1 appears to have lower average fracture toughness than DGEBA-D400. However, the comparison is complicated by the large standard deviation of the control sample. The data scattering may be reduced further through the use of additional test specimens.

Table 2.2 Mechanical Properties of the Epoxies

Resin	Compression					Fracture Toughness
	E (GPa)	σ_y (MPa)	σ_r (MPa)	$\sigma_y - \sigma_r$ (MPa)	G_R (MPa)	K_q (MPa·m ^{0.5})
DGEBA-D400	2.68	73	45	28	76	1.20 ± 0.57
DGEBA-D230-D2000 8.9-1.1	2.04	64	47	17	90	0.85 ± 0.19

2.3.2 Multifunctional Prepolymer Approach

2.3.2.1 Crosslink Density from Stoichiometry

In this study, the difunctional epoxide and amine act as chain extenders, while the tetrafunctional reagents are the crosslinkers for network formation. In Figure 2.5, the average crosslink density ($1/M_c$) is estimated using Equation 2.1, and plotted together with volumetric density measured using water displacement method (ASTM D792).

DGEBA-D230 and TGDDM-Aniline are the most lightly and heavily crosslinked resin, respectively. As expected, the two Topologically Heterogeneous Network (THN) epoxies, TGDDM-Aniline-D230 and TGDDM-Aniline-DGEBA-D230 have intermediate crosslink densities. The volumetric density increases with increasing crosslink density. This is an expected result since the additional crosslinks reduce free volume of the polymer^{23,24}. As discussed in later sections, the crosslink density estimated from stoichiometry agree well with experimental values.

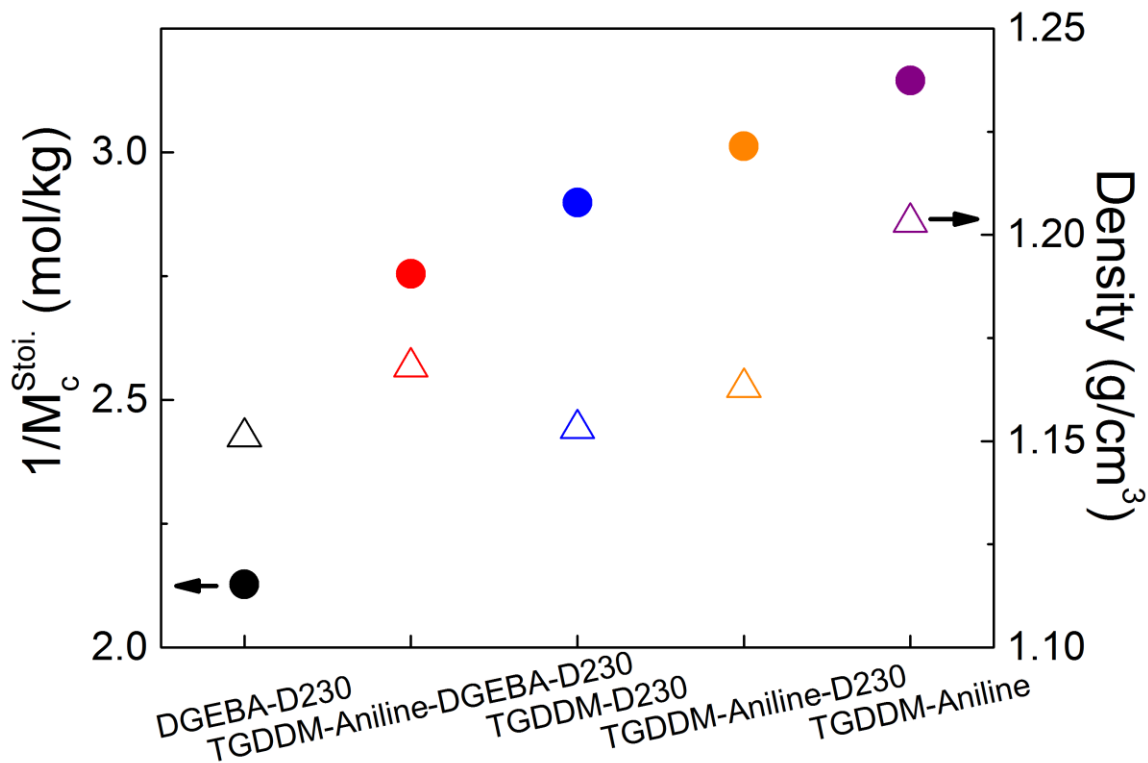


Figure 2.5 Crosslink densities (solid circles), and volumetric densities (unfilled triangles) of epoxies.

2.3.2.2 Dynamic Mechanical Properties

Plotted in Figure 2.6(a) and Figure 2.6(b) are the storage and loss moduli of the epoxies, respectively. Only a single glass transition is detected for each sample. This result indicates that the molecular heterogeneity is not sufficient to generate macroscopically phase separated materials. The T_g values of the epoxies increase with increasing crosslink density due to additional restriction on the motion of the polymer chains [Figure 2.6(a)].

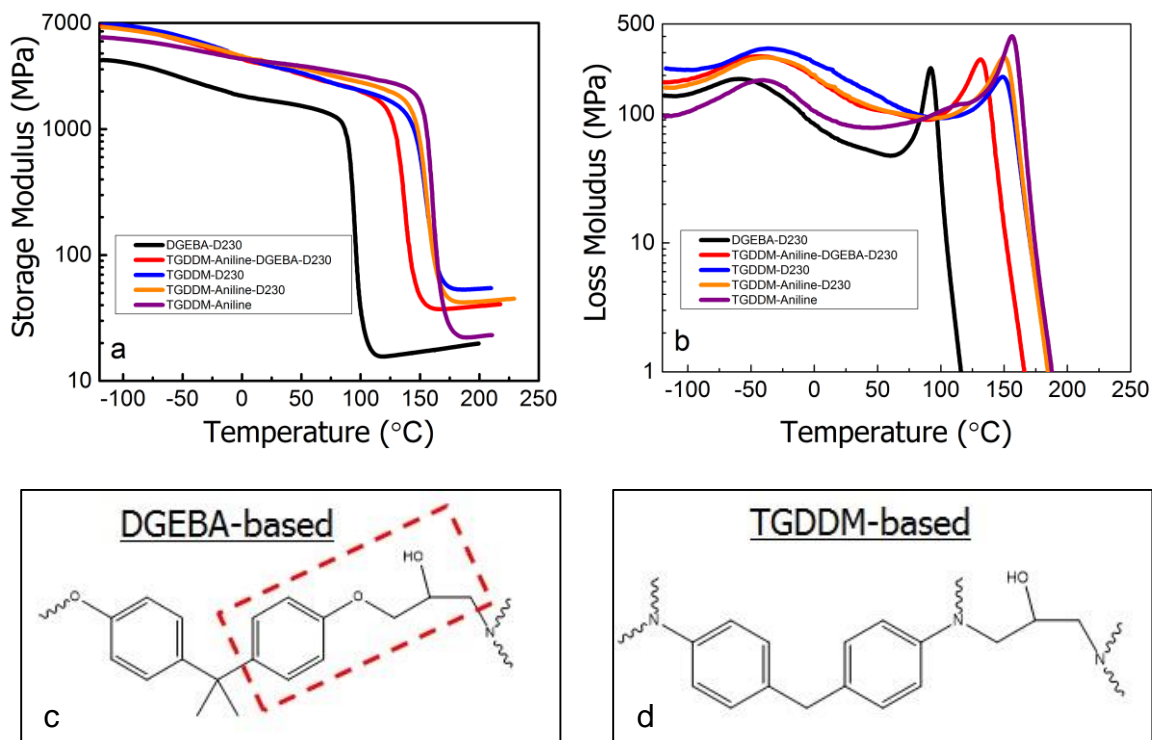


Figure 2.6 (a) Storage moduli and (b) Loss moduli of epoxies. (c) Network repeat segment of DGEBA-based resin with hydroxylpropylether unit and phenyl group highlighted. (d) Network repeat segment of TGDDM-based resin.

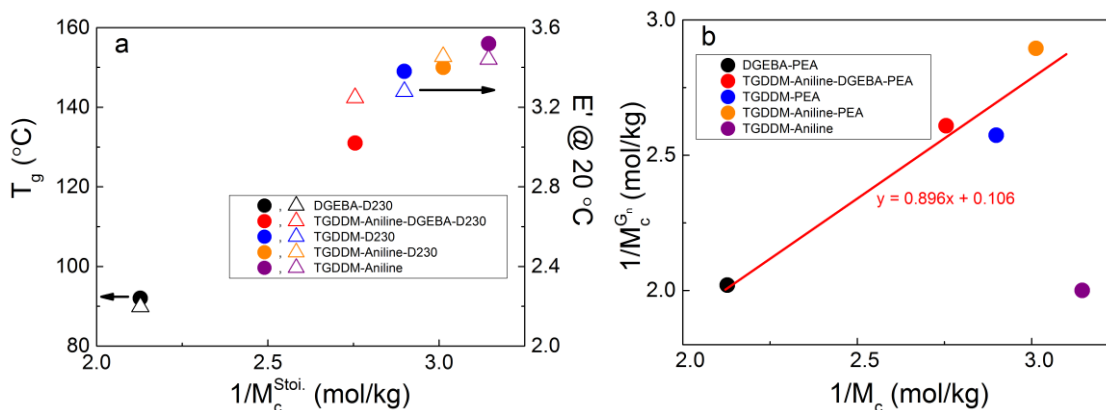


Figure 2.7 (a) Glass transition temperature (solid circle) and storage moduli (unfilled triangle). (b) Comparison between crosslink densities obtained from rubbery plateau moduli, and stoichiometry.

As shown in Figure 2.7(a), at room temperature or 20 °C, the TGDDM-based epoxies are about 1 GPa stiffer than DGEBA-D230. At lower temperatures, however, the

occurrence of beta transition complicates the moduli comparison [Figure 2.6(a)]. After the glass transition, the storage modulus increases linearly with increasing temperature in the rubber plateau regime. The behavior is typical of chemically crosslinked polymers tested on DMA²². The molecular weight between crosslinks ($M_c^{G_n}$) is related to the rubbery plateau modulus (G_n) by

$$M_c^{G_n} = \frac{\rho_r RT}{G_n} \quad (2.2)$$

where $G_n = E'/3$, E' is the storage modulus, ρ_r is the density in rubbery state, R is the gas constant, and T is temperature in absolute Kelvin. Although tightly crosslinked epoxies are expected to deviate from ideality due to non-Gaussian chain conformation⁴¹, good qualitative agreement has been obtained^{10,16}.

The crosslink densities from rubbery plateau moduli are estimated using volumetric densities at room temperature, and plotted against those from stoichiometry in Figure 2.7(b). A linear trend is observed among the epoxies except for TGDDM-Aniline. The T_g and storage modulus measurements in Figure 2.7(a) suggest that TGDDM-Aniline has reached high conversion. However, the deviation from linearity in Figure 2.7(b) indicates that this control sample is not fully cured even at 200 °C. Assuming that complete conversion could be theoretically attained by following the trend line shown in the figure, with steric hindrance the degree of cure for TGDDM-Aniline is limited to 68%. The topological constraints imposed by the rigid constituents impede the diffusion and further reaction of residual functionalities of TGDDM and aniline at the final postcure temperature.

In Figure 2.6(b), distinct differences in the beta and alpha transitions are observed among the epoxies. The beta transition of DGEBA-D230 occurred at around -60 °C. The result is in agreement with the recent work of Monnerie and coworkers⁴², who attributed

the appearance of beta transition of DGEBA-based epoxies to the localized and cooperative motions of the network repeat units, including the hydroxypropylether segment and the phenyl ring [Figure 2.6(c)]. In marked contrast, TGDDM-Aniline exhibits a higher beta transition near $-40\text{ }^{\circ}\text{C}$, probably because it has different network connectivity [Figure 2.6(d)]. The shape of its beta transition also appears more symmetric, with smaller drop in loss modulus when approaching the alpha transition. Furthermore, the apparent overlap between the beta and alpha transitions is more pronounced for DGEBA-D230 than TGDDM-Aniline. The THN epoxies showed much broader beta transitions near $-40\text{ }^{\circ}\text{C}$, which extend farther beyond room temperature and overlap slightly with their alpha or glass transitions. This result is expected from their enhanced chemical heterogeneity. However, the broad beta transition of the neat resin TGDDM-D230 seems to be an exception.

Shown in Figure 2.8(a) are the normalized alpha transitions of the epoxies. The loss moduli are normalized with respect to the peak maxima and the temperatures shifted by T_g 's. The alpha transitions are highly asymmetric. They are broader on the low temperature side or glassy regime of the transition and narrower on the high temperature side or rubbery regime. The alpha transition is a manifestation of large-scale cooperative motion of polymer chains²⁴. Its breadth can therefore be considered a measure of mobility of network segments.

The full width at half maximum (FWHM) of the transitions are plotted against $1/M_c$ in Figure 2.8(b). The neat resins DGEBA-D230 and TGDDM-Aniline show the narrowest width. In contrast, the THN epoxies have much broader transitions. Topological difference in stiffness and crosslink density are considered responsible for the increased width.

TGDDM-D230 again appears to be the exception. The reason for this discrepancy may be that TGDDM-based resins have broader transitions than DGEBA-based resins when cured using a tetrafunctional amine. However, further work is needed to confirm the hypothesis.

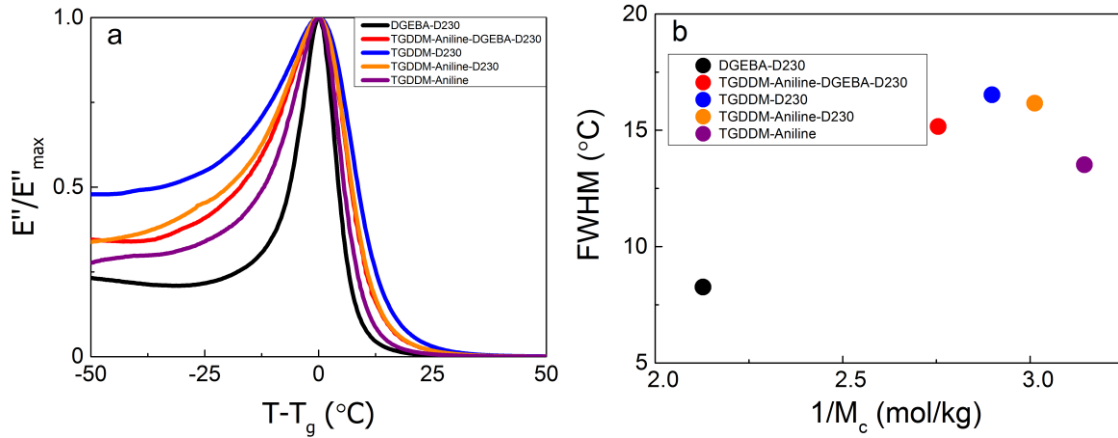


Figure 2.8 (a) Normalized alpha transitions, (b) Corresponding full widths at half maximum (FWHM) of the transitions.

The increases in the widths of both beta and alpha transitions are indicative of enhanced mobility of the network segments. Despite their relatively high T_g 's, the THN resins show higher propensity for microstructural rearrangement in the glassy state. As discussed in the next section, this can facilitate energy dissipation during mechanical deformation, and result in tougher resins.

2.3.2.3 Compressive Behavior

Shown in Figure 2.9(a) are the stress-strain curves of the epoxies. As listed in Table 2.3, the Young's modulus (E), yield stress (σ_y), rejuvenated stress (σ_r), strain softening ($\sigma_y - \sigma_r$), and strain hardening modulus (G_R) generally scale with $1/M_c$. However, marked differences in strain localization responses are observed among the resins. In Figure 2.9(a), DGEBA-D230 is the most ductile resin, as expected from its flexible constituents. In

contrast, TGDDM-Aniline has a large post-yield stress drop, and fails before significant strain hardening can take place. For the THN epoxies, however, the incorporation of flexible diepoxide and diamine reduces the extent of stress softening by nearly 70% from that of TGDDM-Aniline (Table 2.3). At the same time, their strain hardening moduli are about twice as large as that of TGDDM-Aniline. These results suggest that the THN epoxies are less prone to premature brittle failure.

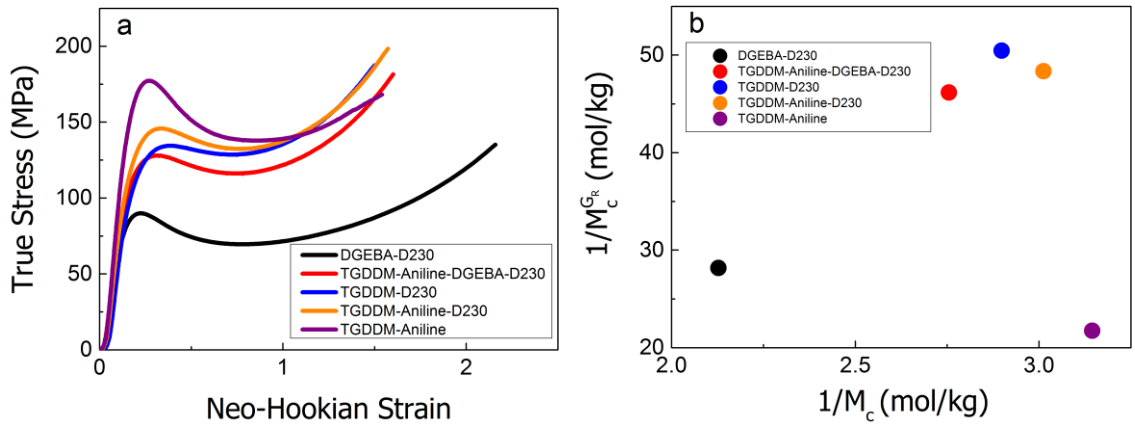


Figure 2.9 (a) Stress-strain curves of THN epoxies and control samples tested in compression, (b) Comparison of crosslink densities obtained from strain hardening moduli and stoichiometry.

Table 2.3 Physical properties of the epoxies.

Resin	$1/M_c$ (mol/kg)	E (GPa)	σ_y (MPa)	σ_r (MPa)	$\sigma_y - \sigma_r$ (MPa)	G_R (MPa)
DGEBA-D230	2.13	2.90	89	70	19	79
TGDDM-Aniline-DGEBA-D230	2.75	3.13	128	116	12	131
TGDDM-D230	2.90	3.18	135	130	5	142
TGDDM-Aniline-D230	3.01	3.35	145	132	13	137
TGDDM-Aniline	3.14	3.78	177	136	41	64

Another measure of molecular weight between crosslinks (M_c^{Gr}) has been calculated from strain hardening modulus (G_R) using the following equation^{26,32}

$$M_c^{G_r} = \frac{\rho_g RT}{G_R} \quad (2.3)$$

It has the same form as Equation 2.2 except that ρ_g is the volumetric density at room temperature. As shown in Figure 2.9(b), the crosslink densities based on strain hardening modulus and stoichiometry differ by one order of magnitude. However, there is good qualitative agreement between them. TGDDM-Aniline is again the exception, suggesting incomplete conversion. Close resemblance of the correlations in Figure 2.7(b) and 2.9(b) confirms that the strain hardening response is indeed associated with crosslink density.

2.3.2.4 Fracture Toughness

In Figure 2.10, the fracture toughness of the resins generally decrease with increase in T_g . At first glance, the trend appears consistent with the literature^{20,38}. An epoxy with higher T_g or yield stress has smaller process zone or damage-accumulation region in front of the crack tip, leading to lower energy dissipation. However, closer inspection reveals that TGDDM-Aniline-DGEBA-D230 actually has relatively high toughness despite its high T_g . Compared to the control sample DGEBA-D230, the T_g of the THN resin is about 40 deg °C higher. However, the associated reduction in fracture toughness is quite small. In fracture toughness testing, the precrack acts as the largest flaw in the material³⁵. Strain softening and hardening are expected to take place before the crack can propagate. Introducing topological heterogeneity improves the strain localization behavior, and ultimately fracture toughness. Such enhancement is not observed in TGDDM-Aniline-D230 probably due to its highly crosslinked structure.

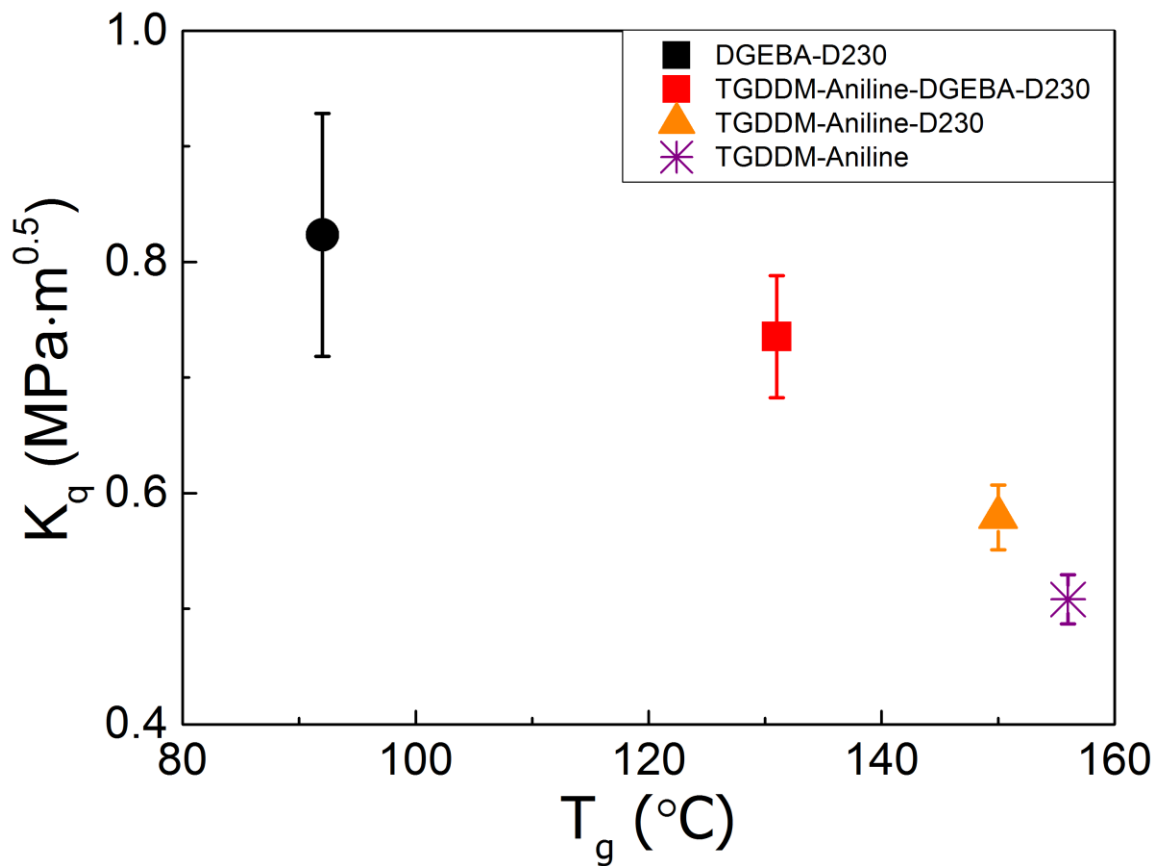


Figure 2.10 Fracture toughness of epoxies.

2.3.2.5 Thermal Stability

Plotted in Figure 2.11(a) are TGA thermograms of the epoxies. DGEBA-D230 shows a single stepwise weight loss near 380 °C. It has the lowest decomposition temperature (T_d) and residue because of low crosslink density and aromatic content [Figure 2.11(b)]. In marked contrast, TGDDM-Aniline exhibits gradual weight loss starting near 300 °C, and then a more sudden drop near 400 °C. Its highly crosslinked network structure and high aromatic content result in twice as much residue as DGEBA-D230. The addition of flexible epoxide and diamine make the THN epoxies less thermally stable. Their residues decrease to about 11%, but still slightly higher than that of TGDDM-D230.

TGDDM-Aniline-D230 decomposes at similar temperatures as TGDDM-Aniline, while TGDDM-Aniline-DGEBA-D230 and DGEBA-D230 have comparable T_d values.

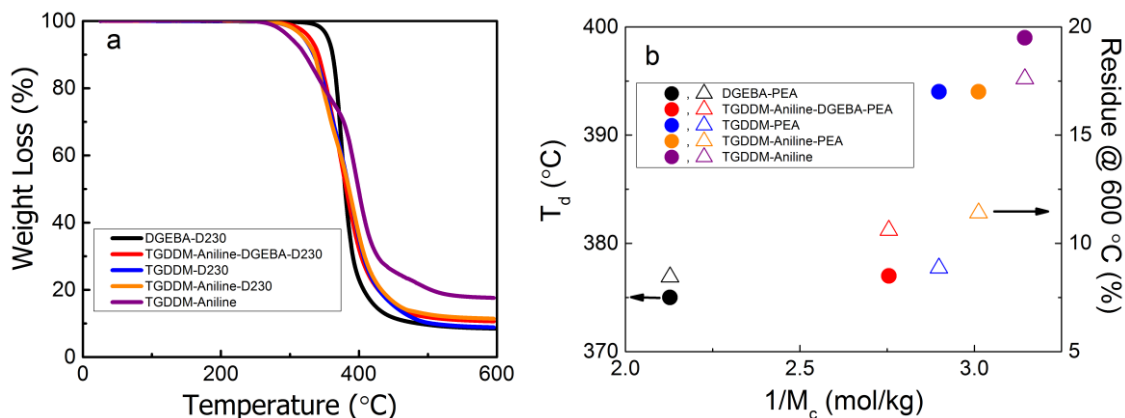


Figure 2.11 (a) TGA thermograms of epoxies, (b) Decomposition temperatures (solid circle) and residues (unfilled triangle).

2.4 Conclusion

In the homologous curative approach, a Topologically Heterogeneous Network (THN) epoxy was prepared from amine curing agents with different molecular weights but the same structure repeat unit. The resulting material contains regions with varying stiffness and crosslink density. Compared to a single amine-cured epoxy with the same average crosslink density, the THN resin shows broader glass transition, and bifurcated dynamic mechanical transition. However, its post-yield response is identical to the control sample, suggesting that the non-linear properties such as rejuvenated stress and strain hardening modulus are dictated by network connectivity.

In the multifunctional THN prepolymer approach, a prepolymer is first prepared from a rigid tetrafunctional epoxide and difunctional amine in off-stoichiometric or 2:1 ratio. Further network heterogeneity is introduced by incorporating a flexible tetrafunctional amine and diepoxide. The resulting THN epoxies have high thermal

stability, glass transition temperatures, elastic moduli, and yield strength. Network heterogeneity is confirmed by broadened beta and alpha transitions. The increase in segmental mobility is associated with enhanced strain localization response. Specifically, the THN resins exhibit about 70% lower strain softening and two-fold increase in strain hardening modulus when compared to the control sample. The THN resin with higher molecular heterogeneity is found to have relatively high fracture toughness despite its high T_g .

2.5 Future Work

Future investigation may focus on evaluating the effects of incorporating prepolymers with different distributions of oligomeric species. In this effort, an arbitrary molar ratio of 2 to 1 was chosen when reacting the tetrafunctional epoxide TGDDM and the difunctional amine aniline. Other off-stoichiometric ratios may be used to alter the distribution of the oligomeric species, as long as they generate viscous liquids below gel point. The fractions of various oligomers in the prepolymers may be determined by Nuclear Magnetic Resonance. An optimal ratio may be obtained for producing high T_g resin with high toughness.

2.6 References

1. Lee, H., and Neville, K., Handbook of Epoxy Resins. McGraw-Hill, New York, (1967).
2. Wang, X. R., and Gillham, J. K., J Appl Polym Sci, 47, 425-446 (1993).
3. deNograro, F. F., Guerrero, P., Corcuera, M. A., and Mondragon, I., J Appl Polym Sci, 56, 177-192 (1995).
4. Ma, J., Mo, M. S., Du, X. S., Rosso, P., Friedrich, K., and Kuan, H. C., Polymer, 49, 3510-3523 (2008).
5. Laiarinandrasana, L., Fu, Y., and Halary, J. L., J Appl Polym Sci, 123, 3437-3447 (2012).
6. deNograro, F. F., LlanoPonte, R., and Mondragon, I., Polymer, 37, 1589-1600 (1996).
10. Crawford, E., and Lesser, A. J., J Polym Sci Pt B-Polym Phys, 36, 1371-1382 (1998).
11. Tan, N. C. B., Bauer, B. J., Plestil, J., Barnes, J. D., Liu, D., Matejka, L., Dusek, K., and Wu, W. L., Polymer, 40, 4603-4614 (1999).
14. Lahlali, D., Naffakh, M., and Dumon, M., Polym Eng Sci, 45, 1581-1589 (2005).
15. Yang, G., Fu, S. Y., and Yang, J. P., Polymer, 48, 302-310 (2007).
16. Detwiler, A. T., and Lesser, A. J., J Mater Sci, 47, 3493-3503 (2012).
18. Bonnaud, L., Pascault, J. P., and Sautereau, H., Eur Polym J, 36, 1313-1321 (2000).
19. Park, S. J., and Lee, J. R., J Mater Sci Lett, 20, 773-775 (2001).
20. Kinloch, A. J., and Young, R. J., Fracture Behaviour of Polymers. Applied Science Publishers, Northern Ireland, (1983).
21. Haward, R. N. (ed) The Physics of Glassy Polymers. 2nd edn. Chapman & Hall, London, (1997).
22. Flory, P. J., Principles of Polymer Chemistry. Cornell University Press, Ithaca, (1953).

23. Nielsen, L. E., Landel, R. F., Mechanical properties of polymers and composites. 2nd edn. Marcel Dekker, New York, (1994).
24. Shaw, M. T., MacKnight, W. J., Introduction to polymer viscoelasticity. 3rd edn. John Wiley & Sons, Hoboken, (2005).
26. van Melick, H. G. H., Govaert, L. E., and Meijer, H. E. H., Polymer, 44, 2493-2502 (2003).
30. Haward, R. N., and Thackray, G., Proc R Soc A, 302, (1968).
31. Haward, R. N., Polymer, 28, 1485-1488 (1987).
32. Detwiler, A. T., and Lesser, A. J., J Appl Polym Sci, 117, 1021-1034 (2010).
33. Hoy, R. S., and Robbins, M. O., J Polym Sci Pt B-Polym Phys, 44, 3487-3500 (2006).
35. Lee, C. Y. C., and Jones, W. B., Polym Eng Sci, 22, 1190-1198 (1982).
38. Crawford, E. D., and Lesser, A. J., Polym Eng Sci, 39, 385-392 (1999).
40. Lesser, A. J., and Crawford, E., J Appl Polym Sci, 66, 387-395 (1997).
41. Charlesworth, J. M., Polym Eng Sci, 28, 230-236 (1988).
42. Heux, L., Halary, J. L., Laupretre, F., and Monnerie, L., Polymer, 38, 1767-1778 (1997).

CHAPTER 3

PREPARATION AND CHARACTERIZATION OF PRESTRESSED DOUBLE NETWORK EPOXIES

3.1 Introduction

In this effort we evaluate the effect of mechanical heterogeneity in baseline energy state on the thermal and mechanical properties of epoxies. Prestress is imposed between cure reactions to alter the energy states of the resulting materials. The synthesis of an Interpenetrating Polymer Network (IPN) is considered a promising route of blending immiscible polymers to create high-performance composites⁴³. An IPN is defined by Sperling and Mishra as the combination of multiple polymer networks where “at least one of which is polymerized/crosslinked in the immediate presence of the other(s).”⁴⁴ Depending on the sequence of network formation, an IPN may be classified as sequential or simultaneous. However, due to different rates of formation of the constituent networks, a true simultaneous IPN is difficult to obtain. Interconnection between the components is also possible, which results in a grafted IPN. Phase separation of network constituents tends to occur because of thermodynamic incompatibility⁴³.

Prestressed Double Network (PDN) elastomers show improved physical characteristics over conventional single network system. However, they differ from traditional IPN's in that their two-step curing process involves the same polymer, and that the second network is introduced while the first undergoes uniaxial extension. The resulting material obeys the two-network hypothesis of Andrews, Tobolsky and Hanson⁴⁵. When allowed to attain a state of ease, the length of a PDN elastomer lies between that of the original unstrained rubber and that of the stretched elastomer when the second network is

formed. Mechanical behavior of PDN elastomers have been described by a variety of elasticity theories⁴⁶⁻⁴⁸. The extent of reinforcement is shown to be dictated by the degree of chain orientation achieved from stretching the first network. Interestingly, a minimum stretch ratio must be surpassed before the Young's modulus, toughness, and strength measured parallel to the direction of stretch start to rise progressively with larger strain level⁴⁹⁻⁵². A similar threshold for drastic changes of modulus and coefficient of thermal expansion (CLTE) is found in PDN thermoplastic elastomers^{51,52}. Since the constituent networks are interlocked and incompletely relaxed, the phenomena was explained in terms of entropic competition and ensuing heat exchange between the two components^{51,52}. The transition is thought to occur when the two networks move from a competitive to collaborative regime.

The synthesis of PDN epoxies is based on step-cure chemistry developed previously¹⁶. The careful choice of aliphatic and aromatic curing agents provides systematic variation in network stiffness while maintaining constant crosslink density across the entire composition range. Favorable reaction kinetics makes it possible to react the aliphatic diamine at low temperature without reacting the aromatic diamine. The second network is formed at higher temperature while deformation is imposed on the partially cured resin. Since typical epoxy is unable to endure large tensile deformation, uniaxial compression is employed for prestressing. The engineering strain level is kept at 50% as the molar ratio between the curing agents is adjusted. The stored latent free energy is expected to alter the thermal and mechanical properties of the resulting materials. Unlike prestressed thermoplastic elastomers reported earlier^{51,52}, PDN epoxies have more

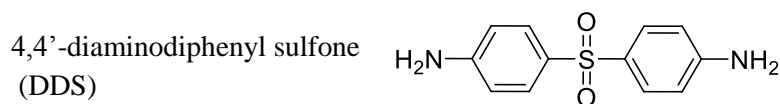
controlled network architecture and are below their glass transition temperatures at room temperature.

3.2 Experimental

3.2.1 Materials

DGEBA (DER 332) was purchased from Dow Chemical, and Jeffamine D230 was courtesy of Huntsman. 4,4'-diaminodiphenyl sulfone (DDS, MW: 248 g/mol) was obtained from Acros Organic. The structure of DDS is given in Table 3.1.

Table 3.1 Chemical structure of new amine.



3.2.2 Network Formation

The initial network formation step of Prestressed Double Network (PDN) epoxies was identical to that of DN epoxies, or control samples without any prestress. D230 and DDS with molar ratios ranging from 9:1 to 1:9 were mixed with stoichiometric amounts of DGEBA at elevated temperatures. DDS was dissolved first at 125 °C, and then D230 was introduced at 80 °C. The aliphatic fraction was reacted first at 100 °C for 6 hours. The partially cured resin was briefly heated to 150 °C to soften and immediately deformed with a PHI melt press to 50% of its original height. DDS was then reacted at 200 °C for 6 hours to yield the second network while the first network was under strain. Samples with 80, 90 and 100% DDS contents were postcured for 4 h at 200 °C and for 2 h at 220 °C.

The resulting epoxy was “prestressed” and “unrelaxed” (Figure 3.1) because the load was released only after cooling it to room temperature. After heating an unrelaxed

epoxy above its T_g to remove the latent free energy, the sample was referred to as “relaxed.” Its thickness was between that of the partially cured resin and that of the unrelaxed resin.

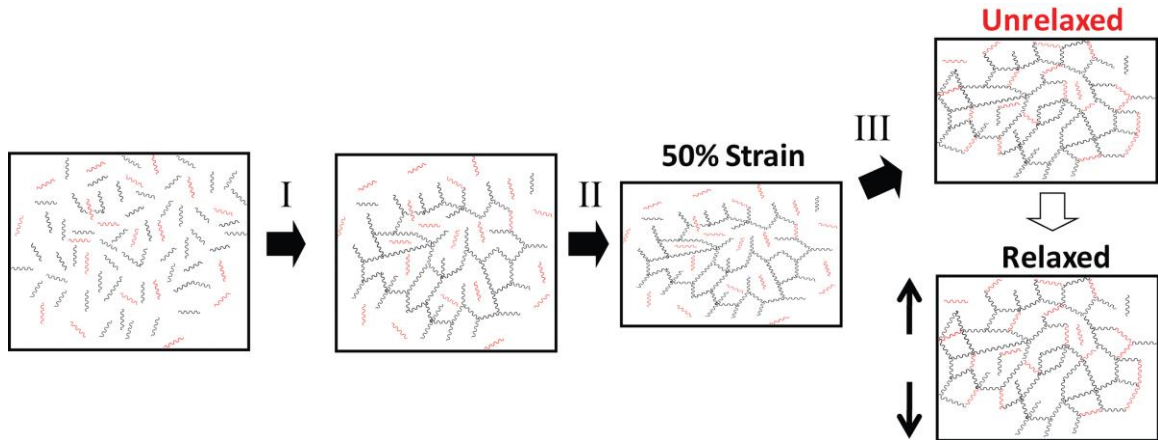


Figure 3.1 Sample preparation scheme of PDN epoxies. The black and red wavy lines stand for D230 and DDS, respectively. After the first cure (Step I), essentially all D230 had reacted to form the first network while most DDS remained unreacted. The partially cured resin was then compressed by 50% compressive strain (Step II). While in the deformed state, DDS was reacted to introduce the second network (Step III). The resulting epoxy is unrelaxed because of the latent free energy stored in it. It became relaxed and had some thickness recovery after heating above its glass transition temperature.

3.2.3 Characterization

3.2.3.1 Thermomechanical Analysis

Thermomechanical analysis was performed with TMA 2940 (TA Instruments) in expansion mode at a constant load of 0.05 N and a heating rate of 3°C/min. Each specimen was tested twice over the same temperature range, and held isothermal for 5 minutes at the end of the first heating to erase previous thermal history. The PDN specimens were tested both parallel *and* perpendicular to the direction of prestressing for possible anisotropy.

3.2.3.2 Dynamic Mechanical Analysis

Dynamic mechanical properties of single cantilever beam specimens were measured on DMA 2980 (TA Instruments) as described in Chapter 1. Relaxed PDN samples were prepared by heating the unrelaxed resins at $T_g + 20$ °C for about 10 minutes in a nitrogen-purged oven.

3.2.3.3 Tensile Testing

Tension test was conducted on Instron 5800 with a high-precision 2” strain gauge at a crosshead speed of 1 mm/min and 20 °C. The specimens were 3 mm thick ASTM D638 Type I tensile bars prepared using a Tensilkut router and standard metal die. Each reported value of Young’s modulus, yield stress and strain at break was an average of 4 to 6 measurements.

3.2.3.4 Fracture Toughness

Fracture toughness was measured as described in Chapter 1. Images of the fractured specimens were taken with a Nikon D40 digital camera and cross polarizers. The fracture surfaces were examined by an optical profilometer Zygo NewView 7300.

3.3 Results and Discussion

3.3.1 Molecular Weight between Crosslinks

The curing agents, D230 and DDS, possess inherently dissimilar chain stiffness and curing kinetics. However, they have the same number of amine functionalities and similar molecular weights. Therefore, the two constituents of Double Network (DN) and

Prestressed Double Network (PDN) epoxies have almost the same molecular weight between the crosslinks (M_c). As listed in Table 3.2, the M_c calculated using Equation 2.1 is about 470 g/mol across the whole composition range. This provides a model system for studying the effects of stiffness and prestress on the material properties.

Table 3.2 Estimated molecular weights between the crosslinks of PDN epoxies

% DDS	0	10	20	30	40	50	60	70	80	90	100
M_c (g/mol)	470.0	470.4	470.8	471.2	471.7	472.1	472.5	472.9	473.3	473.7	474.2

3.3.2 Thermomechanical Properties

The deformation step can create anisotropic materials that behave differently in directions parallel and perpendicular to the prestressing. Plotted in Figure 3.2 are the first heating traces of representative Double Network (DN) and Prestressed Double Network (PDN) epoxies on TMA. With increasing aromatic amine content, a similar increase in T_g is detected in DN and unrelaxed PDN resins. The increase is due to the substitution of flexible D230 with rigid DDS crosslinks, which places additional constraint on the molecular motion of polymer chains within the networks²⁴.

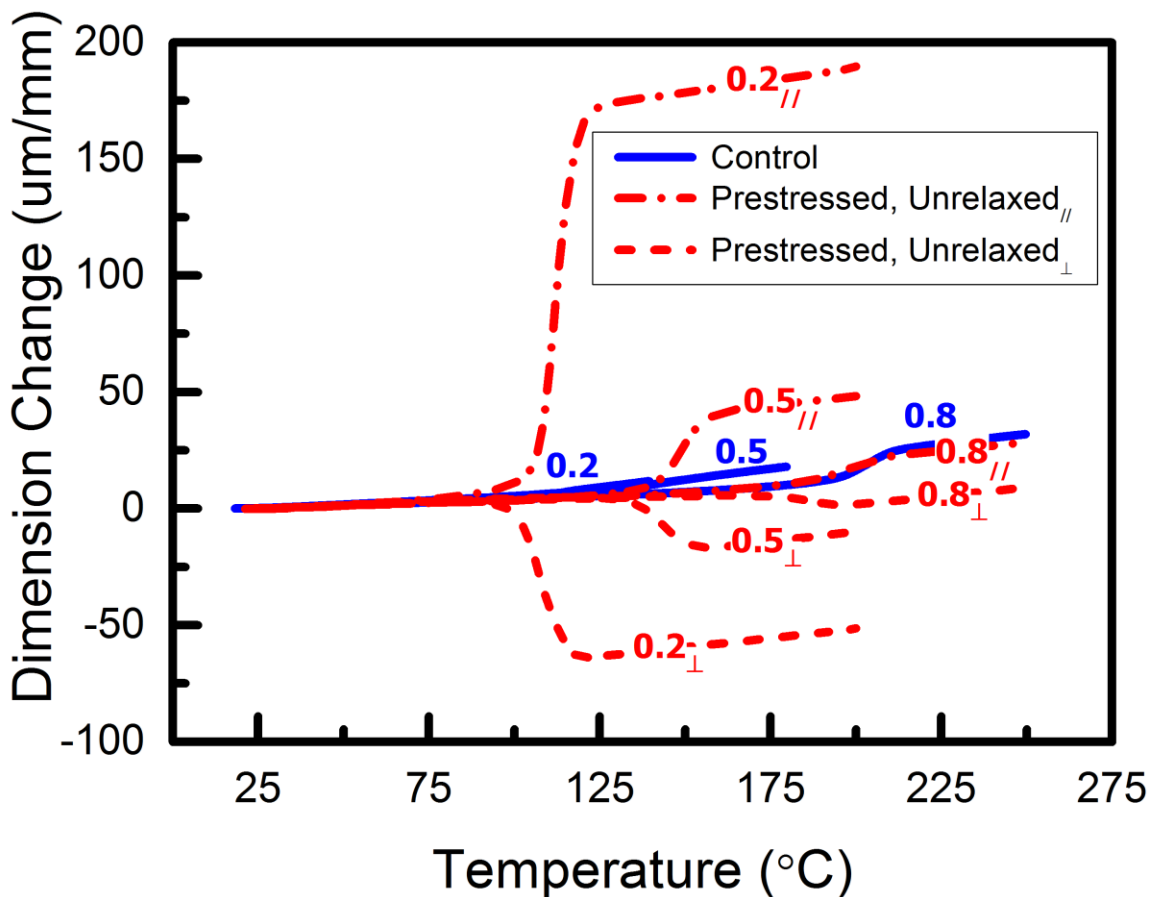


Figure 3.2 Dimension changes of epoxies during first heating on TMA. The numbers 0.2, 0.5, and 0.8 denote the molar fractions of DDS used to synthesize the resins. Control: DN epoxies without prestress; Prestressed, Unrelaxed_{//}: unrelaxed PDN epoxies tested parallel to the prestressing direction; Prestressed, Unrelaxed_⊥: unrelaxed PDN epoxies tested perpendicular to the prestressing direction.

Interestingly, the unrelaxed PDN epoxy with 20% DDS content (PDN 0.2U) exhibits much greater dimension change near its T_g and wider transition temperature span than the corresponding DN epoxy (DN 0.2). The expansion in the direction parallel to prestressing is more pronounced than the contraction in the direction perpendicular to prestressing, nearly a factor of three in the case of PDN 0.2U. These results indicate that that glass transitions of PDN epoxies can be severely complicated by their thermomechanical history, or the prestressed network formation process. The unrelaxed

resin is at a metastable state⁵³, due to the latent free energy stored in it. The input of thermal energy during the first heating accelerates the segmental motion of the macromolecules and facilitates structural recovery of the aliphatic network to its initial or undeformed state. However, the deformation is not completely reversible due to straining of the interlocking DDS network, which is formed while the first network is in a deformed state.

As shown in Figure 3.2, the magnitude of dimension change during the glass transition also diminishes with increasing aromatic content. Little difference exists between the traces of DN 0.8 and PDN 0.8U tested parallel to the prestressing direction. The observation suggests that the prestress decreases with DDS fraction. In other words, partially reacted resins did not necessarily experience an equal level of stress when subjected to the same amount of strain. This is an expected result considering that the gel point estimated from Flory-Stockmayer theory is 0.58 for networks based on a difunctional epoxide monomer and tetrafunctional amines⁵⁴. Although a small amount of DDS may react during the first cure, the overall extent of the first crosslinking reaction is expected to decrease with increasing amount of the aromatic curing agent. Accordingly, partially cured resins with higher aromatic content are probably sol-glasses, which have lower network connectivity and can flow more easily under load when heated above T_g . The presence of unreacted small DDS molecules and lightly crosslinked polymer chains can help relieve the compressive stress caused by the imposed deformation.

A qualitative measure of the prestress in the resins is given in Figure 3.3, which is obtained by normalizing the thickness recovery of a resin going from the glassy to the rubbery state with its thickness prior to testing. The stepwise dimension change of unrelaxed PDN epoxies decreases significantly with increasing DDS fraction. It appears to

level off at 60% DDS content before dropping again. Little difference is observed between DN 0.8 and PDN 0.8U. The result indicates that PDN epoxies with 80% aromatic content or greater have no prestress in them. However, a more rigorous analysis considering cure shrinkage and elastic recovery is needed to confirm the result.

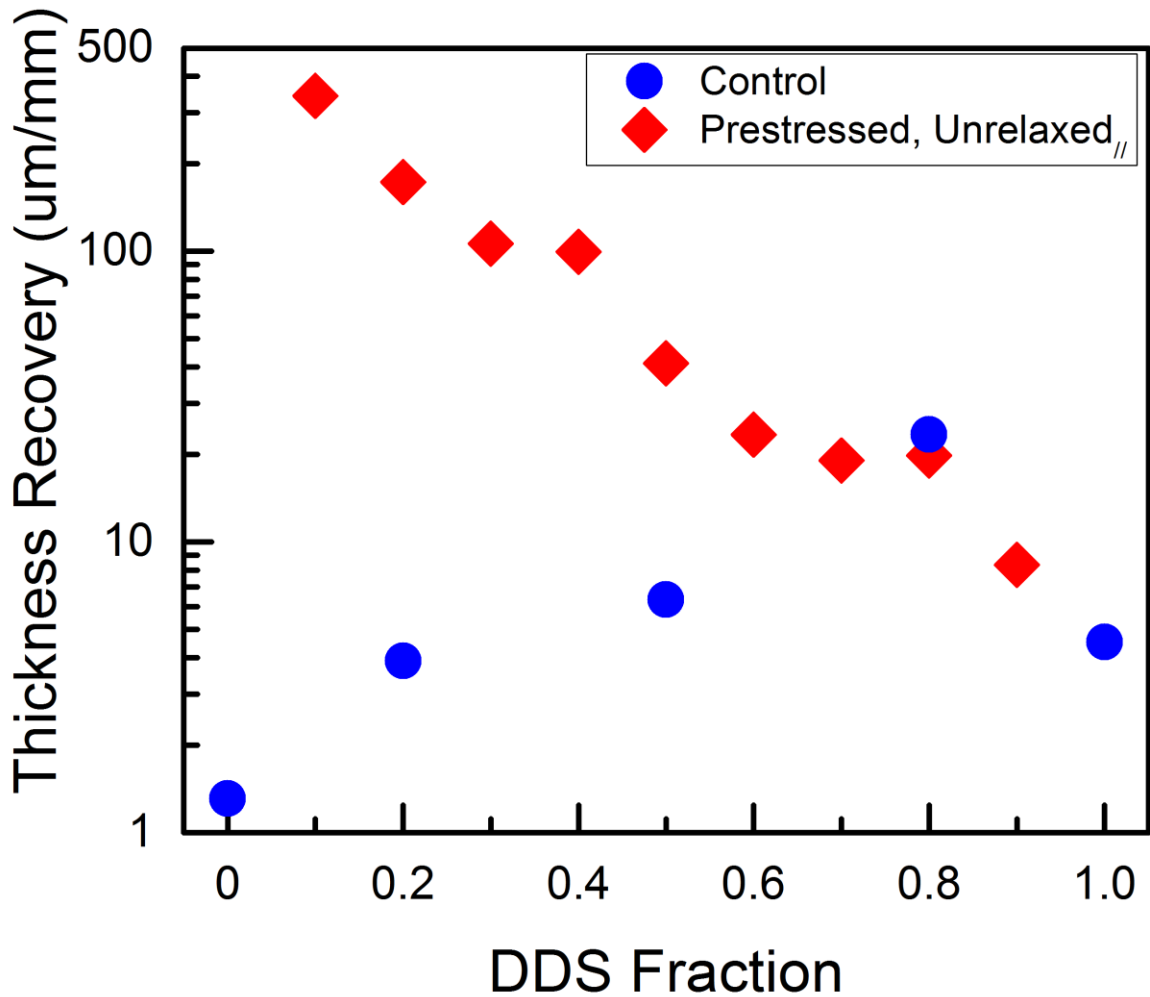


Figure 3.3 Dimension changes of epoxies going from glassy to rubbery state normalized by thickness prior to testing.

Figure 3.4 shows the second heating traces of the same epoxies. With the erasure of previous thermal history, PDN epoxies show less drastic dimension changes near the

glass transition. For example, the magnitude is one order less for PDN 0.2R when compared to the unrelaxed resin.

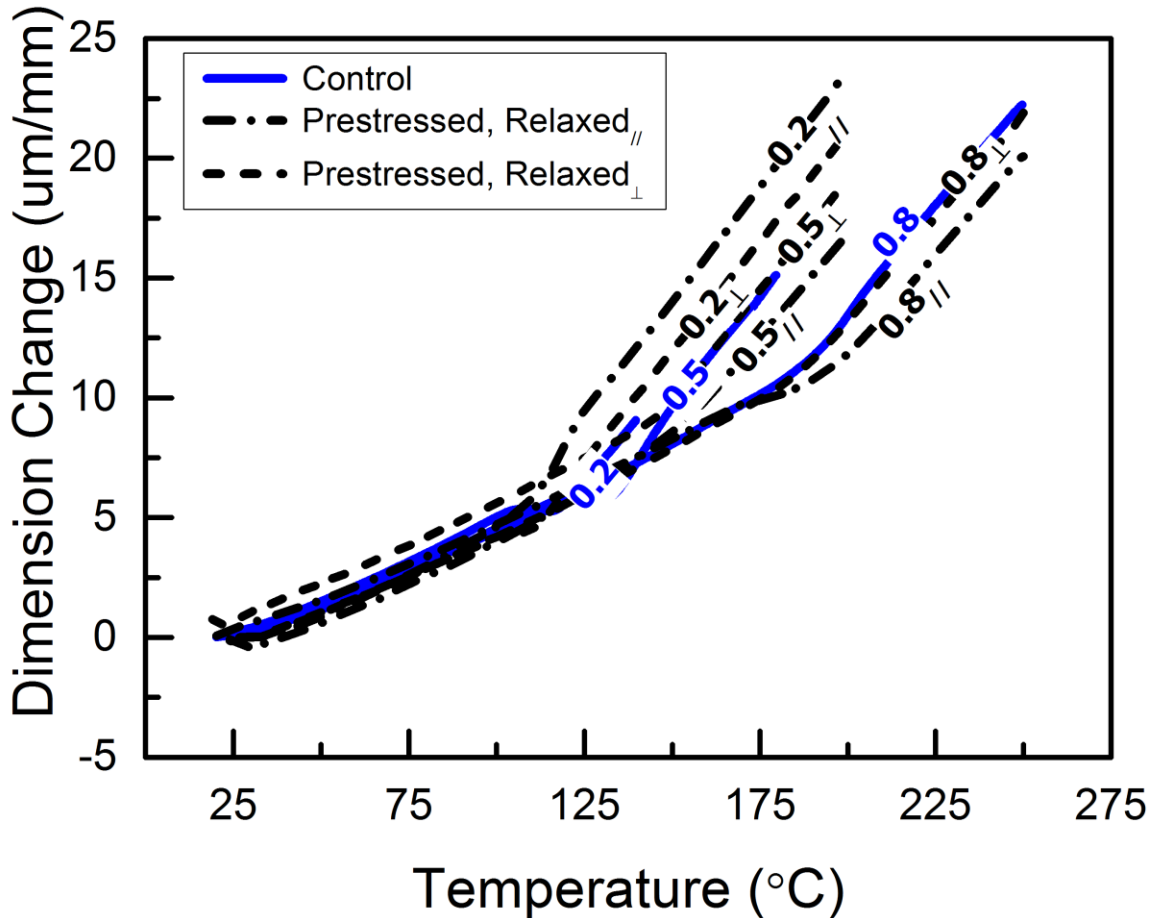


Figure 3.4 Dimension changes of epoxies during second heating on TMA. Prestressed, Relaxed_{//}: relaxed PDN epoxies tested parallel to the prestressing direction; Prestressed, Relaxed_⊥: relaxed PDN epoxies tested perpendicular to the prestressing direction.

The glass transition temperatures of unrelaxed and relaxed PDN resins tested on the TMA in the direction parallel to prestressing [Figure 3.5(a)], and in the direction perpendicular to prestressing [Figure 3.5(b)] are plotted against DDS fraction along with the control samples. The effects of anisotropy and latent free energy on T_g are negligible. The T_g 's of PDN epoxies stay the same when measured parallel and perpendicular to the

prestressing direction. Furthermore, no appreciable difference in T_g is observed among the unrelaxed and relaxed resins.

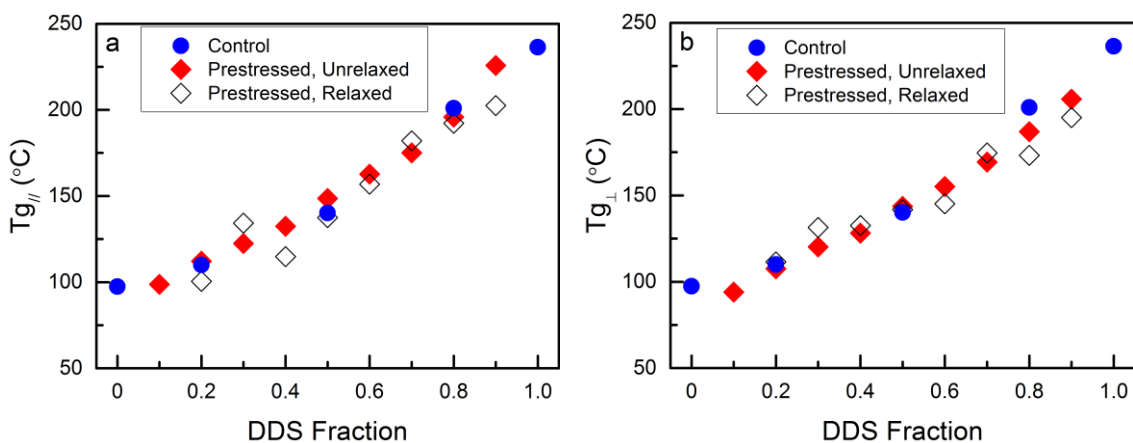


Figure 3.5 Glass transition temperatures of epoxies measured on TMA. (a) Parallel to the prestressing direction, (b) Perpendicular to the prestressing direction.

As illustrated in Figure 3.6(a) and 3.6(b), both the rubbery and glassy coefficients of linear thermal expansion (CLTE) of the PDN epoxies and the control samples are generally insensitive to change in network composition. These results are consistent with the findings of Ogata and coworkers, who reported that the rubbery CLTE of epoxies decreases with increasing crosslinking density, and that the glassy CLTE increases with increasing crosslinking density⁵⁵. Since the molar crosslinking density is uniform among all PDN resins, no change in CLTE due to composition is expected. The effect of testing directions is also negligible. The presence of latent free energy does not result in decreased CLTE as in the case of DN thermoplastic elastomers^{51,52}. The discrepancy is probably due to the limited degree of chain orientation achievable by deforming the epoxies to 50% strain in compression.

The maximum strain level that typical epoxies can sustain without fracture is considerably lower than elastomers, due to the much higher crosslinking density of epoxies.

The deformation step between cure reactions induces biaxial orientation. For a brittle polymer, however, property improvement from biaxial orientation can be less significant than that from uniaxial orientation due to finite extensibility of the polymer chains²³.

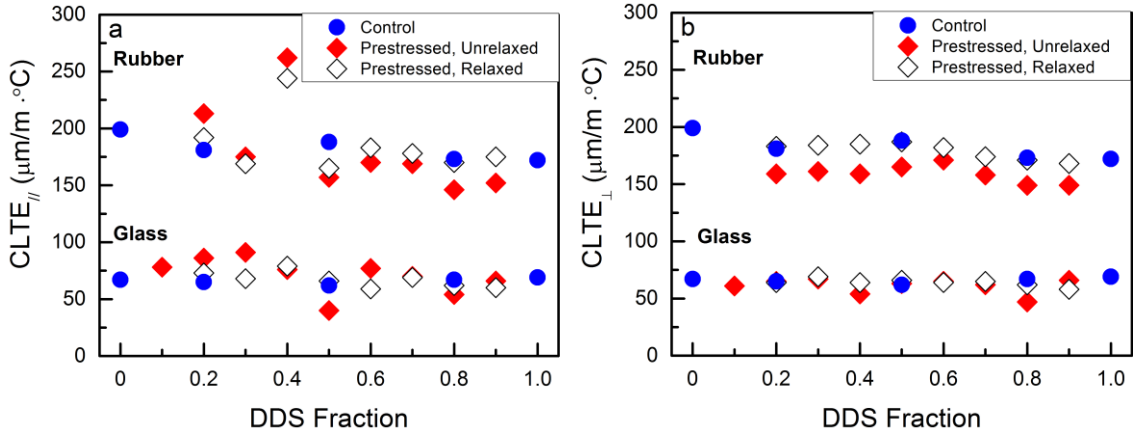


Figure 3.6 Coefficients of linear thermal expansion of epoxies. (a) Measured parallel to the prestressing direction, (b) Measured perpendicular to the prestressing direction.

3.3.3 Dynamic Mechanical Properties

Plotted in Figure 3.7(a) and 3.7(b) are the storage and the loss moduli of representative PDN epoxies and the control samples. Only a single T_g is detected for each sample. Macroscopic phase separation was not triggered by prestressing between cure reactions. No effect of prestressing is observed in the moduli or T_g . However, the T_g values measured by DMA (Figure 3.8) tend to be about 10 °C higher than those tested on TMA (Figure 3.5) because of the difference in the experimental time scale²⁴. The data points for the control samples are taken from previous work¹⁶.

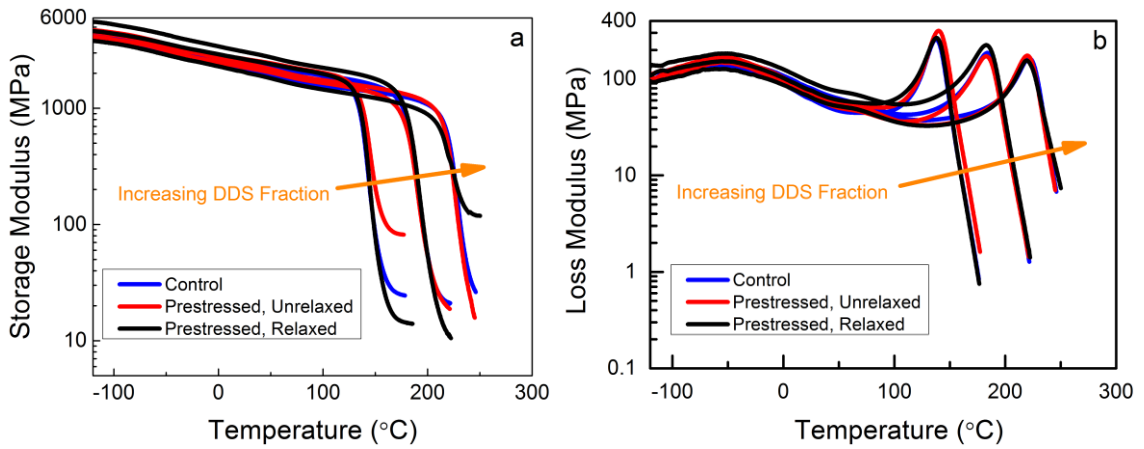


Figure 3.7 Dynamic mechanical measurements of some representative epoxies. (a) Storage moduli, (b) Loss moduli.

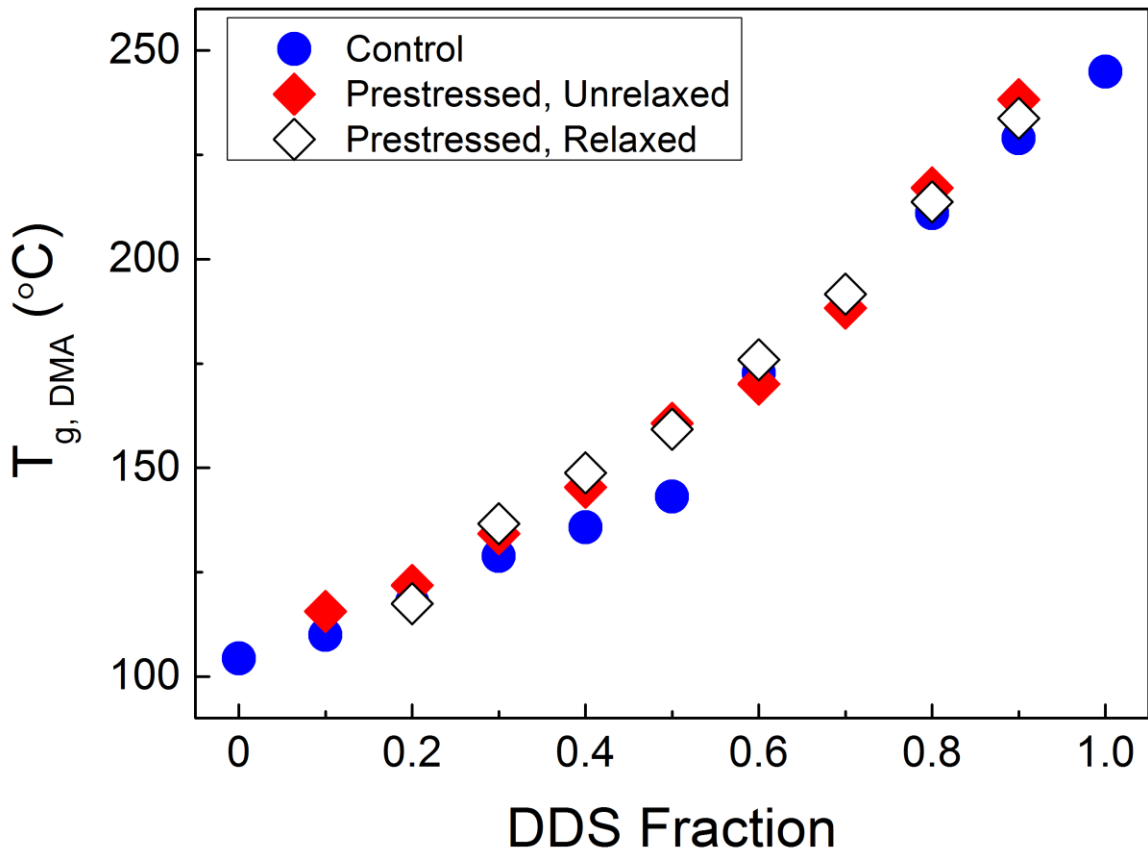


Figure 3.8 Glass transition temperatures of epoxies measured on DMA.

The beta transition peaks normalized with respect to the peak maxima of loss moduli are shown in Figure 3.9. The transitions occur at around -60 °C for all PDN epoxies and control samples. The transition has been attributed to the localized motion of network repeat units⁴². Since the same structural units are present in all resins, no change in the beta transition temperatures is expected. The shape of the transition peaks shows little variation with change in DDS fraction, or removal of latent free energy.

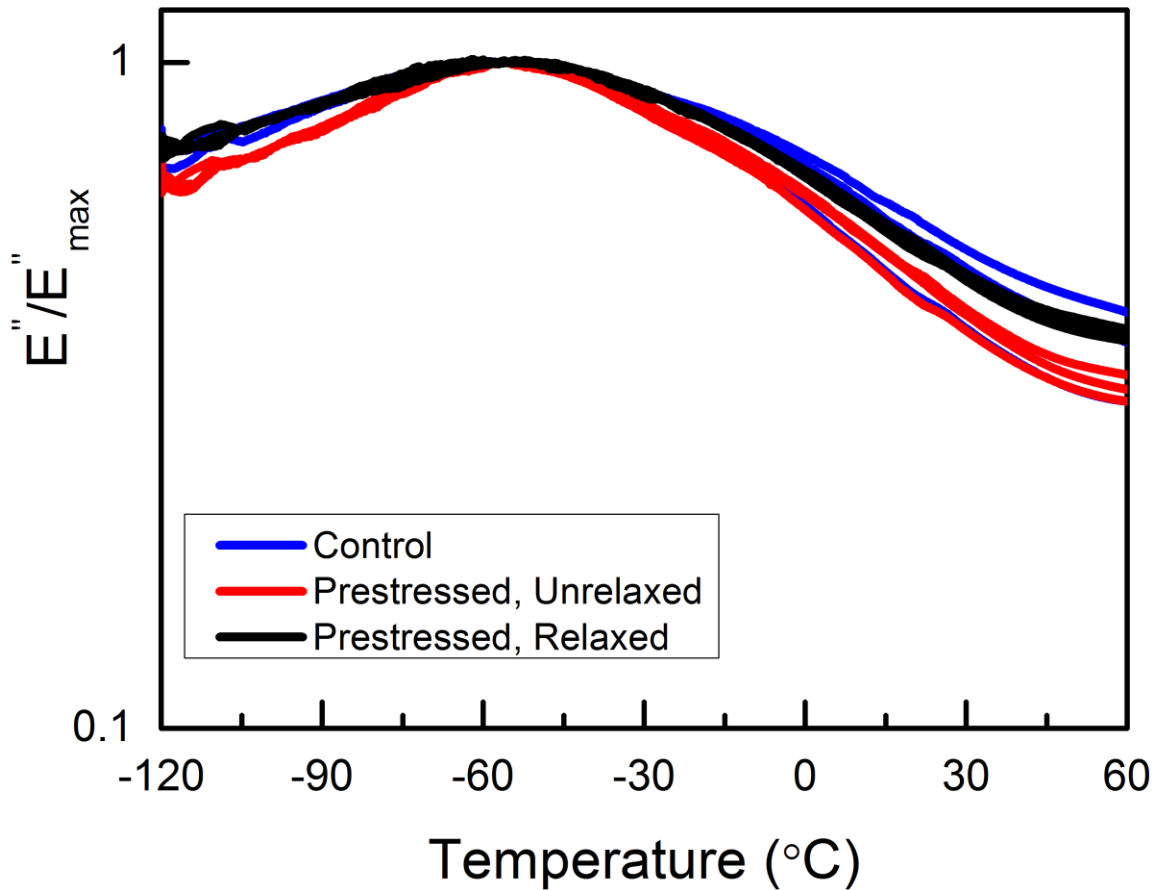


Figure 3.9 Normalized beta transitions

Shown in Figure 3.10(a) are the normalized alpha transitions of the same epoxies illustrated in Figure 3.7(b). The full width at half maximum (FWHM) of the alpha transitions of the PDN epoxies are given in Figure 3.9(b), along with those of the control

samples taken from previous work¹⁶. As in Chapter 2, the peak shapes are highly asymmetric and more stretched in the lower temperature region. The resins cured with 0 and 100% DDS have the narrowest alpha transition width. For the control samples and unrelaxed PDN resins, the transition width increases toward intermediate DDS fraction and appears to maximize around 60% DDS. Even though all of the resins appear homogeneous on the macroscopic scale, these results suggest that network heterogeneity exists on the molecular scale. Unlike the Topologically Heterogeneous Network epoxies in Chapter 2, the molecular weight between crosslinks is constant across the composition range in this study. The molecular heterogeneity is therefore attributed to the difference in the stiffness between the aliphatic and aromatic curing agents.

For relaxed PDN resins shown in Figure 3.10(b), the transition width increases with increasing DDS fraction. The result suggests that the removal of latent free energy may also affects segmental mobility. However, the 80% DDS composition appears to be the exception, and more testing are needed to confirm the hypothesis.

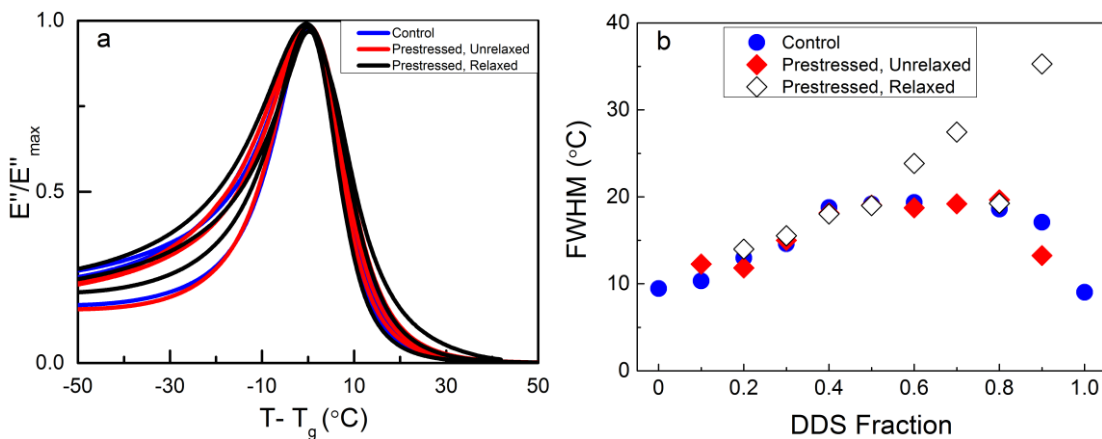


Figure 3.10 (a) Normalized alpha transitions, (b) Full width at half maximum (FWHM) of the transitions.

3.3.4 Tensile Response

Shown in Figure 3.11 are tensile stress-strain curves of the control samples cured with purely D230 (DN 0), purely DDS (DN 1), and 50% DDS content (DN 0.5), as well as unrelaxed PDN epoxy with 50% DDS content (PDN 0.5U). The most ductile resin, DN 0, deforms through yield and exhibits the largest elongation at break. The most rigid resin, DN 1, is expected to show the smallest elongation at break. However, as shown in Table 3.3, PDN 0.5U fails at similar strain level as DN 1. In contrast, DN 0.5 fails at considerably higher strain. The result underscores the finite extensibility of network chains in the prestressed resin. As a result of the compression step, some polymer chains in the aliphatic network are already stretched and aligned in the tensile testing direction prior to testing. Based on the compression testing results in previous work¹⁶, at 50% compressive strain, the first network of the PDN epoxy is already in the strain hardening region. Thus, only a small amount of additional strain can be tolerated before reaching the extensibility limit of the network.

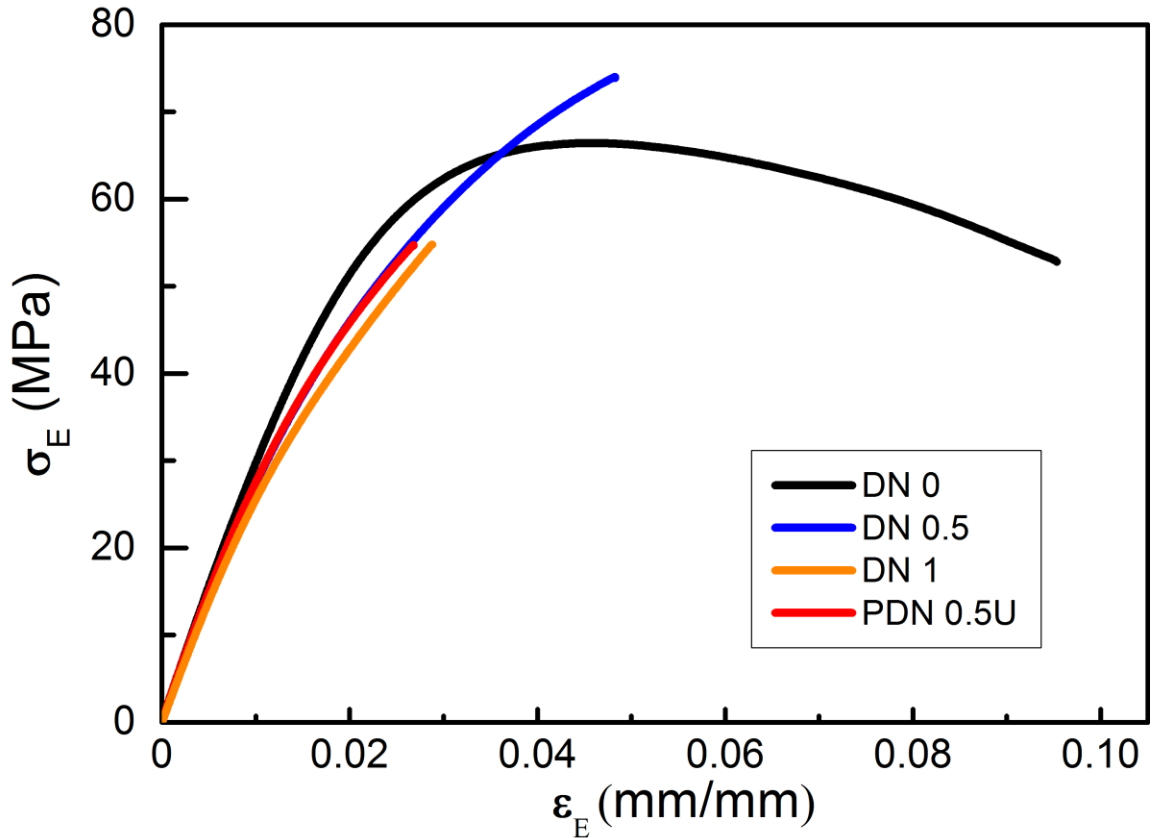


Figure 3.11 Tensile stress-strain curves of epoxies. DN 0: cured purely with D230; DN 1: cured purely with DDS; DN 0.5: cured with 50% DDS content; PDN 0.5U: prestressed, unrelaxed resin with 50% DDS content.

The Young's moduli are also given in Table 3.3. DN 0 and DN 1 show the highest and lowest moduli, respectively. The tensile modulus of DN 0.5 also appears to obey the rule of mixtures. However, unlike DN elastomers, no reinforcement is seen when comparing DN 0.5 and PDN 0.5U. Again, the diminished response is probably due to the brittle nature of the resins, which restricts the degree of chain orientation achievable by prestressing the partially cured resin to 50% compressive strain.

Table 3.3 Tensile testing results

Resin	E (GPa)	σ_y (MPa)	ϵ_{break} (mm/mm)
DN 0	2.95	66.8	0.086
DN 1	2.48	n/a	0.028
DN 0.5	2.68	n/a	0.049
PDN 0.5U	2.70	n/a	0.026

3.3.5 Fracture Toughness

As shown in Figure 3.12, the control samples cured with 0, 40, 50, and 100% DDS contents have about the same fracture toughness (K_q). In marked contrast, the unrelaxed PDN resins with 40% and 50% DDS contents exhibit more than 30% increase in K_q over the control samples. The result is rather interesting because no additive is incorporated, and the prestressed epoxies are single-phase materials as suggested by T_g measurements on TMA and DMA. The elastic moduli also remain the same, according to DMA and tensile test.

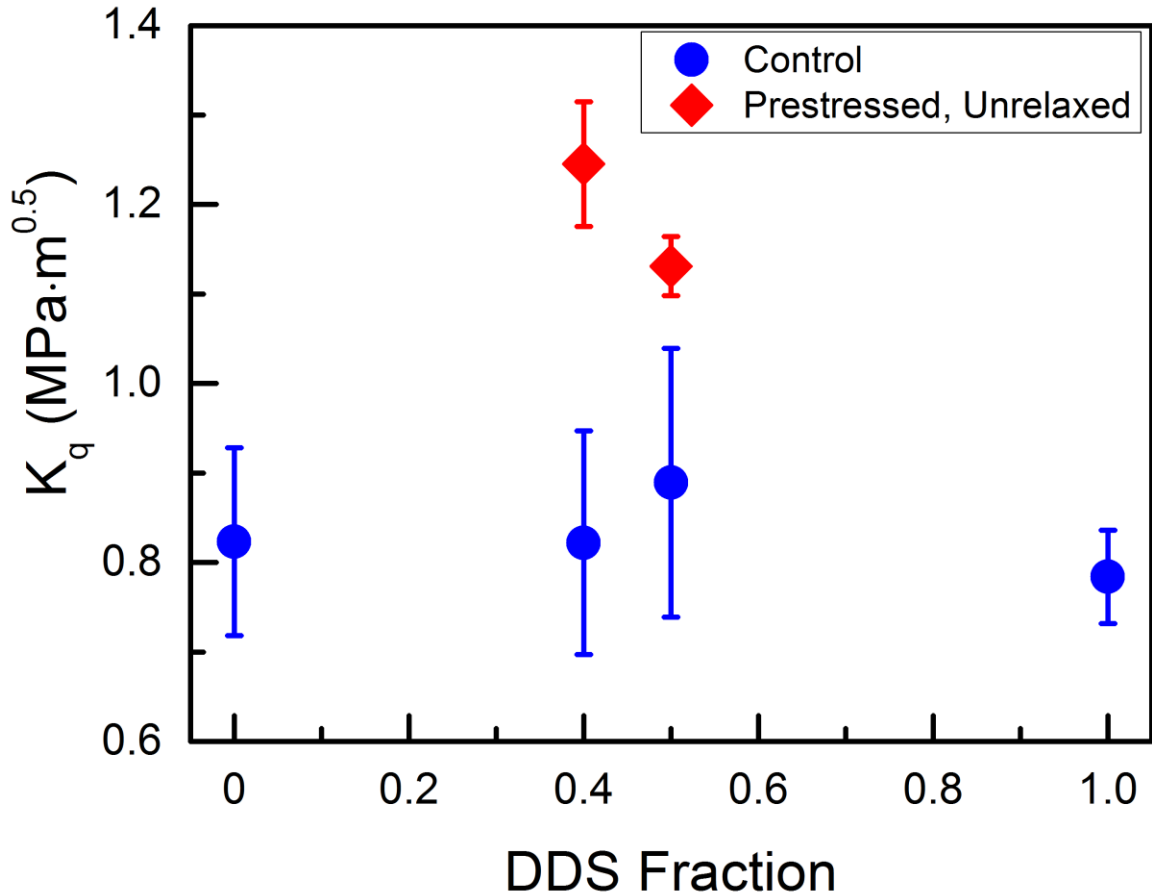


Figure 3.12 Fracture toughness of unrelaxed PDN epoxies and control samples.

The PDN resins appear anisotropic since higher K_q values are measured at the radial direction than the tangential direction (Figure 3.13). Improvement in mechanical properties via the utilization of other types of prestress has been reported for other glassy polymers. Archer and Lesser studied the mechanical response of polymethylmethacrylate (PMMA) with externally applied compressive prestress⁵⁶. Although the deformation was small, significant improvement in impact performance is observed. Weon et al. oriented PMMA using large strain simple shear, and found significant increases in both fracture toughness and impact resistance⁵⁷.

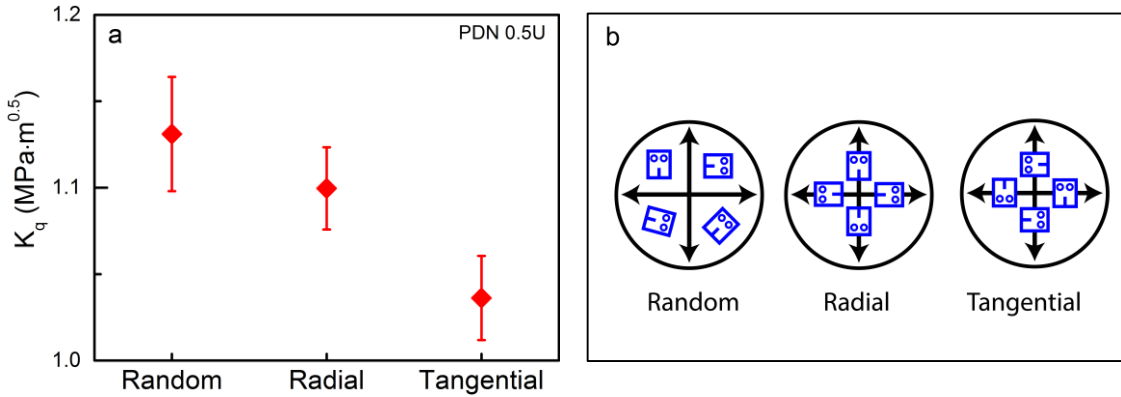


Figure 3.13 (a) Fracture toughness of unrelaxed PDN epoxies with 50% DDS content tested along different precrack directions, (b) Precrack directions.

The fracture surface of prestressed epoxies show interesting features. Shown in Figure 3.14(a) and 3.14(b) are polarized digital images of mini-CT specimen of a control sample with 50% DDS content (DN 0.5) and an unrelaxed PDN epoxy (PDN 0.5U), respectively. The propagating cracks are arrested before these two specimens fail completely. The whitening regions or stress concentrations on DN 0.5 are due to the mini-CT specimen fabrication process and fracture toughness testing. In marked contrast, a marble-like texture is seen extending across the surface of PDN 0.5U. Such feature is the direct results of the compression step, which induced orientation. Strong birefringence is preserved even after polishing the sample to expose regions away from the fracture surfaces.

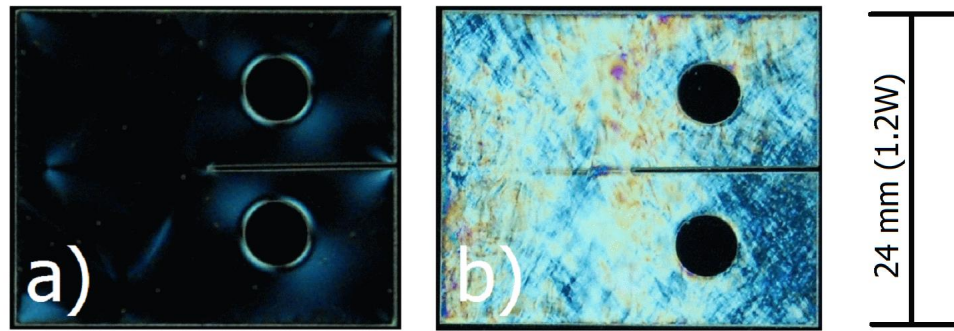


Figure 3.14 Polarized digital images of representative miniature compact tension specimens after fracture. (a) control sample with 50% DDS content, (b) unrelaxed PDN epoxy with 50% DDS content.

Fracture surfaces of a representative PDN 0.5U mini-CT specimen are shown in Figure 3.15. The control samples have smooth and mirror-like fracture surfaces, which are characteristic of brittle failure in unmodified epoxies. The center or plane-strain region of the fracture surface of PDN resins is also featureless [Figure 3.15(b)]. However, the edge or plane-stress regions exhibit significant surface irregularities or tortuosity [Figure 3.15(a) and 3.15(c)]. The result suggests that pronounced local plastic deformation has taken place during the fracture events, promoting energy dissipation. The underlying mechanism for the increase in toughness is attributed to the combination of opening and in-plane shear failure modes. If in-plane shear is fully activated, the toughness of polymeric glasses can increase by an order of magnitude⁵⁸.

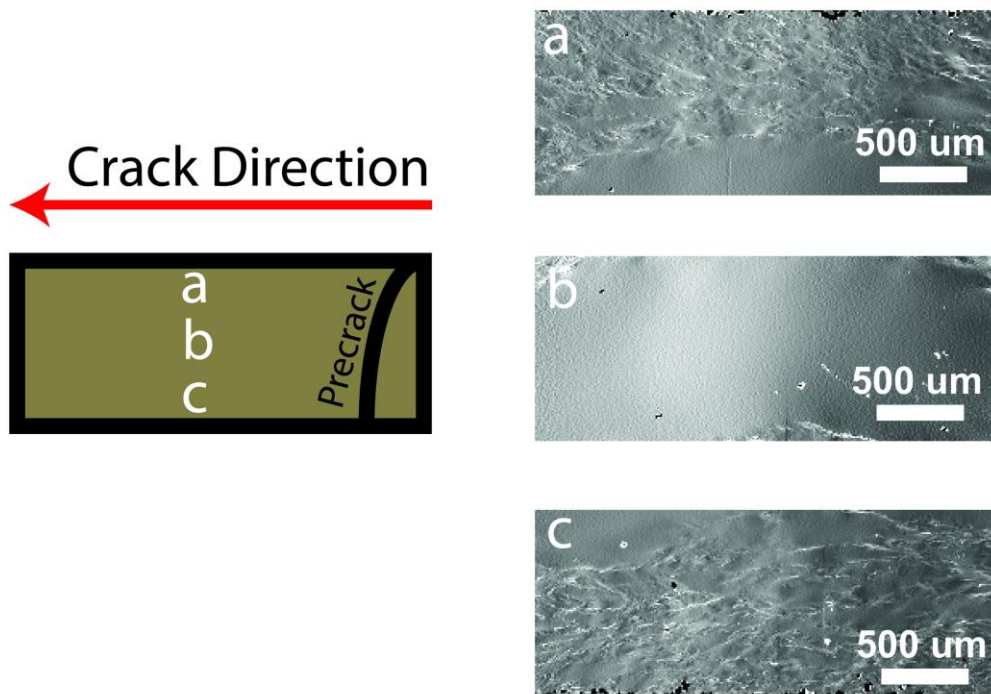


Figure 3.15 Fracture surfaces of an unrelaxed PDN epoxy with 50% DDS content. The sketch at the left shows the relative positions where the images are taken on the mini-CT specimen.

3.4 Conclusion

This chapter presents a novel preparation method for Prestressed Double Network (PDN) epoxies, which is a new type of Interpenetrating Polymer Network (IPN) thermoset. The synthesis steps involve the use of two amine curatives with similar molar mass but different stiffness and cure kinetics. Constant molecular weight between crosslinks exists across the entire composition range. The rigid second network is introduced while the ductile first network is under 50% compressive strain.

The mechanical heterogeneity or prestress does not alter the coefficients of linear thermal expansion. Network heterogeneity is qualitatively described by systematic variation in alpha transition width. The prestress has little effect on T_g values, but in certain

cases appears to broaden the alpha transition width. About 30% increase in fracture toughness is achieved without changing elastic modulus. This enhancement is accompanied by strong birefringence and visible roughness on the fracture surface. The toughening mechanisms is attributed to the combination of opening and in-plane shear failure modes.

3.5 Future Work

Future investigation may focus on examining the non-linear mechanical behavior of the prestressed, relaxed epoxies. As discussed in the chapter, relaxed resins are allowed to attain new states of equilibrium, with thickness between that of the undeformed and the prestressed states. Compared to the control samples without any prestress, the relaxed resins have the same elastic moduli and T_g values. However, they show much broader alpha transitions at high DDS fractions, which may result in improved tensile behavior and fracture toughness. In addition, compression testing may be conducted to study the strain localization response of prestressed epoxies.

3.6 References

16. Detwiler, A. T., and Lesser, A. J., *J Mater Sci*, 47, 3493-3503 (2012).
23. Nielsen, L. E., Landel, R. F., *Mechanical properties of polymers and composites*. 2nd edn. Marcel Dekker, New York, (1994).
24. Shaw, M. T., MacKnight, W. J., *Introduction to polymer viscoelasticity*. 3rd edn. John Wiley & Sons, Hoboken, (2005).
42. Heux, L., Halary, J. L., Laupretre, F., and Monnerie, L., *Polymer*, 38, 1767-1778 (1997).
43. Lipatov, Y. S., and Alekseeva, T. T., *Adv Polym Sci*, 208, 1-227 (2007).
44. Sperling, L. H., and Mishra, V., *Polym Adv Technol*, 7, 197-208 (1996).
45. Andrews, R. D., Tobolsky, A. V., and Hanson, E. E., *J Appl Phys*, 17, 352-361 (1946).
46. Flory, P. J., *Trans Faraday Soc*, 56, 722-743 (1960).
47. Santangelo, P. G., and Roland, C. M., *Rubber Chem Technol*, 67, 359-365 (1994).
48. Meissner, B., and Matjka, L., *Polymer*, 44, 4611-4617 (2003).
49. Kaang, S., Gong, D., and Nah, C., *J Appl Polym Sci*, 65, 917-924 (1997).
50. Aprem, A. S., Joseph, K., and Thomas, S., *J Appl Polym Sci*, 91, 1068-1076 (2004).
51. Singh, N. K., and Lesser, A. J., *J Polym Sci, Part B: Polym Phys*, 48, 778-789 (2010).
52. Singh, N. K., and Lesser, A. J., *Macromolecules*, 44, 1480-1490 (2011).
53. Oleynik, E., *Prog Colloid Polym Sci*, 80, 140-150 (1989).
54. Odian, G. *Principles of polymerization*. John Wiley & Sons, Hoboken, (2004).
55. Ogata, M., Kinjo, N., and Kawata, T., *J Appl Polym Sci*, 48, 583-601 (1993).
56. Archer, J. S., and Lesser, A. J., *J Appl Polym Sci*, 114, 3704-3715 (2009).

57. Weon, J. I., Creasy, T. S., Sue, H. J., and Hsieh, A. J., *Polym Eng Sci*, 45, 314-324 (2005).

58. Archer, J. S., and Lesser, A. J., *J Polym Sci Pt B-Polym Phys*, 49, 103-114 (2011).

CHAPTER 4

PREPARATION AND CHARACTERIZATION OF ASYMMETRIC DOUBLE NETWORK EPOXIES

4.1 Introduction

The aim of this research is to investigate the effect of another type of chemical heterogeneity, or asymmetric stiffness between component networks on the engineering performance of Double Network (DN) epoxies. DN hydrogels with asymmetric stiffness are developed by Gong and coworkers as a potential candidate for artificial soft tissues⁵⁹. Formed via radical chemistry, they exhibit excellent strength and toughness even at 90 wt% water content. During their synthesis, a highly crosslinked polyelectrolyte network is swollen with an aqueous solution of monomer and crosslinker for a lightly crosslinked neutral polymer network. Due to isotropic expansion, the polyelectrolyte chains are merely extended and have no preferred orientation.

Gong and coworkers observed that a high molar ratio of second component to the first is needed to obtain the unusual synergistic effect from the two fragile polymer networks⁵⁹. Chain entanglement has been related to load transfer within the matrix⁶⁰. The toughening mechanism is associated with microscale fragmentation of highly crosslinked polyelectrolyte, which improves energy dissipation during deformation⁶¹. The breakdown of the more brittle component has also been related to large strain hysteresis⁶² and necking⁶³. The approach has recently been utilized to toughen elastomers⁶⁴. However, similar investigation using thermosets or systems with glass transition temperatures (T_g 's) above room temperature has not been reported.

The DN epoxies discussed in Chapter 3 consist of a Jeffamine D230-based aliphatic network and 4,4'-diaminodiphenyl sulfone (DDS)-based aromatic network. They are considered symmetric with respect to crosslink density since the two miscible curing agents have similar molecular weights. In marked contrast, the constituents of the Asymmetric Double Network epoxies have different crosslink densities (Figure 4.1).

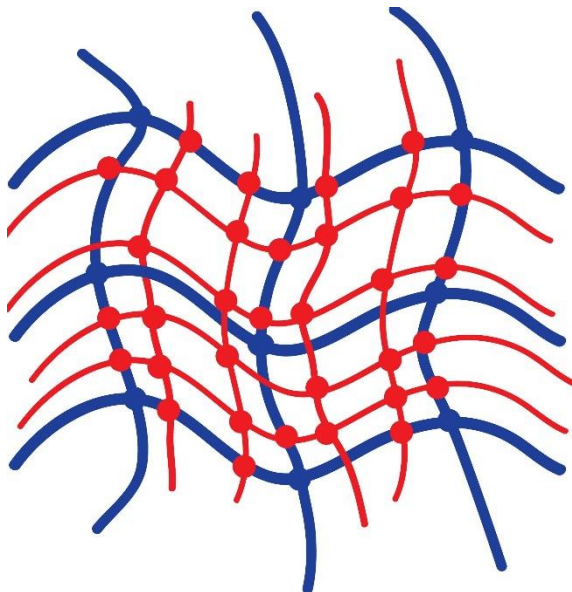
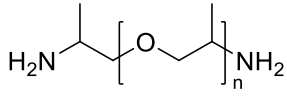
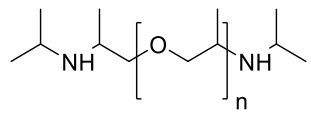
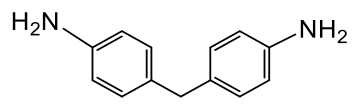


Figure 4.1 Schematic presentation of Asymmetric Double Network epoxies. The loosely crosslinked aliphatic network is colored blue. The densely crosslinked aromatic network is colored red.

One key element in the synthesis of asymmetric epoxies is a difunctional aliphatic amine that increases the chain length between crosslink junctions but does not introduce any additional crosslinks. The chain extender, Jeffamine SD231, is chosen since it has the same polypropylether backbone as the tetrafunctional amine D230 (Table 4.1). The resulting chain-extended aliphatic network therefore has essentially the same stiffness as the network based on purely D230, but with higher molecular weight between crosslinks (M_c).

Table 4.1 Chemical structure of new amines.

Primary Polyetheramine (D230, n ~ 2.5; D400, n ~ 6.1; D2000, n ~ 33)	
Secondary Polyetheramine (SD231, n ~ 2.5)	
4,4'-diaminodiphenyl methane (DDM)	

The effect of hydrogen bonding on the ductility of asymmetric epoxies is evaluated by comparing two structurally similar aromatic curing agents, DDS and 4,4'-diaminodiphenyl methane (DDM). During the polymerization and crosslinking reactions of an epoxy, a pendant hydroxyl group is generated for each oxirane ring on the epoxide monomer that has been opened by an amino hydrogen¹. The sulfone group in DDS can form hydrogen bonding with these newly formed hydroxyl units (Table 4.1). In contrast, DDM does not have such polar moiety to participate in non-covalent bonding.

Comparisons of physical properties are made among epoxies with different network architectures but the same T_g or average crosslink density. Combinations of different fabrication approaches that promote network heterogeneity are also investigated. In Chapter 2, a rigid multifunctional prepolymer is reacted with flexible reagents to generate within the final materials regions of varying stiffness and crosslink densities. Despite the improvement in strain localization response, increase in fracture toughness is limited by the highly crosslinked network structures. In this work, chemical heterogeneity in an asymmetric epoxy is amplified by the use of a different prepolymer. Specifically, the

difunctional epoxide diglycidyl ether of bisphenol A (DGEBA) is reacted with aniline in 2:1 ratio to generate a viscous liquid below gel point. As illustrated in Figure 4.2(a), the prepolymer may consist of short linear and cyclic oligomers. The linear dimer is expected to be the major reaction product. Unlike the multi-functional prepolymer shown in Figure 2.1, however, the cyclic species in the DGEBA-based prepolymer contain zero residual epoxide functionality and cannot participate further in either polymerization or crosslinking reaction [Figure 4.2(b)].

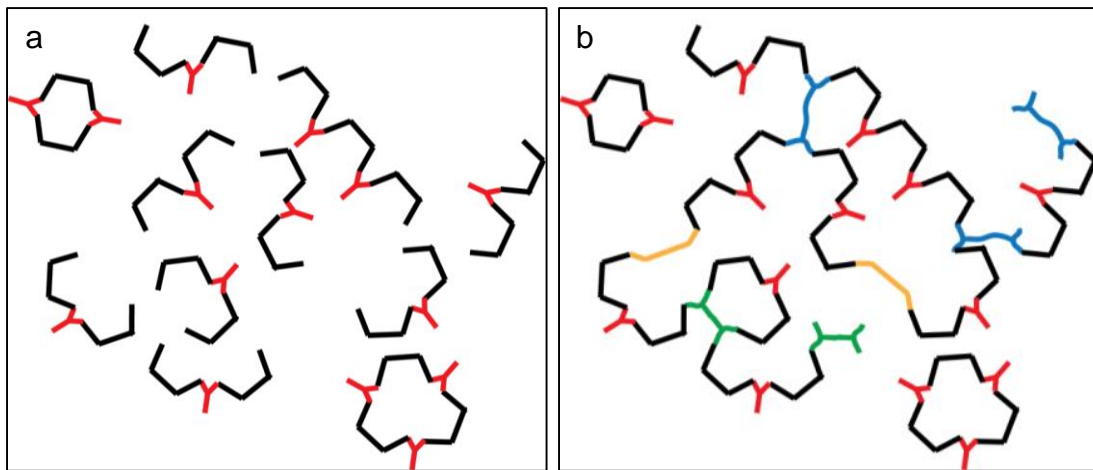


Figure 4.2 (a) Chain-extended prepolymer, (b) DGEBA-Aniline-D230-SD231-DDM 5-4-1. Colored segments: black, DGEBA; red, aniline; orange, SD231; blue, D230; and green, DDM.

As discussed in Chapter 3, the toughness of prestressed elastomers improves with increasing amount of prestressing. However, 50% compressive strain is the highest extent of deformation that can be imposed on the partially cured symmetric epoxy without causing catastrophic failure. In contrast, the aliphatic component of the asymmetric epoxy is expected to be more ductile, because of loosely crosslinked structure. Larger deformation can therefore be imparted between cure reactions, and may result in more than 30% enhancement in toughness.

4.2 Experimental

4.2.1 Materials

Jeffamine D230, D400, and SD231 (MW ~ 315 g/mol) were courtesy of Huntsman. DGEBA (DER 332) was obtained from Dow Chemical. DDS was purchased from Acros Organic. Aniline was ordered from Sigma Aldrich. 4,4-diaminodiphenylmethane (DDM, MW: 198 g/mol) was supplied by Alfa Aesar. The structures of the new chemicals are given in Table 4.1.

4.2.2 Network Formation

Stoichiometric amount of epoxides and amines were used for all resins. During the synthesis of an Asymmetric Double Network epoxy, the aromatic curing agent DDS or DDM was first dissolved into DGEBA at 120 °C or 75 °C. SD231 and D230 were then introduced successively at 60 °C. The ratio of amine hydrogens contributed by the reagents D230-SD231-DDS or D230-SD231-DDM were kept at 6-2-2 and 5-4-1. The DDS formulations were first cured at 100 °C for 6 h, then postcured at 200 °C for 6 h. The DDM formulations were first cured at 80 °C for 3 h, and 100 °C for 1 h. Postcure was conducted at 160 °C for 2 h, and 200 °C for 3 h. The compositions and cure schedules were chosen so that the partially cured resins were above the gel point.

The preparation of DGEBA-D400 and the symmetric epoxies based on D230 and DDS are given in Chapter 2 and 3, respectively. The control samples also included resins cured with a single tetrafunctional amine. DGEBA-DDM was cured at 80 °C for 3 h, 160 °C for 2 h, and 200 °C for 3 h.

DGEBA was reacted with aniline in 2:1 molar ratio at 80 °C for 3.5 h to generate a chain-extended prepolymer. The prepolymer was then reacted with D230, SD231, and DDM to produce DGEBA-Aniline-D230-SD231-DDM 5-4-1. The prestressed resin of DGEBA-D230-SD231-DDM 5-4-1 was prepared as described in Chapter 2, but with a compressive strain of 70%.

4.2.3 Characterization

4.2.3.1 Differential Scanning Calorimetry

Differential scanning calorimetry was conducted as described in Chapter 2.

4.2.3.2 Dynamic Mechanical Analysis

DMA measurement was performed as described in Chapter 1.

4.2.3.3 Compression Testing

Compression test of postcured resins was performed as described in Chapter 1. Compression test of partially cured resin was carried out at $T_g + 20$ °C with silicone oil (Alfa Aesar) as lubricant.

4.2.3.4 Tensile Testing

Tension test was performed on Instron 5800 using ASTM type IV tensile bars at 20 °C and a crosshead speed of 1 mm/min.

4.2.3.5 Fracture Toughness

Fracture toughness testing was conducted as described in Chapter 1.

4.3 Results and Discussion

4.3.1 Molecular Weight between Crosslinks

Listed in Table 4.2 are the average molecular weights between crosslinks (M_c) calculated for the network components and the entire resins using Equation 2.1. As expected, the asymmetric epoxies are more loosely crosslinked than the symmetric epoxy DGEBA-D230-DDS 5-5 or any other control sample. The aromatic curing agent DDM (MW: 198 g/mol) is shorter than DDS (MW: 240 g/mol). Since the aromatic networks are only present in low molar fractions, however, the asymmetric resins with the same amine hydrogen ratios have nearly identical M_c 's. Within each asymmetric resin, the M_c of the aliphatic network is about twice that of the aromatic network. In the case of DGEBA-Aniline-D230-SD231-DDM 5-4-1, the difference is more than four-fold.

Table 4.2 Molecular weights between crosslinks of the epoxies.

Resins	M _c (g/mol)		
	Aliphatic Network	Aromatic Network	Entire Resin
DGEBA-D230	-	-	470
DGEBA-D400	-	-	565
DGEBA-DDS	-	-	474
DGEBA-DDM	-	-	449
DGEBA-D230-DDS 5-5	470	474	472
DGEBA-D230-SD231-DDS 5-4-1	1072	474	914
DGEBA-D230-SD231-DDM 5-4-1	1072	449	910
DGEBA-D230-SD231-DDS 6-2-2	808	474	637
DGEBA-D230-SD231-DDM 6-2-2	808	449	631
DGEBA-Aniline-D230-SD231-DDM 5-4-1	1958	449	1648

4.3.2 Differential Scanning Calorimetry

The DSC thermograms of the partially cured and postcured resins are given in Figure 4.3. The numbers next to the curves are the corresponding T_g values. A single glass transition temperature is detected for each resin, indicating macroscopically homogeneous material. As shown in Figure 4.3(a), partially cured DGEBA-D230-DDS 5-5 has a T_g of 54 °C. (The endothermic peak immediately following the glass transition is due to physical aging.) Compared to this symmetric epoxy, the asymmetric epoxies have much lower T_g 's. The result is expected from the plasticization effect of the chain extender SD231. The reduction became nearly twice as pronounced when the molar fraction of SD231 is doubled.

The DDM-based epoxies have lower T_g 's than DDS-based epoxies. Unlike DDS, the aromatic curing agent DDM lacks polar moiety that can form hydrogen bonding with the hydroxyl group generated from the opening of the oxirane ring on the epoxide monomer. The difference in T_g 's is also nearly twice as pronounced when the molar fraction of SD231 is doubled.

The exothermic peaks that appear at elevated temperatures correspond to the crosslinking reactions of unreacted aromatic curing agents. The DDM-based epoxies react almost immediately to form the aromatic networks after heating above 100 °C, or the highest cure temperature imposed earlier. In contrast, the DDS-based epoxies do not react further until heated above 150 °C. The discrepancy is due to the electron withdrawing sulfone group in DDS, which lessens the reactivity of the molecule toward any residual epoxide in the partially cured resin.

In Figure 4.3(b), the postcured asymmetric epoxies again have much lower T_g 's than the symmetric epoxy DGEBA-D230-DDS 5-5. The T_g values are also lower than the resin cured with purely D230 or DGEBA-D230. This arises since the reduction in T_g caused by the chain-extended aliphatic network component outweighs the increase in T_g imparted by the minor aromatic network component. Due to hydrogen bonding, the T_g of the control sample DGEBA-DDS is about 30 °C higher T_g than DGEBA-DDM. However, little difference is observed among asymmetric networks with the same ratio of amine hydrogens. The T_g values of the 6-2-2 and 5-4-1 formulations only differ by 3 and 4 °C, respectively. The result again suggests that the T_g 's of the asymmetric epoxies is dominated by the major constituent or aliphatic network.

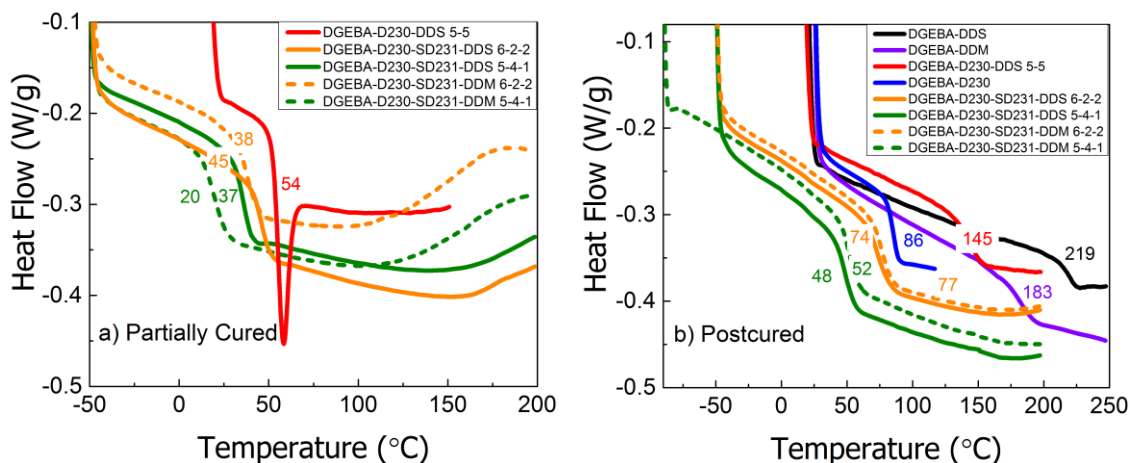


Figure 4.3 (a) DSC thermograms of partially cured resins, (b) DSC thermograms of postcured resins. The numbers next to the curves are glass transition temperatures of the epoxies. Exothermic direction up.

In Figure 4.4(a), comparison is made among resins with different network architectures but the same T_g 's at around 50 °C. The numbers next to the curves are again the corresponding T_g values. The most crosslinked DGEBA-D400 is the least heterogeneous, and has the narrowest glass transition width (see Chapter 2). The asymmetric networks show broader transition, because of the asymmetric stiffness or chemical heterogeneity in the resins.

Plotted in Figure 4.4(b) are the DSC thermograms of partially cured and postcured DGEBA-Aniline-D230-SD231-DDM 5-4-1 with corresponding T_g values. A structurally diverse prepolymer based on DGEBA and aniline (Figure 4.2) is incorporated into these resins to further enhance the chemical heterogeneity. Compared to asymmetric epoxies with the same amine hydrogen ratio of 5-4-1 shown in Figure 4.3, the T_g values of the partially cured and postcured resins containing the prepolymer are about 20 °C higher. This is a rather interesting result since DGEBA-Aniline-D230-SD231-DDM 5-4-1 is only half as crosslinked (Table 4.2). The prepolymer is about twice as long as DGEBA after reacting

with aniline in 2:1 molar ratio. However, the plasticization effect caused by the increase in chain length is overcome by the increase in T_g imparted by the incorporation of rigid aniline. The partially cured resin in Figure 4.4(b) also shows an exothermic peak at elevated temperature, corresponding to the formation of the aromatic network.

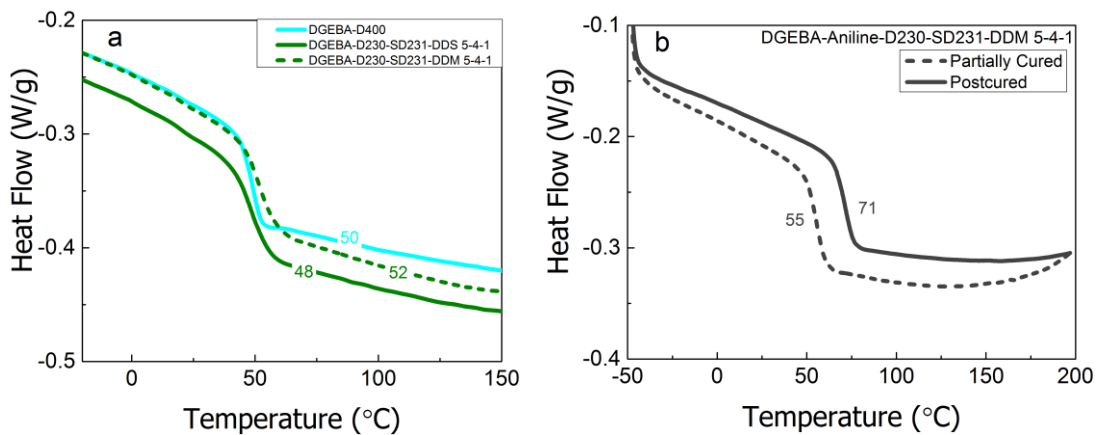


Figure 4.4 (a) DSC thermograms of resins with the same T_g values, (b) DSC thermograms of partially cured and postcured DGEBA-Aniline-D230-SD231-DDM 5-4-1. The numbers next to the curves are glass transition temperatures of the epoxies.

4.3.3 Dynamic Mechanical Properties

Plotted in Figure 4.5(a) and 4.5(b) are the storage and loss moduli of the epoxies, respectively. The numbers next to the storage moduli are the corresponding T_g values. Again, only single glass transition temperature is detected for each sample, indicating that all epoxies are homogenous on the macroscopic scale. Little difference in storage moduli measured at 20 °C is observed among the asymmetric networks with the same amine nitrogen ratio (Table 4.3). The result suggests that the stiffness is primarily dictated by the aliphatic network, and independent of the aromatic curing agents. The observation is also consistent with the similarity in their T_g values discussed in previous section. The difference in moduli between 6-2-2 and 5-4-1 formulations are within data scattering. The

four control samples, DGEBA-D230, DGEBA-D400, DGEBA-DDM, and DGEBA-DDS, have about the same stiffness.

As shown in Figure 4.5(b), the beta transitions of the epoxies in general have similar widths and occur at around the same temperature or $-60\text{ }^{\circ}\text{C}$. This is an expected result since the transition is attributed to localized motion of chain segments⁴², and same network repeat units are present in all tested resins. As commented in Chapter 2, subtle differences exist in the peak intensity, shape, and overlapping regions with the alpha or glass transitions. These changes will be incorporated into a governing parameter in Chapter 5. The T_g values measured on DMA [Figure 4.5(a)] and the associated data scatter are higher than those measured on DSC due to the difference in the experimental time scale²⁴. However, the overall trend is the same as shown in Figure 4.3(b).

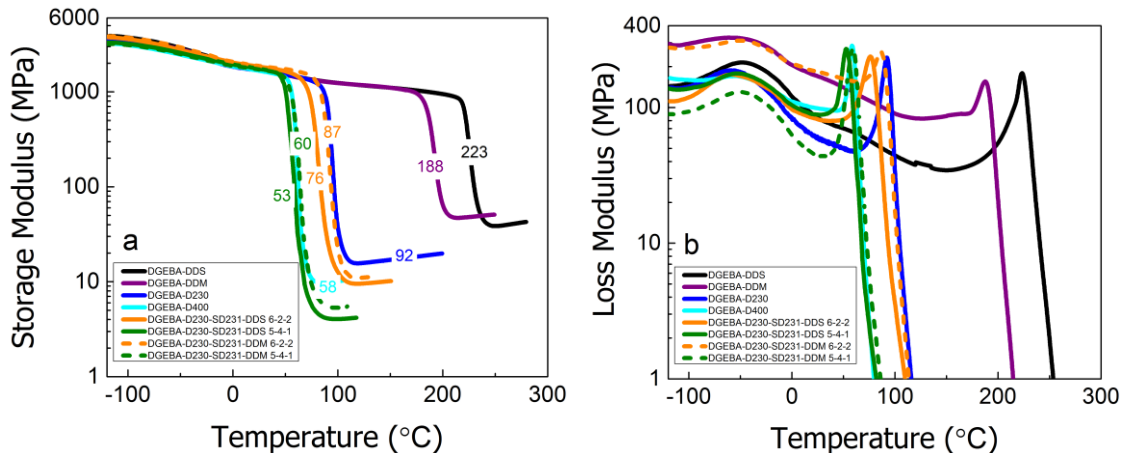


Figure 4.5 (a) Storage moduli of epoxies. The numbers on the curves are glass transition temperatures of the epoxies. (b) Loss moduli of the same epoxies.

The normalized alpha or glass transitions, and the corresponding full widths at half maximum (FWHM) are plotted in Figure 4.6(a) and 4.6(b), respectively. As in previous two chapters, the peak shapes are highly stretched and broader in the lower temperature

region. In Figure 4.6(a), some subtle differences exist in the peak amplitude at the onsets of the transitions. These will be addressed in a more quantitative manner in the next chapter.

In Figure 4.6(b), the asymmetric epoxies have slightly broader alpha transitions than DGEBA-D400, suggesting more heterogeneous network structures. However, they have similar transition widths as DGEBA-D230. The reasons for the observed phenomenon are twofold. Firstly, the aliphatic chain extender SD231 and curing agent D230 have similar stiffness. The two amines have the same number of polyetheramine repeat units as the backbones (Table 4.1). Although two amino hydrogens in D230 are replaced by isopropyl units to yield SD231, the difference in end-groups has negligible effect on overall stiffness of the reagents (see Chapter 5). Secondly, the aromatic networks in the asymmetric resins are only present in low molar fractions. In the case of symmetric epoxies illustrated in Figure 3.10(b), the alpha transition width increases toward intermediate compositions, and is the broadest when the two constituents exist in nearly equal amounts.

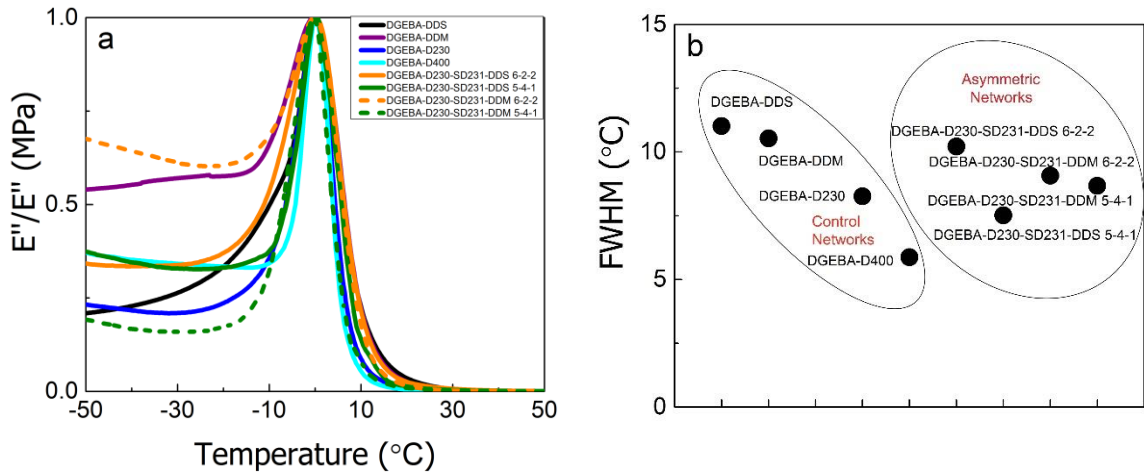


Figure 4.6 (a) Normalized alpha transition, (b) Full width at half maximum (FWHM) of the transitions.

Shown in Figure 4.7(a) are the storage and loss moduli of DGEBA-D230-SD231-DDM 5-4-1 resins without and with prestress. Although 70% compressive strain is imposed

on the asymmetric resin compared to 50% on the symmetric epoxies in Chapter 3, no effect of further prestressing is detected in storage moduli or T_g values. Again, these diminished responses compared to the prestressed elastomers commented in Chapter 3 are probably due to limited degree of orientation that can be achieved in more highly crosslinked epoxies before fracture occurs. The widths of the corresponding alpha transitions in Figure 4.7(b) are largely unaffected by the presence or removal of latent free energy since a difference of 2 °C in the full width at half maximum (FWHM) is within data scatter. These results are also consistent with the dynamic mechanical behavior of Prestress Double Network epoxies in Chapter 3. As shown in Figure 3.10(b), the alpha transition widths are insensitive to prestressing at low molar fractions of the aromatic network.

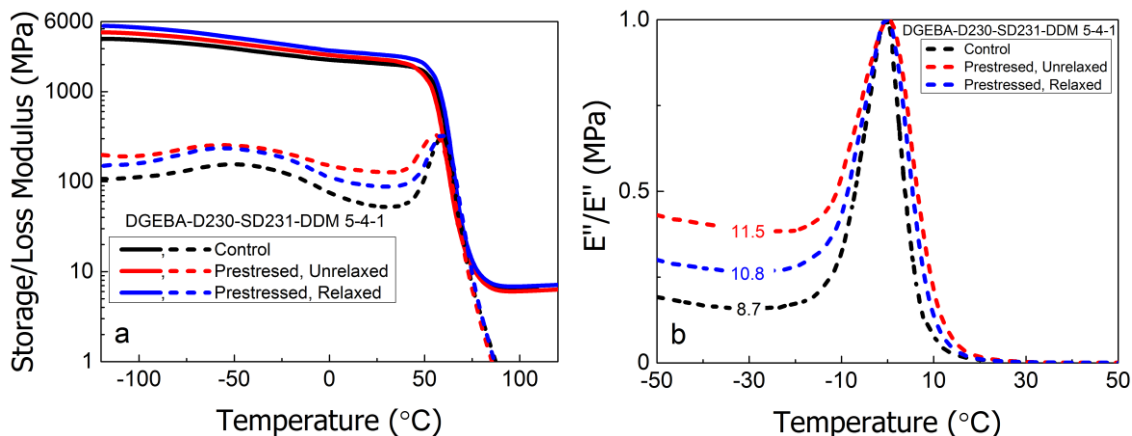


Figure 4.7 (a) Storage moduli (solid lines) and loss moduli (dash lines) of DGEBA-D230-SD231-DDM 5-4-1 resins without and with prestress, (b) Normalized alpha transitions of the same epoxies. The numbers on the curves are the full widths at half maximum (FWHM) of the transitions.

In agreement of the DSC measurements, the T_g of prepolymer-based DGEBA-Aniline-D230-SD231-DDM 5-4-1 is about 20 °C higher than the asymmetric epoxies with the same amine hydrogen ratio (Figure 4.8). The increase in T_g imparted by the incorporation of rigid anilines again outweighs the plasticization effect of chain extending

the monomer DGEBA. However, the prepolymer-based resin has the same storage modulus as DGEBA-D230 (Table 4.3). The result suggests that the molecular packing which dictates the linear property remains unaffected with the substitution of the diepoxide monomer DGEBA by the prepolymer.

The beta transition of the prepolymer-based resin shown in Figure 4.8 is at around $-60\text{ }^{\circ}\text{C}$, which is characteristic of DGEBA-based epoxies^{3,42,65}. The alpha transition is located at $83\text{ }^{\circ}\text{C}$ and has a transition width of $17.1\text{ }^{\circ}\text{C}$. The width is almost twice as broad as the asymmetric resins in Figure 4.6(b). The result is consistent with Topologically Heterogeneous Network epoxies in Chapter 2, and suggests that the use of chain-extended prepolymer results in significantly more heterogeneous network structure.

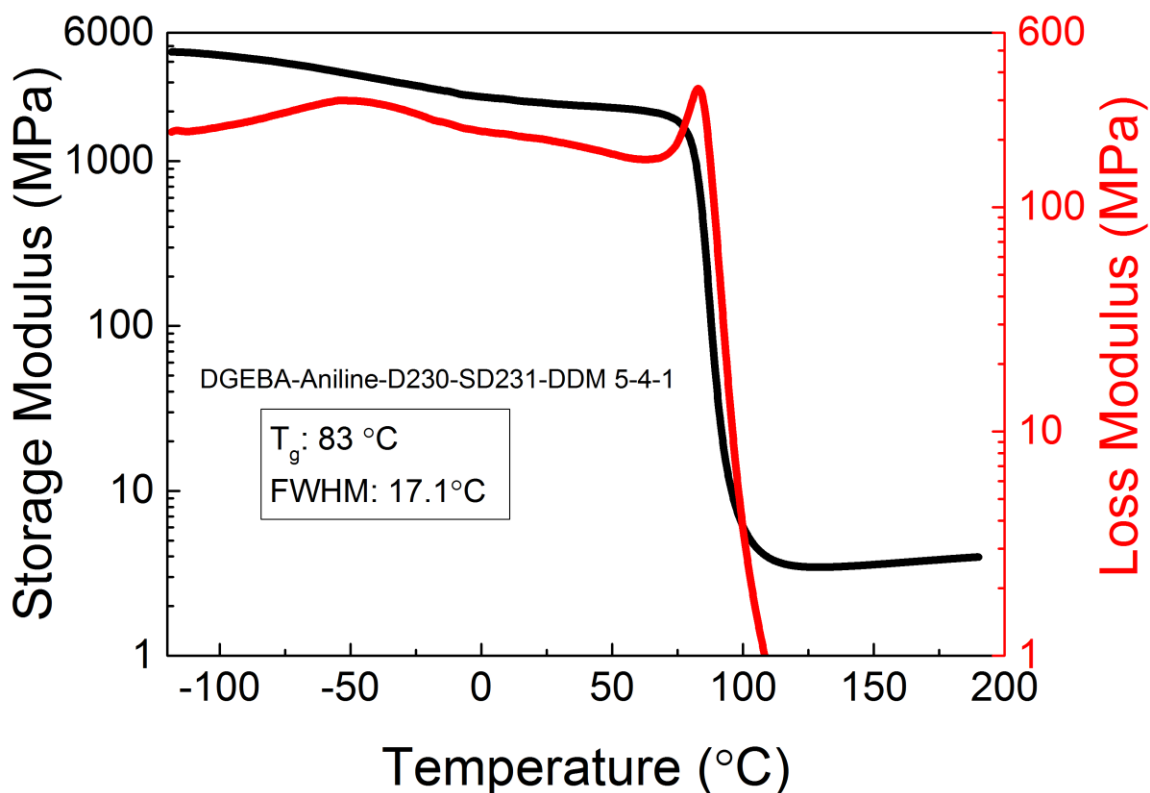


Figure 4.8 Storage and loss moduli of DGEBA-Aniline-D230-SD231-DDM 5-4-1.

4.3.4 Compressive Behavior

Plotted in Figure 4.9(a) are the stress-strain curves of partially cured asymmetric resins. DGEBA-D230-DDS 5-5 from previous work¹⁶ is also included in the figure as the control sample. The numbers next to the curves are the corresponding molecular weight between crosslinks (M_c 's) of the *aliphatic networks*. The curves of asymmetric epoxies with amine hydrogen ratio of 6-2-2 overlap almost exactly. The resins show little improvement in ductility. Like DGEBA-D230-DDS 5-5, they fail almost immediately when deformed beyond 50% compression ratio. DGEBA-D230-SD231-DDS 5-4-1 has a 10% better strain to break. In marked contrast, DGEBA-D230-SD231-DDM 5-4-1 shows significantly more ductile behavior. It fails at around 15% compression ratio, or 85% compressive strain. The enhanced extensibility is probably due to the lack of hydrogen bonding between the unreacted DDM molecules and the hydroxyl groups generated from the opening of the oxirane rings on the epoxide monomers. The particular formulation is therefore the most promising for the synthesis of prestressed asymmetric epoxy.

In order to synthesize the prestressed epoxy, partially cured DGEBA-D230-SD231-DDM 5-4-1 is compressed by 80% strain after heating above its T_g . The aromatic network is then introduced in the deformed state. Upon release of the load, however, only 70% compressive strain is retained in the unrelaxed resins due to large elastic recovery in thickness.

Plotted in Figure 4.9(b) are the stress-strain curves of postcured asymmetric resins and the control samples. The numbers next to the curves are the *average* M_c 's of the resins. The curves of asymmetric epoxies with the same amine hydrogen ratio overlap almost exactly until reaching the rejuvenated stresses. Afterward the DDM-based formulations

show earlier onset of upturn in stress than the DDS-based formulations. The same behavior is observed between the control samples DGEBA-DDM and DGEBA-DDS. The difference is due to higher crosslink density of the aromatic network prepared from DDM than that from DDS (Table 4.2). The polymer chains in a more crosslinked network approach their extensibility limit faster, leading to faster onset of strain hardening⁶⁶.

As shown in Figure 4.9(b), the strain at break increases with the increase in M_c . For the symmetric epoxies with the same crosslink densities, DGEBA-DDS, DGEBA-D230-DDS 5-5, and DGEBA-D230, the strain at break also increases with the increase in the molar fraction of the flexible aliphatic networks. These improvements in extensibility are expected since the motion of the polymer chains are less restricted compared to more crosslinked or rigid structures. In fact, some asymmetric network test specimens with 5-4-1 formulation can reach 73% compressive strain and sustain 48 kiloNewtons (kN) without forming any visible cracks or catastrophic failures.

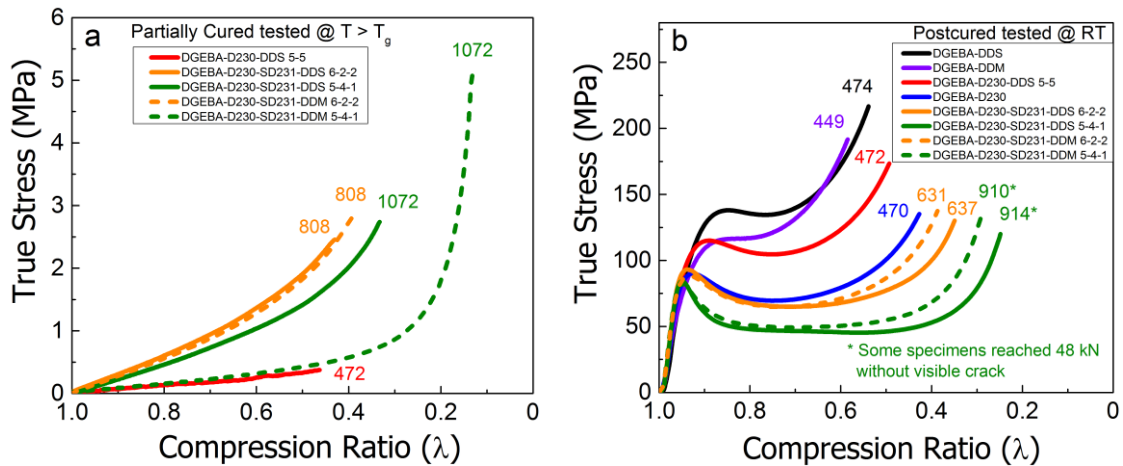


Figure 4.9 (a) Stress-strain curves of partially cured resins. The numbers next to the curves are molecular weights between crosslinks of the aliphatic networks. (b) Stress-strain curves of postcured resins. The numbers next to the curves are the average molecular weights between crosslinks of the epoxies.

The compressive properties of the postcured resins are listed in Table 4.3. The elastic moduli (E 's) obtained from the compression test show the same trend as the storage moduli measured at 20 °C by DMA. Again, the reasons that the asymmetric epoxies have the same moduli as DGEBA-D230 are twofold. Firstly, the chain extender SD231 has similar stiffness as the aliphatic curing agent D230. Secondly, only low molar fractions of aromatic networks are present.

In agreement with previous work^{12,13}, the yield stresses (σ_y 's) of most epoxies listed in Table 4.3 decrease with the decrease in T_g . Although the asymmetric epoxies with amine hydrogen ratio of 6-2-2 have about 10 °C lower T_g values than DGEBA-D230, they have similar yield stresses as the control sample. This discrepancy is probably due to their faster physical aging kinetics. The resins are closer to their equilibrium states because of the smaller differences between their T_g 's and room temperature²¹. Their network segments are expected to have higher mobility than those in DGEBA-D230. Consequently, the accelerated densification of the epoxies manifested itself as apparently higher yield stresses²⁷.

The rejuvenated stresses (σ_r 's) decrease with decreasing T_g for all epoxies. The result suggests that σ_r is an intrinsic network characteristic unaffected by prior thermal history or physical aging. This is consistent with previous findings with entangled thermoplastics^{27,25}.

With the decrease in T_g , the extent of strain softening ($\sigma_y - \sigma_r$) increases, and the strain hardening moduli (G_R) decrease. According to Govaert and coworker²⁷, severe strain localization are expected for the asymmetric epoxies. However, they are actually more ductile than DGEBA-DDS and DGEBA-DDM, which have much smaller strain softening

and higher G_R . As illustrated in Figure 3.11 and 3.12, DGEBA-DDS behaves in a very brittle manner when tested in tension and has low fracture toughness. Unlike the Topologically Heterogeneous Networks epoxies in Chapter 2, a more quantitative description of strain localization is necessary for comparing epoxies with more diverse range of stiffness and crosslink densities. More detailed discussion is presented in Chapter 5.

Table 4.3 Physical properties of the epoxies.

Resin	DSC	DMA	Compression				
	T_g	$E' @ 20\text{ }^\circ\text{C}$ (GPa)	E (GPa)	σ_y (MPa)	σ_r (MPa)	$\sigma_y - \sigma_r$ (MPa)	G_R (MPa)
DGEBA-DDS	219	2.71	2.61	138	135	3	162
DGEBA- DDM	183	2.67	2.42	118	118	0	154
DGEBA-D230-DDS 5-5	145	2.65	2.78	115	105	10	120
DGEBA-D230	86	2.60	2.90	89	70	19	79
DGEBA-D230-SD231-DDS 6-2-2	74	2.90	2.81	92	64	28	66
DGEBA-D230-SD231-DDM 6-2-2	77	2.94	2.79	89	66	23	79
DGEBA-D230-SD231-DDS 5-4-1	48	2.76	2.91	84	45	39	46
DGEBA-D230-SD231-DDM 5-4-1	52	2.71	2.91	83	49	34	66
DGEBA-D400	50	2.64	2.68	73	45	28	76
DGEBA-Aniline-D230-SD231-DDM 5-4-1	71	2.59	2.99	94	62	32	54

In Figure 4.10, true stress is plotted against neo-hookian strain for the postcured resins with the same T_g values. The stress-strain curve of DGEBA-Aniline-D230-SD231-

DDM 5-4-1 is also included in the figure. The numbers next to the curves are again *average* M_c 's of the resins. Compared to DGEBA-D400, the asymmetric epoxies with the same T_g value of about 50 °C have similar elastic moduli and rejuvenated stresses but higher yield stresses and lower strain hardening moduli. As discussed in the previous paragraph, the apparently more severe strain localization of the asymmetric resins is accompanied by much better extensibility. This discrepancy will be addressed using a compression-based ductility parameter in Chapter 5.

Some test specimens of DGEBA-Aniline-D230-SD231-DDM 5-4-1 can also sustain 48 kN without fracturing. Compared to the other asymmetric epoxies with the same amine hydrogen ratio, the prepolymer-based resin has similar elastic and strain hardening moduli (Table 4.3). These are some rather interesting results since DGEBA-Aniline-D230-SD231-DDM 5-4-1 is only half as crosslinked. As discussed in the DSC section, however, the plasticization effect of using longer prepolymer is overcome by the increase in stiffness imparted by the incorporation of rigid aniline. The prepolymer-based resin also has the same extent of strain softening as the asymmetric epoxies with amine hydrogen ratio of 5-4-1, despite its higher yield and rejuvenated stresses (Table 4.3). The results suggest that the additional chemical heterogeneity introduced by replacing the monomer DGEBA with the prepolymer produces a stronger, higher- T_g epoxy while maintaining the elastic modulus and strain localization response.

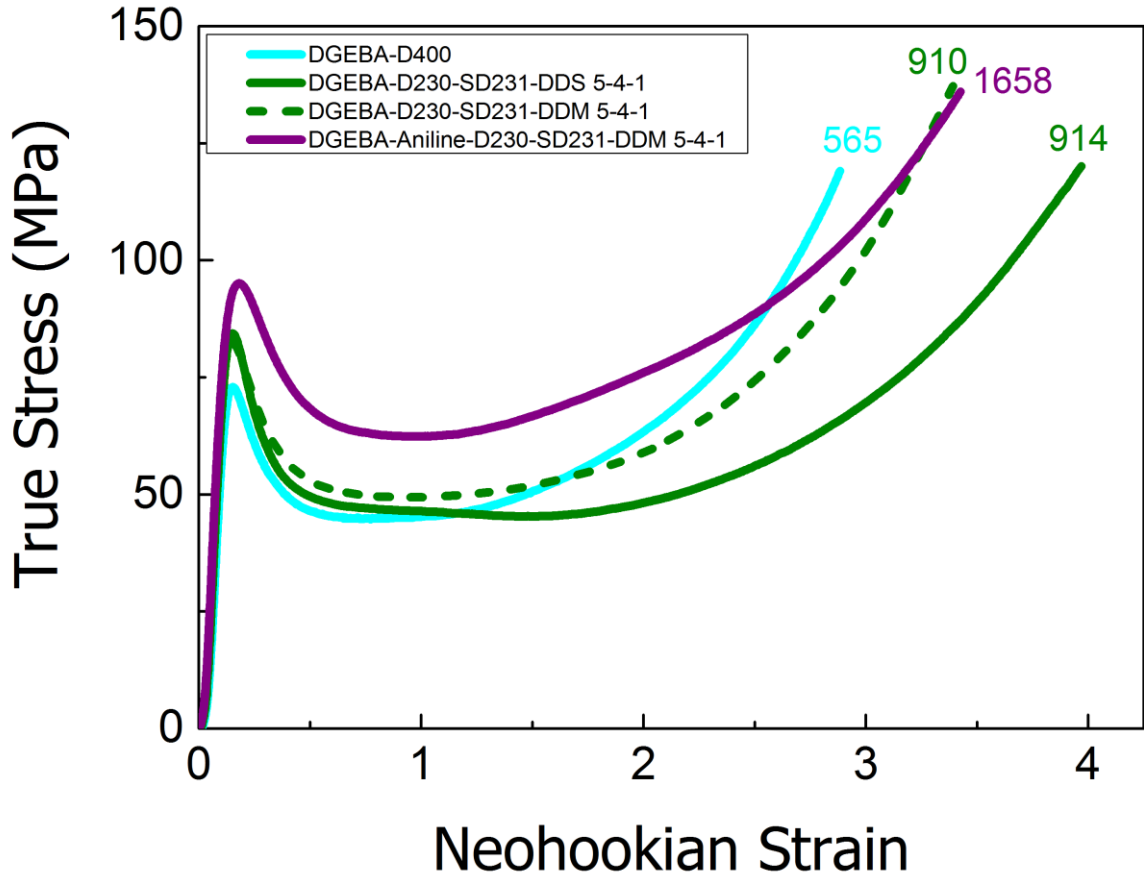


Figure 4.10 Stress-strain curves of postcured resins with the same T_g values, and DGEBA-Aniline-D230-SD231-DDM 5-4-1. The numbers next to the curves are the average molecular weights between crosslinks for the epoxies.

4.3.5 Tensile Responses

Plotted in Figure 4.11(a) are the stress-strain curves of DDM-based asymmetric epoxies tested in tension. Both resins fail after yielding, like DGEBA-D230 in Figure 3.11. As illustrated in Figure 4.11(b), however, they show onsets of necking and shear band formation.

The magnitude of the tensile moduli in Table 4.4 are lower than those in Table 3.3 due to the limitation of smaller test specimen geometry. The 2-inch clip gage was too large for attachment to ASTM type IV tensile bars. The displacements recorded by the Instron

crosshead were therefore used to calculate the strain. The two DDM-based asymmetric epoxies again have the same modulus (Table 4.4), since the linear property is dictated by the major constituents or aliphatic networks with similar stiffness.

The yield stresses obtain from uniaxial tension test (Table 4.4) are lower than those from uniaxial compression (Table 4.3), because of lower hydrostatic stress experienced by the test specimens^{8,9,21}. As in Figure 4.9(b), however, DGEBA-D230-SD231-DDM 6-2-2 has a higher yield stress than the 5-4-1 formulation. This is due to its higher T_g , or less severe plasticization by the chain extender SD231.

As shown in Figure 4.11(a), the 6-2-2 formulation also has a higher failure strain. This result appears to agree with less severe strain localization of the epoxy (Table 4.3). However, it is inconsistent with its lower compressive extensibility in Figure 4.9(b). The premature failure of DGEBA-D230-SD231-DDM 5-4-1 in tension is probably due to flaws in the test specimens that act as stress concentrators.

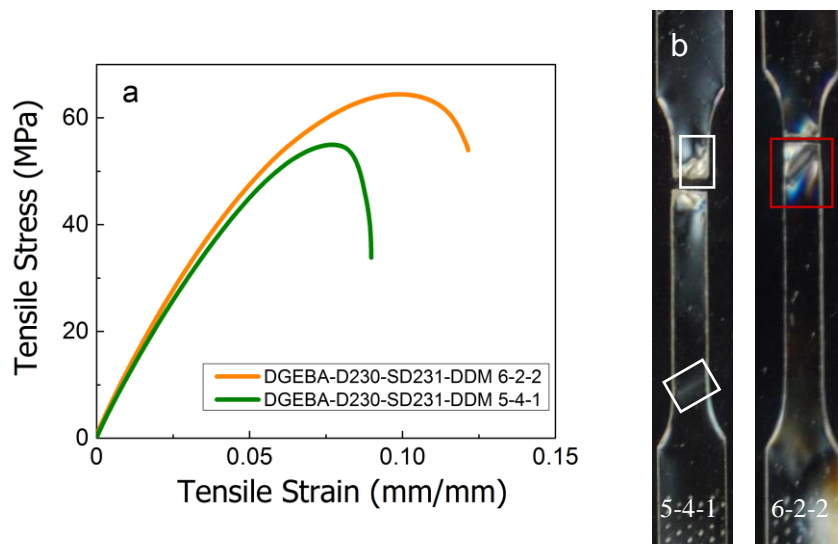


Figure 4.11 (a) Stress-strain curves of DDM-based asymmetric networks tested in tension, (b) Polarized images of tensile bars after test. 5-4-1 & 6-2-2: amine hydrogen ratio of the curing agents D230-SD231-DDM. The boxed regions indicate the onsets of necking and shear banding.

Table 4.4 Tensile properties of DDM-based asymmetric epoxies.

Resin	E (GPa)	σ_y (MPa)	ϵ_b (mm/mm)
DGEBA-D230-SD231-DDM 6-2-2	1.33	64	0.13 ± 0.02
DGEBA-D230-SD231-DDM 5-4-1	1.29	54	0.09 ± 0.01

4.3.6 Fracture Toughness

Plotted in Figure 4.12 are the fracture toughness of DDM-based asymmetric epoxies without and with prestress. The data points for DGEBA-Aniline-D230-SD231-DDM 5-4-1, and the symmetric epoxies in Chapter 3 are also included. The fracture toughness of DGEBA-D230-SD231-DDM 6-2-2 is the same as the symmetric epoxies without any prestress. In marked contrast, the 5-4-1 formulation without any prestress has

comparable toughness as prestressed DGEBA-D230-DDS 5-5. Unlike the tensile test discussed earlier, however, fracture toughness testing is more sensitive to intrinsic material properties since the precrack acts as the largest flaw in the compact tension specimen²⁰.

Prestressing DGEBA-D230-SD231-DDM 5-4-1 by 70% compressive strain increases the fracture toughness even further. The prestressed asymmetric epoxy is tougher than the prestressed symmetric epoxies. However, the relative toughness improvement over a resin without any prestress remains at around 30%.

The prepolymer-based resin DGEBA-Aniline-D230-SD231-DDM 5-4-1 has higher T_g , or yield stress than DGEBA-D230-SD231-DDM 5-4-1. Based on previous work^{20,38}, it is expected to have a lower fracture toughness due to smaller process zone size. As shown in Figure 4.12, however, the prepolymer-based resin is actually tougher than the asymmetric epoxy with the same amine hydrogen ratio. Unlike the Topologically Heterogeneous Network epoxies in Chapter 2, the enhanced chemical heterogeneity imparted by the incorporation of the prepolymer DGEBA-Aniline results in tougher resin with relatively high T_g .

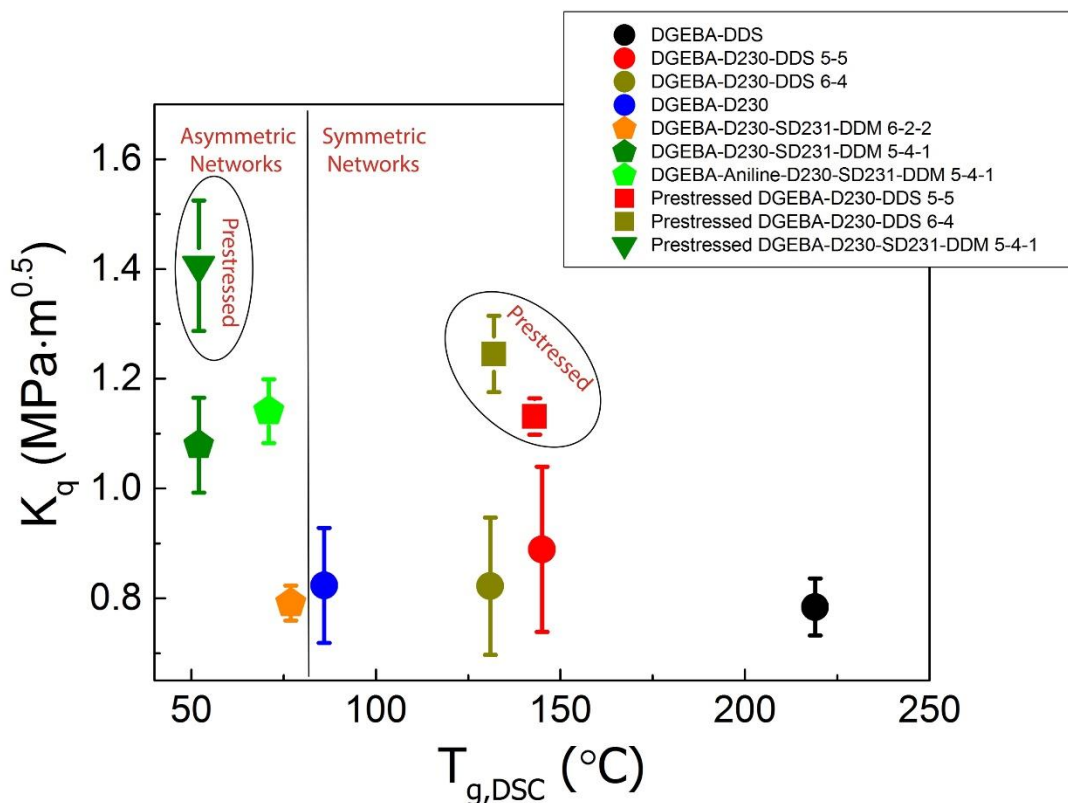


Figure 4.12 Fracture toughness of DGEBA-based epoxies.

4.4 Conclusion

This chapter presents the synthesis and characterization of Asymmetric Double Network epoxies, which consist of high molar fractions of loosely crosslinked aliphatic networks and low fractions of highly crosslinked aromatic networks. The synthesis involves the use of a chain extender SD231, which has similar stiffness as the aliphatic curing agent D230. Two structurally similar aromatic curing agents are used to examine the effect of hydrogen bonding. Combination with fabrication strategies discussed in Chapter 2 and 3 are also evaluated.

Unlike the chemical heterogeneity in Chapter 2 and the mechanical heterogeneity in Chapter 3, the asymmetric stiffness does not result in broadened alpha transition width.

Compared to the control sample with the same T_g value, the asymmetric resins are stronger and more ductile in compression. They yield and show onsets of necking when tested in tension.

The DDM-based asymmetric epoxy with 5-4-1 amine hydrogen ratio among the curing agents has the best extensibility when partially cured because of the lack of hydrogen bonding. When postcured, its fracture toughness is comparable to prestressed symmetric resin in Chapter 3. After prestressing the particular formulation by 70% compressive strain, the fracture toughness improves further. However, the relative enhancement stays the same or around 30%. Replacing the diepoxide monomer DGEBA with the prepolymer DGEBA-Aniline generates a tough epoxy with relatively high T_g .

4.5 Future work

Future investigation may focus on understanding the reaction kinetics of amines used to prepare the asymmetric networks. Isothermal cure or polymerization study may be conducted using Differential Scanning Calorimetry. In the previous effort of symmetric networks, the aliphatic curing agent D230 and aromatic curing agent DDS react at different temperatures. Consequently, sequential Interpenetrating Polymer Networks are obtained. During the synthesis of DDM-based asymmetric networks, however, some fraction of the aromatic curing agent may react during the initial cure. In order to minimize the advancement in reaction conversion during storage, the partially cured resins were kept at $-10\text{ }^\circ\text{C}$ in a freezer, and tested within 12 hours after preparation.

Furthermore, it is important to confirm that chain extension by difunctional SD231 occurs before crosslinking by tetrafunctional D230. After the two primary amine

hydrogens of D230 react with the epoxide monomers, the resulting linear oligomers are expected to be less reactive than the shorter, less hindered aliphatic chain extender SD231.

4.6 References

1. Lee, H., and Neville, K., Handbook of Epoxy Resins. McGraw-Hill, New York, (1967).
3. deNograro, F. F., Guerrero, P., Corcuera, M. A., and Mondragon, I., J Appl Polym Sci, 56, 177-192 (1995).
8. Kody, R. S., and Lesser, A. J., J Mater Sci, 32, 5637-5643 (1997).
9. Lesser, A. J., and Kody, R. S., J Polym Sci Pt B-Polym Phys, 35, 1611-1619 (1997).
12. Lesser, A. J., and Calzia, K. J., J Polym Sci Pt B-Polym Phys, 42, 2050-2056 (2004).
13. Calzia, K. J., and Lesser, A. J., J Mater Sci, 42, 5229-5238 (2007).
16. Detwiler, A. T., and Lesser, A. J., J Mater Sci, 47, 3493-3503 (2012).
20. Kinloch, A. J., and Young, R. J., Fracture Behaviour of Polymers. Applied Science Publishers, Northern Ireland, (1983).
21. Haward, R. N. (ed) The Physics of Glassy Polymers. 2nd edn. Chapman & Hall, London, (1997).
24. Shaw, M. T., MacKnight, W. J., Introduction to polymer viscoelasticity. 3rd edn. John Wiley & Sons, Hoboken, (2005).
25. van Breemen, L. C. A., Engels, T. A. P., Klompen, E. T. J., Senden, D. J. A., and Govaert, L. E., J Polym Sci Pt B-Polym Phys, 50, 1757-1771 (2012).
27. van Melick, H. G. H., Govaert, L. E., and Meijer, H. E. H., Polymer, 44, 3579-3591 (2003).
38. Crawford, E. D., and Lesser, A. J., Polym Eng Sci, 39, 385-392 (1999).
42. Heux, L., Halary, J. L., Laupretre, F., and Monnerie, L., Polymer, 38, 1767-1778 (1997).

59. Gong, J. P., Katsuyama, Y., Kurokawa, T., and Osada, Y., *Adv Mater* (Weinheim, Ger), 15, 1155-1158 (2003).
60. Huang, M., Furukawa, H., Tanaka, Y., Nakajima, T., Osada, Y., and Gong, J. P., *Macromolecules*, 40, 6658-6664 (2007).
61. Tanaka, Y., *EPL*, 78, 56005 (2007).
62. Webber, R. E., Creton, C., Brown, H. R., and Gong, J. P., *Macromolecules*, 40, 2919-2927 (2007).
63. Na, Y. H., Tanaka, Y., Kawauchi, Y., Furukawa, H., Sumiyoshi, T., Gong, J. P., and Osada, Y., *Macromolecules*, 39, 4641-4645 (2006).
64. Ducrot, E., Chen, Y., Bulters, M., Sijbesma, R. P., and Creton, C., *Science*, 344, 186-189 (2014).
65. Dammont, F. R., and Kwei, T. K., *J Polym Sci A-2*, 5, 761-769 (1967).
66. Treloar, L. R. G., *The physics of rubber elasticity* Oxford University Press, New York, (2005).

CHAPTER 5

DUCTILITY AND GOVERNING PARAMETERS

5.1 Introduction

The objective of this chapter is to further examine the structure-process-property relationships of the epoxies presented in the last three chapters. The focus is on understanding the connections of heterogeneous network architectures with fracture toughness and post-yield responses. Ductility parameters are proposed based on dynamic mechanical spectroscopy and compression test. Furthermore, glass transition temperature (T_g) and cohesive energy density (E_c) are used to correlate with non-linear mechanical properties.

5.1.1 DMA-based Ductility Parameter

In their work²⁵, Govaert and coworkers treat the beta and alpha transitions as simple delta functions. As illustrated in Figure 5.1(a), only the differences between the test temperature (T_{test}) and the peak temperatures of the dynamic mechanical transitions (T_β and T_α) are considered. As discussed in Chapter 2 through Chapter 4, however, distinct differences are observed in transition width, intensity, and peak shape due to molecular heterogeneity. In order to account for such variations in mechanical spectra or segmental mobility in a more quantitative manner, a dimensionless ductility parameter is proposed based on a weighted integral approach depicted in Figure 5.1(b).

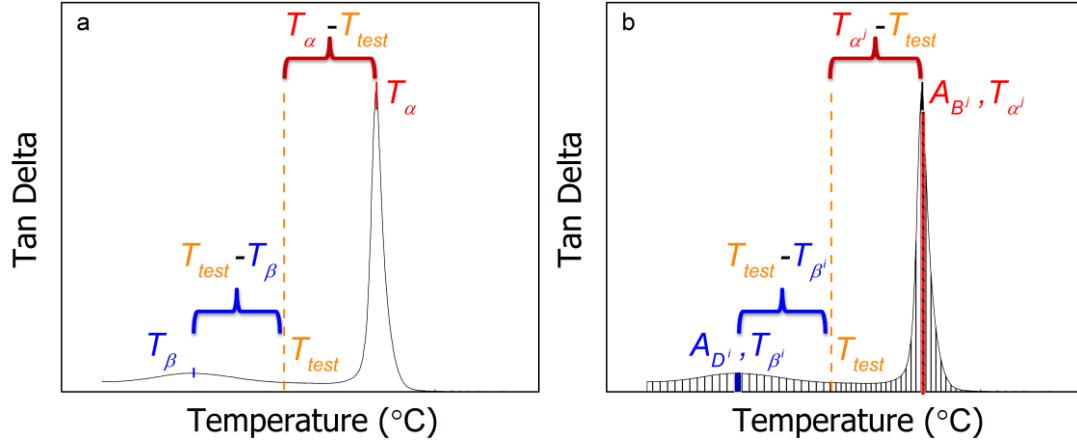


Figure 5.1 (a) Delta function approach; (b) Weighted integral approach.

The weighted integral approach involves tan delta, which is the dimensionless ratio of loss modulus to storage modulus. Polymers tend to become more ductile with increasing temperature, and more brittle with decreasing temperature. Hence, the areas under the tan delta curve is divided into two regions with respect to T_{test} . As shown in Figure 5.1(b), the regions below and above T_{test} are referred to as the ductile and brittle contributions (A_D and A_B), respectively. Previous studies suggest linear dependence of mechanical properties on temperature^{13,25,67}. Therefore, each integral in the two regions A_D and A_B is weighted by its proximity to T_{test} . The ductility parameter d is then defined as the ratio between the sums of the weighted integrals.

$$d \equiv \frac{\sum_{i=1}^{i=n} A_{D^i} \cdot |T_{test} - T_{\beta^i}|}{\sum_{j=1}^{j=m} A_{B^j} \cdot |T_{\alpha^j} - T_{test}|} \quad (5.1)$$

The beta transition has been commonly modeled as a thermally activate process^{68,69}. In a typical DMA experiment, the storage modulus continuously increases with decreasing temperature. However, the tan delta of an epoxy does not reach zero even at -150 °C, or

the lower temperature limit of the DMA instrument. A baseline correction is therefore applied before integrating a spectrum. The procedure is illustrated in Figure 5.2. The onset of beta transition is defined as the intersection point of the raw data curve and a Gaussian-type fitting function. A baseline connecting the onset of beta transition and the end of alpha transition is then subtracted from the raw data curve, after removing data points outside the two limits.

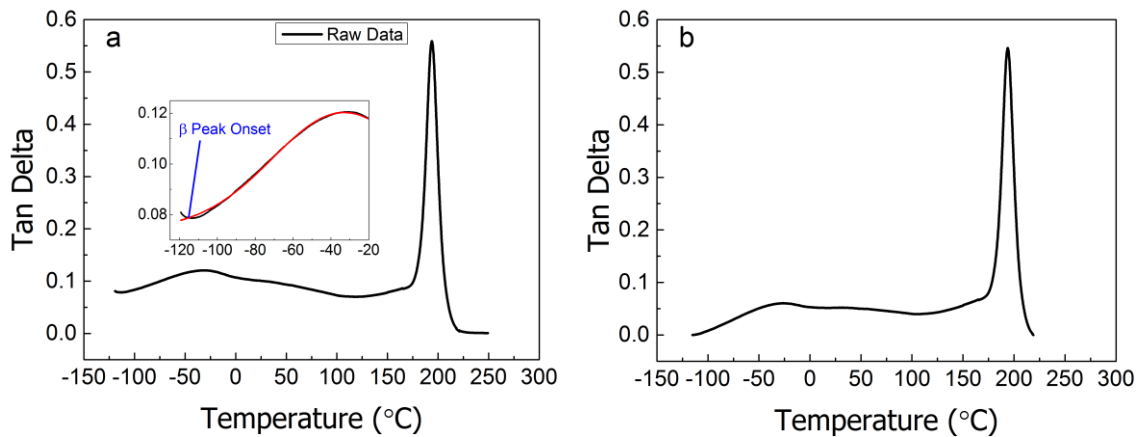


Figure 5.2 (a) Before baseline subtraction. Inset shows how the onset of beta transition is defined; (b) After baseline subtraction.

5.1.2 Compression-based Ductility Parameter

According to Haward and Thackray, the mechanical behavior of glassy polymers can be decomposed into elastic and viscous contributions³⁰. They argued that the initial response is controlled by intermolecular forces, and the post-yield response is dictated by an entropic network. A neck stability criteria incorporating the yield stress and strain hardening modulus is correlated with the strength of polymer in tension²¹. Govaert and coworkers has extended the criteria further by introducing a strain localization factor that includes the effects of thermal treatment and mechanical history²⁷. Good agreement is

observed in engineering thermoplastic²⁷, but limited success is found with thermosets due to their highly crosslinked structures³².

When tested in tension, epoxies tend to fail without forming a neck. With the asymmetric networks in Chapter 4, however, shear banding is observed [Figure 4.11(b)]. The shear band stability criteria from an earlier study⁵⁸ is therefore more appropriate for thermosets.

$$\frac{\sqrt{2}\sigma_r}{3G_R} = \frac{\lambda_E - 1/\lambda_E}{K_y - 1} \quad (5.2)$$

where σ_r is the rejuvenated stress, G_r is the strain-hardening modulus, K_y is the ratio of yield stress to rejuvenated stress, and λ_E is the equilibrium factor or orientation needed to stabilize the shear band. The equation is based on the force equilibrium between materials inside and far away from the shear band.

A kinematic approach is also considered. Although the compressive strain at break do not reflect the strength of thermoplastics²⁷, it reveals the extensibility limit of thermosets. The kinematic factor λ_K is taken as the maximum displacement expressed in term of neo-hookian strain.

$$\lambda_K = \lambda^2 - 1/\lambda \quad (5.3)$$

where λ is the compression ratio at break.

The compression-based ductility parameter is defined as the ratio λ_E/λ_K . The parameter accounts for the effects of shear banding and finite extensibility. It is used to correlate the non-linear properties with fracture toughness of epoxies.

5.1.3 Glass Transition Temperature and Cohesive Energy Density

Calzia and Lesser demonstrated that the glass transition temperature (T_g) and cohesive energy density (E_c) are two molecular parameters that govern the yield response of epoxies^{12,13}. The T_g reflects network stiffness, and the values were obtained from differential scanning calorimetry (DSC). The E_c reveals network strength, and the values were obtained from numerical simulation involving energy minimization of an amorphous cell with 6 network repeat units. Both parameters include the effects of backbone stiffness, crosslink density, crosslinker functionality, and intermolecular interactions.

Jones and coworkers⁷⁰ also independently reported that the yield stress of epoxies is dictated by E_c . They utilized a group interaction theory that involved reduction of degree of freedom from crosslinking. The E_c values were estimated using the cohesive energies (E_{coh} 's) and molar volumes (V 's) previously tabulated by Fedors for different chemical structure units⁷¹. Jones and coworker also applied their theory to predict elastic modulus, and coefficient of thermal expansion⁷².

5.2 Experimental

The DMA, compression, and fracture toughness testing results of epoxies in Chapter 2 through 4 were re-examined using ductility parameters proposed in the introduction section of this chapter. TGDDM-Aniline was not included in the discussion due to incomplete conversion (see Chapter 2).

In this investigation, E_c was estimated using Fedors' group contribution theory with the same network repeat units assumed by Equation 2.1 for calculating the molecular weight between crosslinks. The E_{coh} and V for the functional group SO_2 were extrapolated

since the values were not tabulated by Fedors. The temperature of compression testing, 25 °C or 298 K, was normalized by T_g values obtained from DSC measurements.

5.3 Results and Discussion

5.3.1 DMA-based Ductility Parameter

In Figure 5.3(a), a linear correlation is observed between yield stress (σ_y) and the DMA-based ductility parameter. In Figure 5.3(b), with the inclusion of prestressed resins, a reverse but linear correlation is obtained for fracture toughness (K_q). A resin with lower yield stress is expected to have higher fracture toughness due to larger process zone or damage-accumulation region in front of the crack tip^{20,38}.

In Figure 5.4, The size of the process zone is estimated using $(K_q/\sigma_y)^2$. A correlation with $R^2 = 0.72$ is obtained. The results in Figure 5.3 and 5.4 are in fact rather surprising. The ductility parameter is based on DMA measurements made at very small strain or 0.1%. However, yielding and fracture occur at much larger strains. The reason may be associated with the similarity in segmental motions induced by thermal force and mechanical deformation⁶⁷. However, further refinement of the weighted integral approach is needed to reduce the data scattering. Investigation of the effect of strain rate or test frequency is outside the scope of this work.

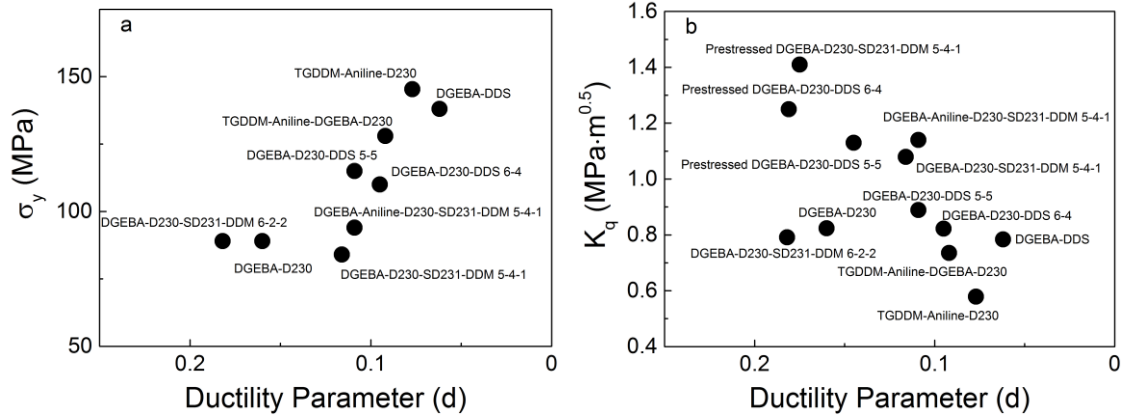


Figure 5.3 Correlations between the DMA-based ductility parameter and (a) yield stress; (b) fracture toughness.

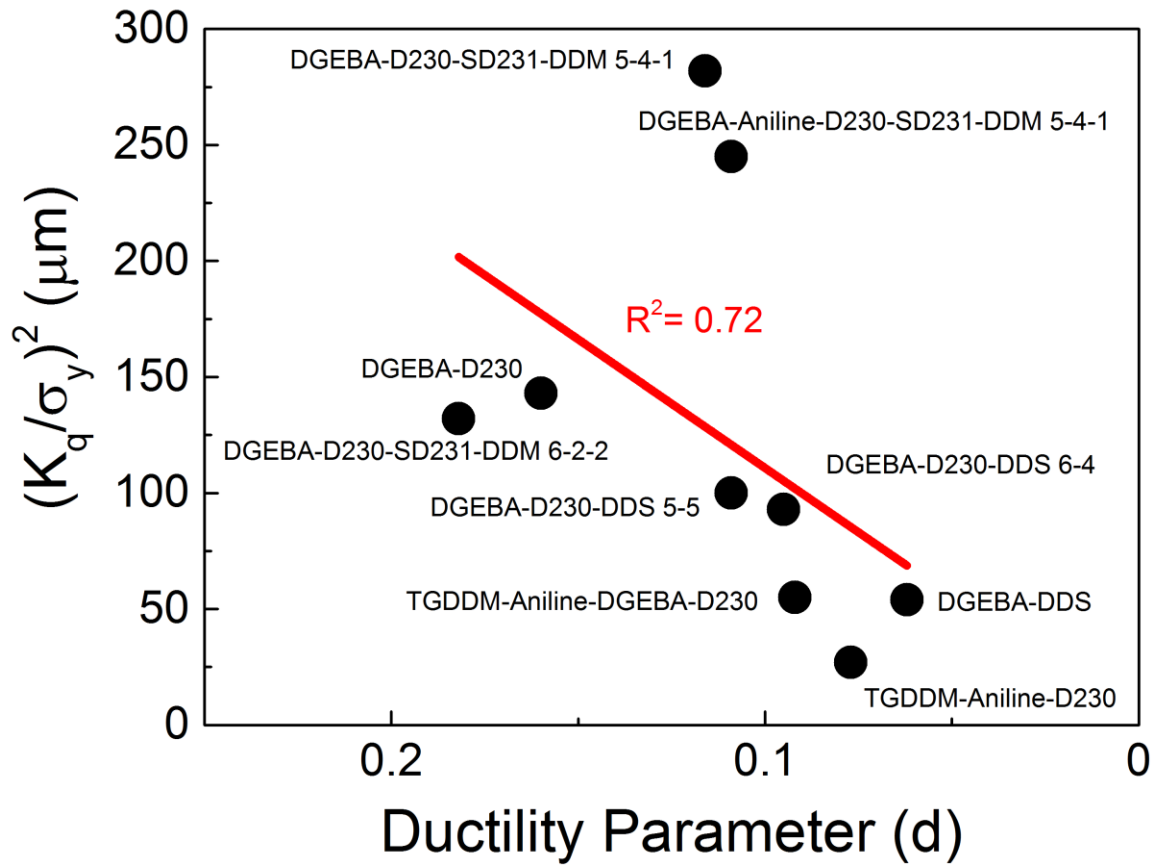


Figure 5.4 Correlation between the DMA-based ductility parameter and process zone size.

5.3.2 Compression-based Ductility Parameter

Almost the same linear correlation is observed in Figure 5.5(a) and 5.5(b), except that the apparent slope of the trend line is steeper with the equilibrium factor (λ_E) than with the kinematic factor (λ_K). Plotting the estimated process zone size against the compression-based ductility parameter λ_E / λ_K produces a better correlation that further separates the resins with close values of λ_E or λ_K . The ratio λ_E / λ_K is a fundamentally better parameter since it incorporates both equilibrium and kinematic considerations. Compared to the DMA-based parameter, the compression-based parameter provides a better correlation, with $R^2 = 0.91$.

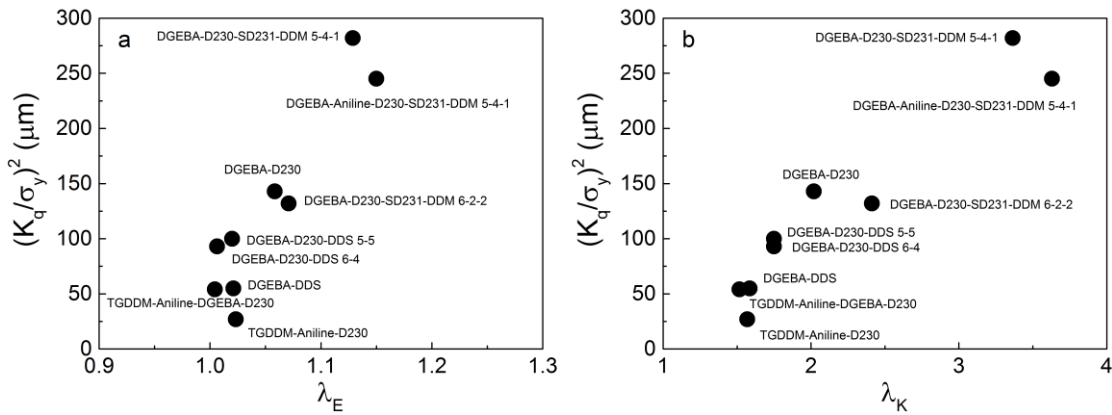


Figure 5.5 Correlations between estimated process zone size and (a) equilibrium factor; (b) kinematic factor.

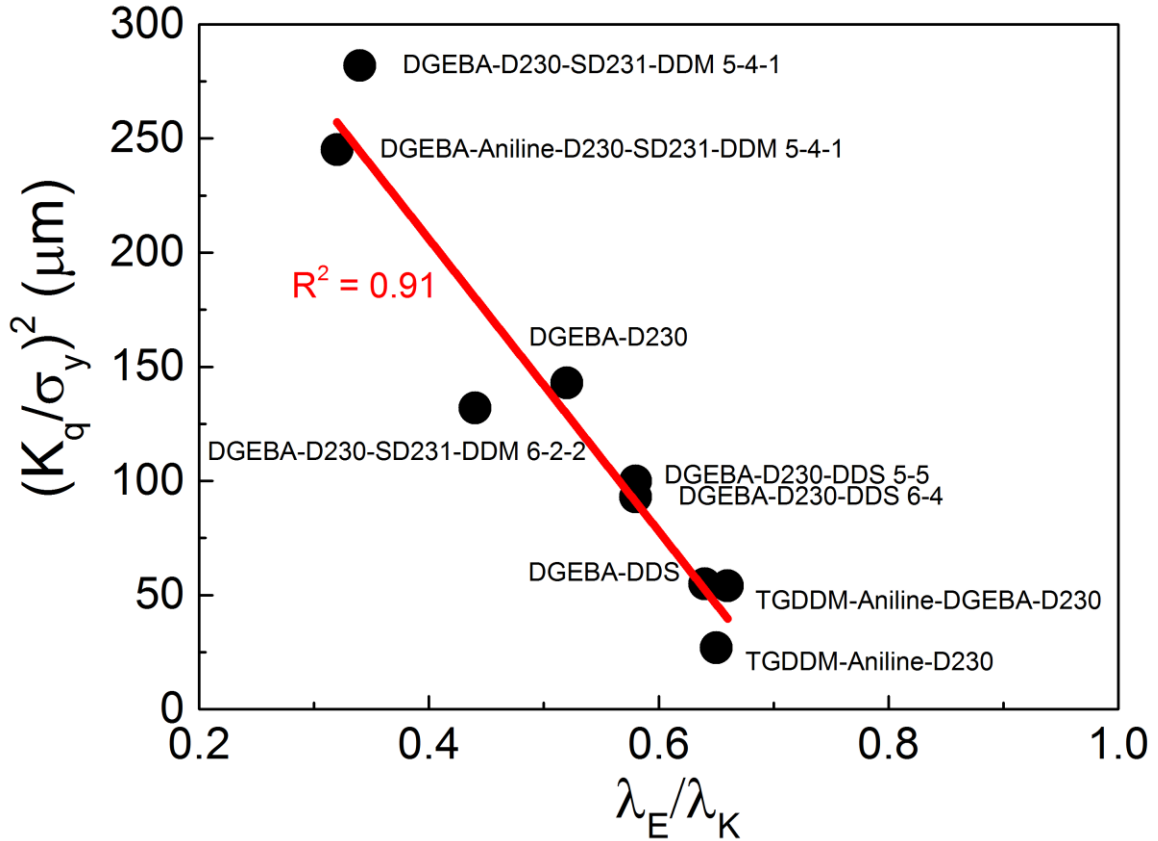


Figure 5.6 Correlation between estimated process zone size and compression-based ductility parameter λ_E/λ_K .

5.3.3 Glass Transition Temperature and Cohesive Energy Density

The cohesive energy (E_{coh}), molar volumes (V), and cohesive energy densities (E_c) of all the reagents used in previous chapters are given in Table 5.1. As expected, the more rigid tetrafunctional epoxide TGDDM has higher E_c than the flexible diepoxide DGEBA. In general, the aromatic amines have higher E_c than the aliphatic amines because of the stiff phenyl ring. Compared to DDM, the curing agent DDS has much higher E_c because of the polar SO_2 group that can participate in hydrogen bonding. In contrast, D230 has similar stiffness as D400 and the chain extender SD231.

Table 5.1 Physical properties of the reagents.

Reagents	MW (g/mol)	E_{coh} (J/mol)	V (cm ³ /mol)	E_c (J/cm ³)
DGEBA	350	118527	236	502
TGDDM	450	154354	258	598
DDS	248	114520	163	704
DDM	198	93940	159	590
Aniline	93	44500	91	491
D230	240	79275	218	364
D400	450	138423	407	340
SD231	315	96595	321	301

The molecular weight between crosslinks (M_c 's), and cohesive energy densities (E_c 's) of the epoxies studied in Chapter 2 to 4 are given in Table 5.2 through 5.4. The Topologically Heterogeneous Network (THN) epoxies do not have a clear correlation between their structures and E_c (Table 5.2). The Double Network (DN) epoxies have the same M_c , but their E_c increase with increasing aromatic content or backbone stiffness (Table 5.3). The Asymmetric Networks (AN) with amine hydrogen ratio of 5-4-1 have about the same T_g and E_c as DGEBA-D400, and DGEBA-D230-D2000 8.9-1.1 (Table 5.2 and 5.4).

Table 5.2 Molecular weights between crosslinks, and cohesive energy densities of Topologically Heterogeneous Networks.

Topologically Heterogeneous Networks (THN)	M_c (g/mol)	E_c (J/cm ³)
DGEBA-D400	565	427
DGEBA-D230-D2000 8.9-1.1	567	429
TGDDM-D230	345	491
TGDDM-Aniline	315	554
TGDDM-Aniline-D230	332	563
TGDDM-Aniline-DGEBA-D230	363	534

Table 5.3 Molecular weights between crosslinks, and cohesive energy densities of Double Networks.

Double Networks (DN)	M_c (g/mol)	E_c (J/cm ³)
DGEBA-D230	470.0	458
DGEBA-D230-DDS 9-1	470.4	467
DGEBA-D230-DDS 8-2	470.8	476
DGEBA-D230-DDS 7-3	471.2	485
DGEBA-D230-DDS 6-4	471.7	495
DGEBA-D230-DDS 5-5	472.1	504
DGEBA-D230-DDS 4-6	472.5	514
DGEBA-D230-DDS 3-7	472.9	524
DGEBA-D230-DDS 2-8	473.3	534
DGEBA-D230-DDS 1-9	473.7	544
DGEBA-DDS	474.2	554

Table 5.4 Molecular weights between crosslinks, and cohesive energy densities of Asymmetric Networks.

Asymmetric Networks (AN)	M_c (g/mol)	E_c (J/cm ³)
DGEBA-D230-SD231-DDS 5-4-1	914	428
DGEBA-D230-SD231-DDM 5-4-1	910	426
DGEBA-D230-SD231-DDS 6-2-2	637	453
DGEBA-D230-SD231-DDM 6-2-2	631	448
DGEBA-Aniline-D230-SD231-DDM 5-4-1	1648	528
DGEBA-DDM	449	524

In Figure 5.7, E_c appears to increase with decreasing M_c . However, no correlation is expected since M_c is estimated using Equation 2.1, which is based purely on network connectivity. In contrast, E_c incorporates the effects of backbone stiffness and intermolecular interactions.

In Figure 5.8 and 5.9, the yield stress (σ_y), rejuvenated stress (σ_r), and strain hardening modulus (G_R) are normalized by E_c and plotted against T/T_g . Data points from Detwiler and Lesser¹⁶ are also included for comparison. The correlation between σ_y and E_c is in agreement with previous work^{13,70}. The correlations with σ_r and G_R suggest that post-yield responses are also governed by T_g and E_c . The larger scattering in Figure 5.9 may be indicative of the network heterogeneity.

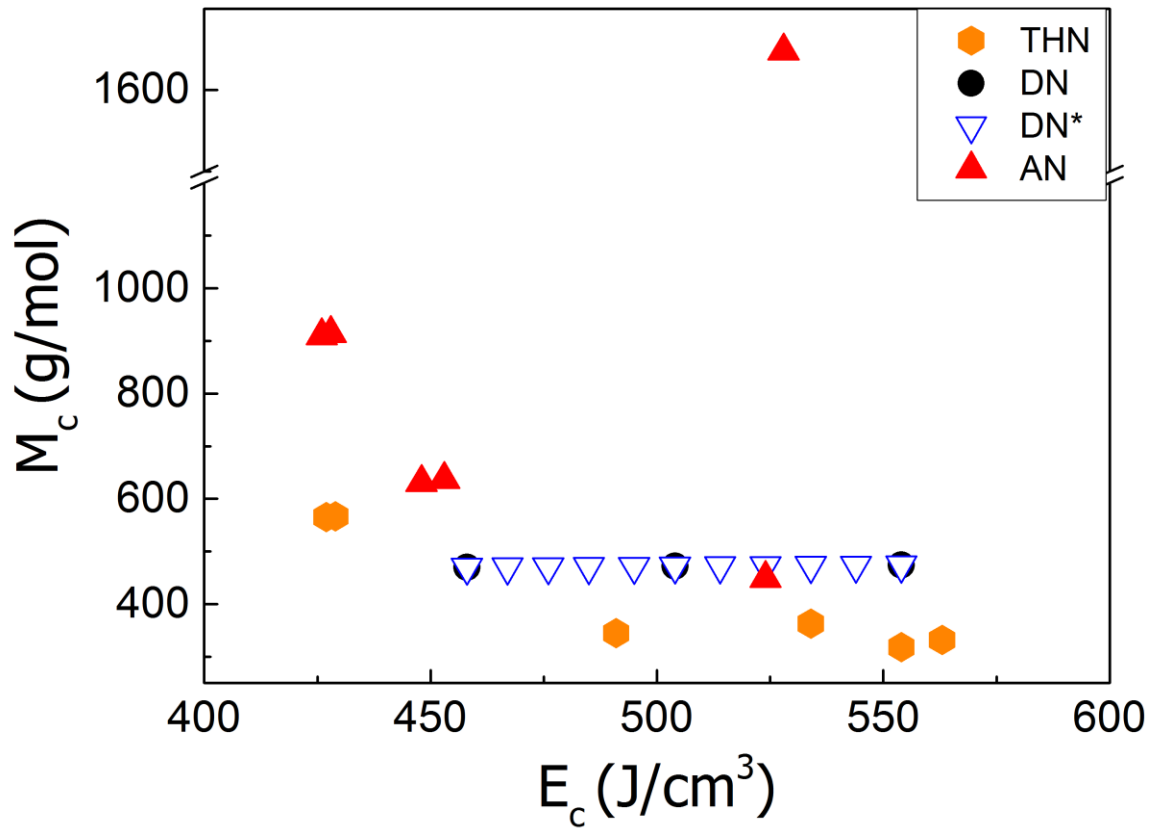


Figure 5.7 Molecular weight between crosslink versus cohesive energy density. THN: Topologically Heterogeneous Networks; DN: Double Networks; DN*: Reference [16]; AN: Asymmetric Networks.

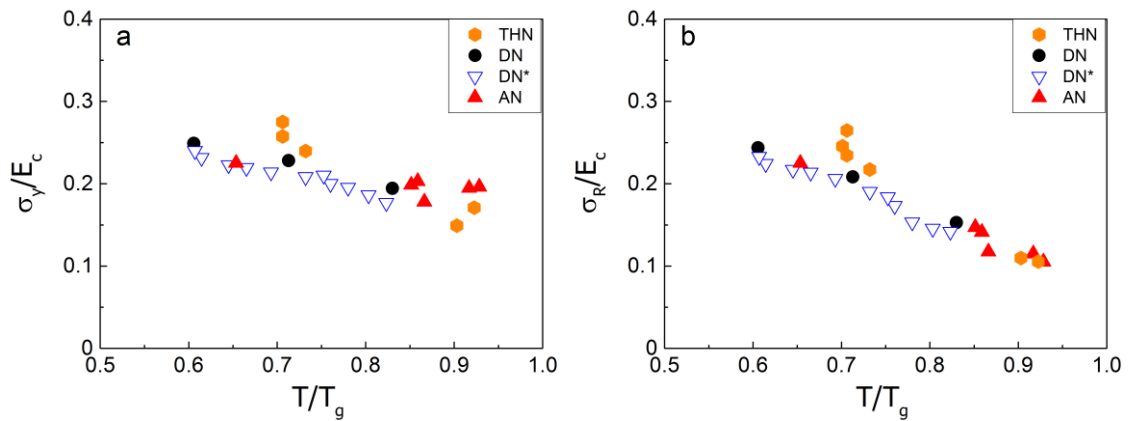


Figure 5.8 Normalized non-linear mechanical properties plotted against normalized test temperature. (a) Yield stress; and (b) Rejuvenated stress.

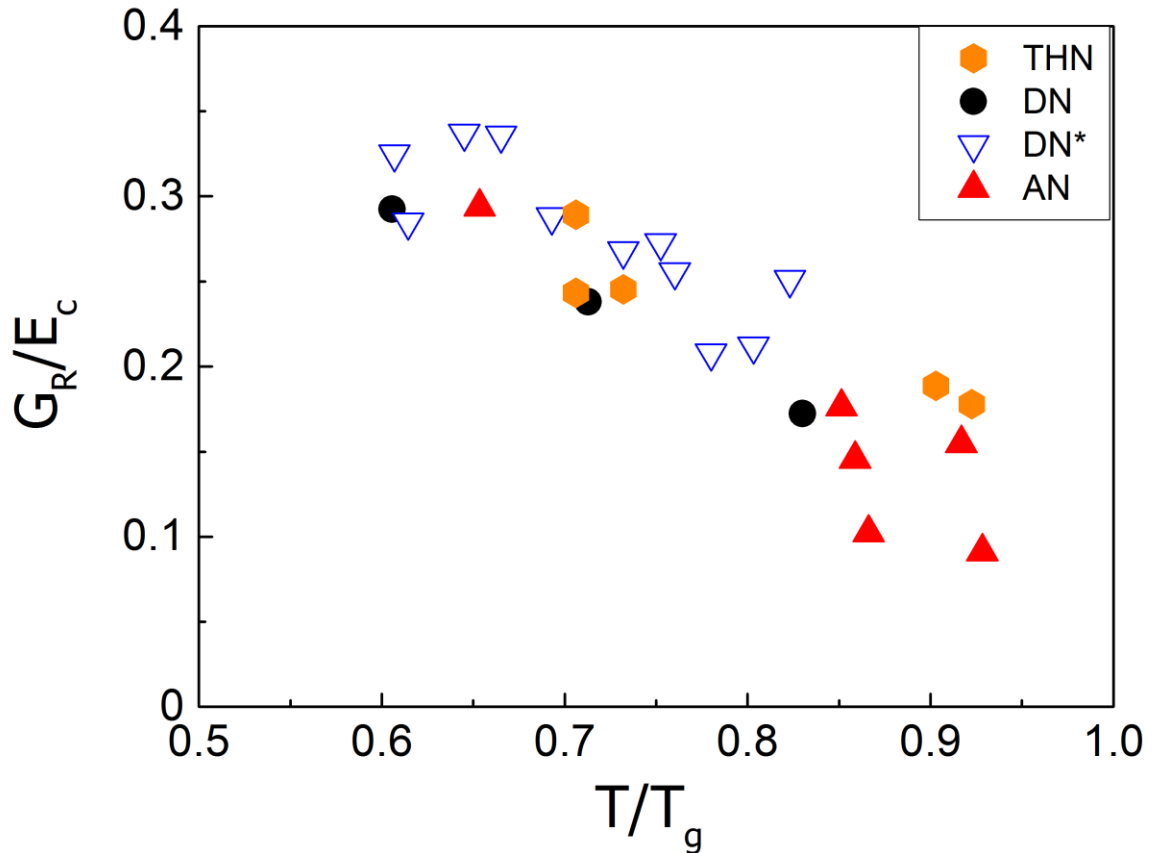


Figure 5.9 Normalized strain hardening modulus against normalized test temperature.

5.4 Conclusion

Two ductility parameters are proposed based on mechanical spectroscopy and compression testing to quantify the effects of chemical and mechanical heterogeneities. The DMA-based ductility parameter utilizes a weighted integral approach to quantitatively describe the influence of segmental mobility. The compression-based ductility parameter considered the balance between shear forces and finite extensibility of network chains. Both correlate well with fracture toughness. However, the compression-based parameter provides much better correlation.

The glass transition temperature and cohesive energy density are proposed as governing parameters for post-yield responses. These parameters captures the chemical heterogeneity within the network structures. Good correlations with rejuvenated stress and strain hardening modulus are obtained.

5.5 Future Work

Future investigation may focus on studying the frequency or strain rate dependence of the DMA-based ductility parameter. In this thesis, the DMA-based ductility parameters are determined at a single frequency of 1 Hz for epoxies with different network heterogeneity. A complementary study would be obtaining the parameters at different frequencies for a single epoxy formulation. Broadband Dielectric Spectroscopy may be used to correlate the ductility parameters with non-linear properties measured at high strain rates.

5.6 References

12. Lesser, A. J., and Calzia, K. J., *J Polym Sci Pt B-Polym Phys*, 42, 2050-2056 (2004).
13. Calzia, K. J., and Lesser, A. J., *J Mater Sci*, 42, 5229-5238 (2007).
16. Detwiler, A. T., and Lesser, A. J., *J Mater Sci*, 47, 3493-3503 (2012).
20. Kinloch, A. J., and Young, R. J., *Fracture Behaviour of Polymers*. Applied Science Publishers, Northern Ireland, (1983).
21. Haward, R. N. (ed) *The Physics of Glassy Polymers*. 2nd edn. Chapman & Hall, London, (1997).
25. van Breemen, L. C. A., Engels, T. A. P., Klompen, E. T. J., Senden, D. J. A., and Govaert, L. E., *J Polym Sci Pt B-Polym Phys*, 50, 1757-1771 (2012).
27. van Melick, H. G. H., Govaert, L. E., and Meijer, H. E. H., *Polymer*, 44, 3579-3591 (2003).
30. Haward, R. N., and Thackray, G., *Proc R Soc A*, 302, (1968).
32. Detwiler, A. T., and Lesser, A. J., *J Appl Polym Sci*, 117, 1021-1034 (2010).
38. Crawford, E. D., and Lesser, A. J., *Polym Eng Sci*, 39, 385-392 (1999).
58. Archer, J. S., and Lesser, A. J., *J Polym Sci Pt B-Polym Phys*, 49, 103-114 (2011).
67. Eyring, H., *J Chem Phys*, 4, 283-291 (1936).
68. MacCrum, N. G., Read, B. E., and Williams, G. (eds) *Anelastic and Dielectric Effects in Polymeric Solids*. John Wiley & Sons, New York, (1967).
69. Kalfus, J., Detwiler, A., and Lesser, A. J., *Macromolecules*, 45, 4839-7847 (2012).
70. Foreman, J. P., D., P., S., B., and R., J. F., *Polymer*, 49, 5588-5595 (2008).
71. van Krevelen, D. W., and te Nijenhuis, K., *Properties of Polymers*. Elsevier Science, Slovenia, (2009).

72. Foreman, J. P., Porter, D., Behzadi, S., Travis, K. P., and Jones, F. R., *J Mater Sci*, 41, 6631-6638 (2006).

BIBLIOGRAPHY

1. Lee, H., and Neville, K., *Handbook of Epoxy Resins*. McGraw-Hill, New York, (1967).
2. Wang, X. R., and Gillham, J. K., *J Appl Polym Sci*, **47**, 425-446 (1993).
3. deNograro, F. F., Guerrero, P., Corcuera, M. A., and Mondragon, I., *J Appl Polym Sci*, **56**, 177-192 (1995).
4. Ma, J., Mo, M. S., Du, X. S., Rosso, P., Friedrich, K., and Kuan, H. C., *Polymer*, **49**, 3510-3523 (2008).
5. Laiarinandrasana, L., Fu, Y., and Halary, J. L., *J Appl Polym Sci*, **123**, 3437-3447 (2012).
6. deNograro, F. F., LlanoPonte, R., and Mondragon, I., *Polymer*, **37**, 1589-1600 (1996).
7. Pfaff, F. A. Mechanical Relaxation Effects in Amine Cured Epoxies. In: SPI Epoxy Resin Formulators Conference, New Orleans, LA, Nov. 3-5 1996.
8. Kody, R. S., and Lesser, A. J., *J Mater Sci*, **32**, 5637-5643 (1997).
9. Lesser, A. J., and Kody, R. S., *J Polym Sci Pt B-Polym Phys*, **35**, 1611-1619 (1997).
10. Crawford, E., and Lesser, A. J., *J Polym Sci Pt B-Polym Phys*, **36**, 1371-1382 (1998).
11. Tan, N. C. B., Bauer, B. J., Plestil, J., Barnes, J. D., Liu, D., Matejka, L., Dusek, K., and Wu, W. L., *Polymer*, **40**, 4603-4614 (1999).
12. Lesser, A. J., and Calzia, K. J., *J Polym Sci Pt B-Polym Phys*, **42**, 2050-2056 (2004).
13. Calzia, K. J., and Lesser, A. J., *J Mater Sci*, **42**, 5229-5238 (2007).
14. Lahlali, D., Naffakh, M., and Dumon, M., *Polym Eng Sci*, **45**, 1581-1589 (2005).
15. Yang, G., Fu, S. Y., and Yang, J. P., *Polymer*, **48**, 302-310 (2007).
16. Detwiler, A. T., and Lesser, A. J., *J Mater Sci*, **47**, 3493-3503 (2012).
17. McAninch, I. M., Palmese, G. R., Lenhart, J. L., and La Scala, J. J., *J Appl Polym Sci*, (2013).

18. Bonnaud, L., Pascault, J. P., and Sautereau, H., *Eur Polym J*, **36**, 1313-1321 (2000).
19. Park, S. J., and Lee, J. R., *J Mater Sci Lett*, **20**, 773-775 (2001).
20. Kinloch, A. J., and Young, R. J., *Fracture Behaviour of Polymers*. Applied Science Publishers, Northern Ireland, (1983).
21. Haward, R. N. (ed) *The Physics of Glassy Polymers*. 2nd edn. Chapman & Hall, London, (1997).
22. Flory, P. J., *Principles of Polymer Chemistry*. Cornell University Press, Ithaca, (1953).
23. Nielsen, L. E., Landel, R. F., *Mechanical properties of polymers and composites*. 2nd edn. Marcel Dekker, New York, (1994).
24. Shaw, M. T., MacKnight, W. J., *Introduction to polymer viscoelasticity*. 3rd edn. John Wiley & Sons, Hoboken, (2005).
25. van Breemen, L. C. A., Engels, T. A. P., Klompen, E. T. J., Senden, D. J. A., and Govaert, L. E., *J Polym Sci Pt B-Polym Phys*, **50**, 1757-1771 (2012).
26. van Melick, H. G. H., Govaert, L. E., and Meijer, H. E. H., *Polymer*, **44**, 2493-2502 (2003).
27. van Melick, H. G. H., Govaert, L. E., and Meijer, H. E. H., *Polymer*, **44**, 3579-3591 (2003).
28. Govaert, L. E., van Melick, H. G. H., and Meijer, H. E. H., *Polymer*, **42**, 1271-1274 (2001).
29. Kierkels, J. T. A., Dona, C.-L., Tervoort, T. A., Govaert, L. E., *J Polym Sci B Polym Phys*, **46**, 134-147 (2008).
30. Haward, R. N., and Thackray, G., *Proc R Soc A*, **302**, (1968).
31. Haward, R. N., *Polymer*, **28**, 1485-1488 (1987).

32. Detwiler, A. T., and Lesser, A. J., *J Appl Polym Sci*, **117**, 1021-1034 (2010).
33. Hoy, R. S., and Robbins, M. O., *J Polym Sci Pt B-Polym Phys*, **44**, 3487-3500 (2006).
34. Kanninen, M. F., and Popelar, C. H., *Advanced fracture mechanics*. Oxford University Press, New York, (1985).
35. Lee, C. Y. C., and Jones, W. B., *Polym Eng Sci*, **22**, 1190-1198 (1982).
36. Yamini, S., and Young, R. J., *Polymer*, **18**, 1075-1080 (1977).
37. Kinloch, A. J., Shaw, S. J., Tod, D. A., and Hunston, D. L., *Polymer*, **24**, 1341-1354 (1983).
38. Crawford, E. D., and Lesser, A. J., *Polym Eng Sci*, **39**, 385-392 (1999).
39. Hinkley, J. A., *J Appl Polym Sci*, **32**, 5653-5655 (1986).
40. Lesser, A. J., and Crawford, E., *J Appl Polym Sci*, **66**, 387-395 (1997).
41. Charlesworth, J. M., *Polym Eng Sci*, **28**, 230-236 (1988).
42. Heux, L., Halary, J. L., Laupretre, F., and Monnerie, L., *Polymer*, **38**, 1767-1778 (1997).
43. Lipatov, Y. S., and Alekseeva, T. T., *Adv Polym Sci*, **208**, 1-227 (2007).
44. Sperling, L. H., and Mishra, V., *Polym Adv Technol*, **7**, 197-208 (1996).
45. Andrews, R. D., Tobolsky, A. V., and Hanson, E. E., *J Appl Phys*, **17**, 352-361 (1946).
46. Flory, P. J., *Trans Faraday Soc*, **56**, 722-743 (1960).
47. Santangelo, P. G., and Roland, C. M., *Rubber Chem Technol*, **67**, 359-365 (1994).
48. Meissner, B., and Matjka, L., *Polymer*, **44**, 4611-4617 (2003).
49. Kaang, S., Gong, D., and Nah, C., *J Appl Polym Sci*, **65**, 917-924 (1997).
50. Aprem, A. S., Joseph, K., and Thomas, S., *J Appl Polym Sci*, **91**, 1068-1076 (2004).
51. Singh, N. K., and Lesser, A. J., *J Polym Sci, Part B: Polym Phys*, **48**, 778-789 (2010).

52. Singh, N. K., and Lesser, A. J., *Macromolecules*, **44**, 1480-1490 (2011).
53. Oleynik, E., *Prog Colloid Polym Sci*, **80**, 140-150 (1989).
54. Odian, G. Principles of polymerization. John Wiley & Sons, Hoboken, (2004).
55. Ogata, M., Kinjo, N., and Kawata, T., *J Appl Polym Sci*, **48**, 583-601 (1993).
56. Archer, J. S., and Lesser, A. J., *J Appl Polym Sci*, **114**, 3704-3715 (2009).
57. Weon, J. I., Creasy, T. S., Sue, H. J., and Hsieh, A. J., *Polym Eng Sci*, **45**, 314-324 (2005).
58. Archer, J. S., and Lesser, A. J., *J Polym Sci Pt B-Polym Phys*, **49**, 103-114 (2011).
59. Gong, J. P., Katsuyama, Y., Kurokawa, T., and Osada, Y., *Adv Mater (Weinheim, Ger)*, **15**, 1155-1158 (2003).
60. Huang, M., Furukawa, H., Tanaka, Y., Nakajima, T., Osada, Y., and Gong, J. P., *Macromolecules*, **40**, 6658-6664 (2007).
61. Tanaka, Y., *EPL*, **78**, 56005 (2007).
62. Webber, R. E., Creton, C., Brown, H. R., and Gong, J. P., *Macromolecules*, **40**, 2919-2927 (2007).
63. Na, Y. H., Tanaka, Y., Kawauchi, Y., Furukawa, H., Sumiyoshi, T., Gong, J. P., and Osada, Y., *Macromolecules*, **39**, 4641-4645 (2006).
64. Ducrot, E., Chen, Y., Bulters, M., Sijbesma, R. P., and Creton, C., *Science*, **344**, 186-189 (2014).
65. Dammont, F. R., and Kwei, T. K., *J Polym Sci A-2*, **5**, 761-769 (1967).
66. Treloar, L. R. G., *The physics of rubber elasticity* Oxford University Press, New York, (2005).
67. Eyring, H., *J Chem Phys*, **4**, 283-291 (1936).

68. MacCrum, N. G., Read, B. E., and Williams, G. (eds) *Anelastic and Dielectric Effects in Polymeric Solids*. John Wiley & Sons, New York, (1967).
69. Kalfus, J., Detwiler, A., and Lesser, A. J., *Macromolecules*, **45**, 4839-7847 (2012).
70. Foreman, J. P., D., P., S., B., and R., J. F., *Polymer*, **49**, 5588-5595 (2008).
71. van Krevelen, D. W., and te Nijenhuis, K., *Properties of Polymers*. Elsevier Science, Slovenia, (2009).
72. Foreman, J. P., Porter, D., Behzadi, S., Travis, K. P., and Jones, F. R., *J Mater Sci*, **41**, 6631-6638 (2006).